CHAPTER I

Introduction

Chromatin is the basic structure for packaging and organizing DNA in the eukaryotic cell

In eukaryotes, DNA is organized in the nucleus into a higher order structure composed of proteins and DNA, called "chromatin". Chromatin promotes genomic stability and organizes genomic information such that it can be utilized in a regulated and organized fashion. Chromatin is made up of repeating units, called nucleosomes, which are composed of 147 base-pairs of DNA wound around the histone octamer [1-3]. The histone octamer consists of two copies of each of the four, highly-conserved histone proteins, H2A, H2B, H3 and H4 [1-3]. The DNA double helix wraps around the histone octamer, making contacts through electrostatic interactions, for spatial compaction [2, 3]. While nucleosomes are essential for packing the genomic DNA into the nucleus, they also restrict the ability of different enzymes to access and metabolize the DNA for standard functions such as repair, replication and transcription [4, 5].

Chromatin is modified in response to external stimuli to alter gene expression and consequently, cellular phenotype

The first step in the process of gene expression is transcription. Nucleosomes impede transcription by sterically hindering direct interaction of transcription factors, transcription cofactors or RNA polymerase II with the DNA double helix [5]. For transcription to proceed effectively, the chromatin structure must be altered to permit the appropriate factors to bind and interact with the double helix throughout the transcription cycle [6]. Coordinated recruitment of a multitude of enzymatic activities in a defined fashion allows (1) the alteration of chromatin structure to facilitate transcription and (2) the re-establishment of the restrictive chromatin structure at the end of the transcription cycle to prevent abnormal DNA metabolism [6]. This imposes an additional level of regulation on gene expression in eukaryotes, as the recruitment of each chromatin modifier to the DNA is exquisitely regulated through a variety of factors [7]. Chromatin modifying factors are regulated by environmental and developmental stimuli, which signal through intracellular signaling pathways to alter the recruitment of these factors to genes [8]. Chromatin modification allows the expression status of different genes, and consequently, the cellular phenotype to be modulated without changing the DNA sequence [7]. The mechanism for altering cellular phenotype without altering the information encoded in the DNA is termed "epigenetics" [7].

Histone post-translational modification is an important mechanism for modifying chromatin structure to influence gene expression

In addition to serving as a structural platform for the DNA, the histone octamer also serves as a signaling hub to integrates information from cellular signaling pathways and dictate how associated DNA should be metabolized. Histones are basic proteins with a central helical "histone fold" structure that makes up the core of the octamer and a disordered, but highly-

conserved N-terminal tail. The histone tail projects off the body of the nucleosome, into solution, where it is accessible to enzymatic modification or protein binding [7]. The histone tails are a major site for post-translational, modification, defined as the covalent addition of functional groups, such as acetyl, methyl or phosphoryl or polypeptides, including ubiquitin, onto chemically labile side chains within the histone tails [9] [10]. Histone post-translational modification alters gene expression of associated genes without changing the DNA sequence; this is one, major mechanism of epigenetic regulation [4, 7].

Posttranslational modifications are thought to exert their influence on chromatin structure, and consequently, gene expression, in one of the following ways. First, addition of a charged group, such as acetyl (-COH) can alter the ability of DNA to associate with the histones by neutralizing the charge on the histones [4]. Second, posttranslational modifications, such as acetylation, methylation or ubiquitination can create or obscure binding sites for conserved protein-protein interaction modules [4]. Conserved histone binding domains can distinguish between post-translationally modified and unmodified residues, allowing these domains to recruit important activities to one modification state, but not the other. This is a mechanism for specific recruitment of essential activities to modify chromatin and facilitate gene expression at particular genes [11, 12].

Histone methylation modulates transcriptional status through altering recruitment of transcription factors and cofactors to specific sites on the histone tail

Histone methylation is the covalent addition of one, two or three methyl groups ($-CH_3$) to a lysine (K, Lys) or arginine (R, Arg) side-chains [13]. Histone methylation is catalyzed by histone methyltransferases (HMTs), and removed by histone demethylases. The first identified

human histone methyltransferase, SUV39H1, specifically methylates lysine 9 at histone H3 (H3K9me) [14].   This enzyme was found to possess a conserved SET (Su(Var), EZH2, Trithorax) domain that is found in all histone methyltransferases, with the exception of DOT1L [14].   The SET domain catalyzes methyltransfer from the cofactor, S-adenosyl methionine (SAM) onto the lysine side-chain through nucleophillic attack of the ε-amine nitrogen.   The structure of SET domains is a highly conserved and made up of four distinct components, the N-SET, SET, i-SET and C-SET domains [15-17].   Both substrate and cofactor are bound tightly into two distinct binding clefts, connected by a narrow pore for methyltransfer.   The reaction proceeds by an Sn2 reaction mechanism where the lysine nitrogen nucleophillicaly attacks the methyl group on S-adenosyl methionine (SAM).   This is accomplished by deprotonation of the nitrogen by a nearby water residue; the water molecule is coordinated by a strictly conserved Tyr [18].   The nucleophilicity of the lysine side chain is enhanced by a "carbonyl cage" that forms around this residue [18].   The SAM cofactor is held in place by a conserved GXG motif such that the methyl group is positioned at the entrance to the methylransfer pore [17].

Methylation negligibly affects the histone-DNA contacts, and thus, does not affect gene expression by inducing major structural changes to the chromatin. Rather, it modulates the recruitment of factors directly involved in gene regulation [10, 13].   Conserved domains, including the plant homeodomain (PHD) fingers and the chomodomains, which have been found to distinguish between methyllysine and unmodified lysine [19-26]. Methyllysine binding modules can be found in proteins or complexes that bind DNA, promote transcription as part of the basal transcription machinery, or modify chromatin. The coordinated recruitment of different transcription factors or cofactors, through recognition of different histone PTMs is a major mechanism by which gene expression is modulated to alter cellular phenotype [11].

Histone methylation can activate or repress transcription, depending on the location of the methyl mark

The most detailed functional studies have focused on defining the role of methylation at residues K4, K9, K27, K36 and K79 of H3 as well as K20 of H4. Unlike other histone modifying enzymes, histone methyltransferases (HMTs) catalyze methylation at highly specific sites [13]. Methylation at each lysine residue is catalyzed by a unique family of enzymes, which are unable to modify other lysine residues besides their specific targets [27]. Histone methylation at each unique lysine residues facilitates a particular set of chromatin modifications, which, in turn, influence transcription in a unique and defined way [27]. Combintorial histone modifications that dictate chromatin structure and gene expression are referred to as the "histone code".

Methylation at H3K9 and H3K27 as well as H4K20 have been associated with transcription repression and gene silencing. H3K9 methylation is enriched in both centromeric and telomeric heterochromatin as well as silenced genes in euchromatin [28-33]. Histone methylation at lysine 27 of H3 (H3K27me) is also associated with gene silencing, and is generally enriched at the promoter of silenced genes in euchromatin rather than in heterochromatin [34]. Methylation at H4K20 is also associated silencing through promoting heterochromatin condensation, in addition to regulating cell cycle progression, DNA damage repair and DNA replication [29, 36]

In contrast to H3K9 and H3K27 methylation, which, promote silencing, methylation at H3K4, K36 and K79 promotes transcription activation [37-39]. H3K4me3 is enriched in gene promoters and peaks around the transcription start site (TSS) of active genes. The localization

pattern of H3K4 methylation suggests a role in transcription initiation and promoter clearance [37, 40]. H3K36 and H3K79 methylation are also correlated with transcription activation, However, these methylation marks are enriched in the coding regions of active genes, rather than the promoter [38, 40]. The existence of distinct localization patterns for H3K4me, H3K36me and H3K79me suggests unique and separate functions of these methyl marks. H3K4 methylation at the promoter signals for one set of alterations to the chromatin structure to permit PolII binding and transcription initiation. While, H3K36 and H3K79 methylation signal for a different set of modifications to chromatin in the coding region, to facilitate transcription elongation.

Histone methylation at different residues can "crosstalk" with other histone methylation to fine tune chromatin modification and gene expression [9]. *A particular histone methylation may promote the binding of enzymes to catalyze chromatin modifications that have similar effects on transcription, while, preventing the binding of HMTs that promote the opposing transcriptional outcome.* For example, H3K4me3, recruits the histone demethylase, PHF8. PHF8 removes the repressive methyl mark at H3K9, which, functions antagonistically to methylation at H3K4 [41]. By this mechanism, H3K4 methylation signals to alter the pattern of chromatin modifications to a more transcriptionally permissive state.

H3K4 methylation recruits factors to remodel chromatin and activate transcription

Methylation at H3K4 stimulates transcription by altering chromatin modification and promoting interaction of PolII with the promoter. Methylation at H3K4 is distinguished from unmodified H3K4 by conserved "reader" modules. For example, PHD fingers that can specifically bind to H3K4me, are present in the H3K4 methyltransferase, MLL1, the H3K9 demethylase, PHF8, the basal transcription factor, TAF3 and the chromatin remodelers, BPTF

and ING2. H3K4 methylation acts to enhance transcription through one of the following mechanisms (1) relieve repression of transcription through removal of repressive chromatin modification (2) remodel nucleosomes to permit transcription (3) enhance existing H3K4 methylation and (4) promote transcription directly though recruitment of the basal transcription machinery [21, 42-47].

The MLL family is a conserved class of histone methyltransferases with diverse functions, but common interactions

H3K4 methylation is catalyzed by SET7/9, as well as the MLL family members [48-51]. The founding member of the MLL family, MLL1, was first identified as the translocated protein in a subset of acute leukemias [52]. In 2002, two separate groups identified MLL1 as a histone methyltransferase, with specificity for H3K4 [50, 51]. Subsequent studies determined that MLL1 has weak catalytic capabilities on its own, but has moderate activity in the presence of a conserved complex of three other proteins, WDR5, RbBP5 and ASH2L, called the MLL core complex [53, 54]. The mechanism by which MLL1 complex activity is regulated by its constituent components is a major focus of this dissertation.

The MLL histone methyltransferase family includes MLL1-4 as well as SET1A and SET1B, and catalyzes H3K4 methylation. Each of these proteins contains a C-terminal SET domain, which catalyzes the addition of a methyl group to the lysine 4 side chain. All members of the MLL family associate with the WDR5/RbBP5/ASH2L sub-complex [54-59]. Despite the fact that all MLL family members have a conserved SET domain, and conserved functional domains and interaction partners, these proteins have distinct functions in gene regulation. To this point, MLL1 and MLL2 are highly similar in sequence, with many conserved domains and

interaction partners, including the MLL core complex. Despite these similarities *MLL1-/-* mice are embryonic lethal at day 13.5 with significant defects in axial skeleton development and yolk sac hematopoiesis while *MLL2-/-* mice are embryonic lethal at 9.5 with more general defects in growth and development [60-62]. The existence of dramatically different phenotypes in these two mouse models suggests distinct gene targets and biological roles for these two highly similar proteins. The other MLL family members, MLL3 and 4, also have unique functions and are involved in steroid hormone-transcription, DNA repair, class switching and development [63-65]. Significant work remains to be done to understand both the unique functions of each MLL family member in gene regulation, and how these unique functions are achieved despite significant sequence homology and conserved interaction partners. Of particular interest is the question of the basic modular structure of the MLL family complexes, the MLL/WDR5/RbBP5/ASH2L core, and how it functions in the MLL family complexes.

MLL1 is an essential regulator of *Hox* gene expression in axial skeleton development and hematopoiesis

Original knockout studies with MLL1 identified a critical role for MLL1 in regulating development of both the axial skeleton and the hematopoietic system, in mice [61, 66]. Further studies found that MLL1 affects these developmental processes through positive regulation, primarily of the 5' *Hox* cluster genes. After initial induction by other factors, *Hox* expression is maintained in the developing embryo through the coordinated action of two classes of histone methyltransferases, the polycomb group (PcG) and the trithorax group (TrxG) [67]. Generally, the polycomb group catalyzes repressive histone methylation at target genes while the trithorax group promotes transcription through activating histone modifications such as H3K4me and

chromatin remodeling. The opposing action of these two classes of proteins finely tunes the expression status of target genes, including, the *Hox* locus.

In metazoans, the *Hox* genes are arranged in clusters on four different chromosomes and oriented 5' to 3', in order of the anterior-posterior expression. Biologically, the *Hox* genes have multiple functions in development. Members of the *HoxA, B* and *C* clusters essential functions in hematopoiesis and are highly expressed in hematopoietic stem cells (HSCs) and early progenitors [68-70]. Modulation of *Hox* expression levels in mice have been shown to impact the hematopoietic system in a variety of ways, through impairing stem cell self renewal, proliferation and differentiation or inducing leukemia, further supporting the essential role for the *Hox* cluster in regulation of the hematopoietic system [68]. The *Hox* family member that has the most dramatic hematopoietic phenotype is *HoxA9*, which is an MLL1 target. *HoxA9* is the most highly expressed *Hox* gene in HSCs indicating it may be the major regulator in this cell type [71]. Deletion of *HoxA9,* significantly impairs the ability of HSCs to self-renew and competitively repopulate the hematopoietic system in a lethally irradiated mouse, and results in defects in multiple hematopoietic lineages [72]. Overexpression of *HoxA9* enhances self-renewal and can also result in transformation and development of leukemia [68]. Deletion of *MLL1* largely mimics deletion of *HoxA9* and overexpression of *HoxA9,* along with *HoxA10, B3* and *B4* can reverse this phenotype [73]. In mice, ectopic overexpression of *HoxA9* and its cofactor, *Meis1* is sufficient to transform progenitor cells and develop leukemia with an extended latency period. In human patients, elevated *HoxA9* expression is found in leukemia and associated with poor prognosis. The most common chromosomal rearrangement found in AML is translocation of NPM1[1]; these leukemias are found to have elevated expression of both *HoxA9* and *Meis1* [68]. Elevated *HoxA9* and *Meis1* expression is the factor most significantly

correlated with poor prognosis in leukemia patients. Leukemia patients with elevated *HoxA9* expression have poor rate of survival relative to patients with median and low *HoxA9* expression [74]. Modulating the levels of *HoxA9* expression through interfering with MLL1 may be one way to improve outcomes in patients with high levels of *HoxA9* expression and consequently poor outlook. However, in order to pharmacologically target MLL1 activity, we must first understand how this enzyme functions and is regulated.

The MLL1 complex SET domain catalyzes H3K4 methylation with assistance form the core complex of WDR5, RbBP5 and ASH2L

The MLL family is unique amongst the histone methyltransferases in that these enzymes have negligible activity independently and must associate with additional factors for catalytic function. Despite sequence conservation of all the major SET domain motifs and residues found to participate in substrate and cofactor binding catalysis, the MLL1 SET domain is weakly active in the absence of the core complex components [75-77]. The structure of the MLL1 SET domain shows that, unlike other methyltransferases, the i-SET region is shifted away from the substrate binding cleft, leaving the substrate Lys side chain exposed to solvent and flexible instead of constrained in an optimal position and chemical environment for methyltransfer, as shown in figure 1.1 [75]. It was postulated that the i-SET region must be induced into a "closed" conformation by another protein in order to facilitate efficient methyltransfer. This hypothesis was supported by a cryoEM structure of the yeast SET1 complex, which is a distant relative of MLL1. Another possibility is that a second protein associates tightly with the SET domain and contributes residues for peptide binding to create a multiprotein active site. Regardless of the mechanism, these structures point to an essential role for associated proteins, specifically the

10

MLL1 complex components, WDR5, RbBP5 and ASH2L, in contributing to active site geometry and chemistry. The functional significance of catalytic stimulation by the core components remains to be determined.

The MLL complex component, WDR5, is a context dependent regulator of developmental transcription

Biochemical studies of the MLL1 complex describe a direct interaction between MLL1 and the conserved β-propeller protein, WDR5, and suggest that this interaction is essential for complex stability and activity [Dou, 2006 #239]. WDR5 was initially identified, by genetic techniques, as the protein, BIG-3, involved in stimulating osteoblast differentiation in response to bone morphogenetic factor 2 (BMP-2) and chondrocyte development [78, 79]. Later studies found that WDR5 was part of a multicomponent complex with MLL1/ALL-1/HRX, along with two dozen other polypeptides [50, 51]. WDR5 was found to play important roles in embryonic stem cell maintenance, hematopoiesis (as part of the MLL1 complex), steroid-mediated transcription, myogenesis and hypoxia-induced epithelial to mesenchymal transition [55, 59, 80-85]. Multiple interaction partners of WDR5 have also been identified, including HDAC3, the MLL complex components, MOF, MSL1v1, PAX7 and the noncoding lincRNA, HOTTIP [80, 81, 84-87]. These functions point to a general role for WDR5 in transcription regulation during development, both embryonic and adult tissue development.

Despite the multitude of binding partners identified, WDR5 is a relatively small protein at 35KDa, with only two, conserved binding pockets that have been structurally defined. Although, more binding surfaces exist that have yet to be identified . WDR5 does not, likely, interact with all its identified binding partners simultaneously [88, 89]. WDR5 has different expression

patterns in development than some of its associated proteins [85]. Therefore, it is possible that WDR5 associates with the available proteins depending on cell type to dictate its function. It is also possible that WDR5 interactions may be regulated by post-translational modification of interacting residues. For instance, one of the major interactions described for WDR5 is its interaction with a conserved Arg residue in the preSET domain of MLL1 [90]. As arginine residues can be post-translationally methylated, it is possible that this association could be regulated by an as yet, unidentified, factor arginine methyltransferase. WDR5 has a multitude of biological functions and many identified interaction partners, yet, it possesses no known enzymatic activity and only two described interaction interfaces. This begs the question, of how such a seemingly simple protein can be so essential and drive so many different processes. This question is central to understanding both the function of WDR5 in the MLL complex for hematopoiesis and leukemia as well as the functions of WDR5 in the different biochemical complexes and developmental processes that it has been described in.

WDR5 is an essential factor in hematopoiesis through stimulation of MLL1 complex activity

WDR5 was identified as part of a complex that contains MLL1 and possesses methyltransferase activity against H3K4 [86]. WDR5 knockdown was found to impair expression of MLL1 target genes, *HoxA9* and *HoxC8* [54]. These knockdown studies establish an essential role for WDR5 in MLL1 target gene expression. This also implicates WDR5 in hematopoiesis and leukemia as these genes are essential for both processes. WDR5 interacts directly with the long intergenic non-coding (linc)RNA, HOTTIP [80]. HOTTIP is transcribed from non-coding DNA in the *Hox* locus and through its direct interaction with WDR5, targets the MLL1 complex across the *5'Hox* locus for transcription activation [80]. In addition to showing a

specific mechanism for WDR5 in hematopoiesis, this study also demonstrates a direct interaction between WDR5 and a non-MLL complex component that is important for gene regulation.

WDR5 regulates transcription in embryonic stem cells

Recent work has identified an essential role for WDR5, both alone, and in concert with the acetyltransferase, MOF, in regulation of an essential transcriptional network that regulates self-renewal of embryonic stem cells (ESC) [82, 85]. Initial studies found that inducing differentiation of embryoid bodies or ESC promotes downregulation of WDR5, along with *Nanog* and *Oct4*, but not MLL1, RbBP5 or ASH2L [85]. *Nanog* and *Oct4* are master regulators of transcription in ESC that were found, along with *Sox2* to be necessary and sufficient for induction of an ES-like phenotype in fibroblasts, described as induced pluripotent stem cells or iPS [91]. Further study of WDR5 found that both *Nanog and Oct4* bind to the WDR5 gene, suggesting a mechanism by which WDR5 is downregulated during differentiation. WDR5 was also shown to bind directly to Oct4 and weakly to Nanog, suggesting a means for WDR5 to interact with the Oct4/Sox2/Nanog transcriptional network in ES cells [85].

WDR5 also cooperates with its previously identified interaction partner, MOF, in regulation of key self-renewal and pluripotency genes in ESC [82]. MOF and WDR5 are part of a larger complex with MLL1, RbBP5 and ASH2L, amongst others [86]. MOF and WDR5 are also found in the MOF-Msl1v1 complex, independent of the MLL1 complex components. In ESC, both MOF and its associated histone modification, H4K16, were downregulated during differentiation, like WDR5, but unlike other MLL complex members [82]. Genetic deletion of MOF downregulates genes associated with pluripotency and self-renewal, much like WDR5 knockdown. Genome-wide mapping shows that WDR5 peaks overlap with 30% of MOF peaks,

and both factors were shown to regulate key ESC regulators, *Nanog and Sox2*. This data indicates that both MOF and WDR5 function to regulate expression of self-renewal and pluripotency genes in ESC. More work remains to be done to tease apart the specific functions for these two proteins and determine to what extent their functions are dependent on each other. It also remains to be determined if WDR5 and MOF interact directly, or if the interaction is mediated by association with other proteins. If the interaction is found to be direct, it will be interesting to map the binding interface and determine if MOF competes with the MLL1 complex members for WDR5 binding, or if this interaction can take place in the context of the MLL1 complex.

Despite the essential role for WDR5 in regulating transcription of the Oct4/Sox2/Nanog transcriptional network in ESC, it is not known to what extent this function is dependent WDR5 function in the context of the MLL1 complex. On one hand, approximately 70% of WDR5 gene targets in ESC overlap with H3K4 trimethylation peaks and the MLL1 complex components were found to co-elute with both WDR5 and Oct4 [85]. However, knockdown of RbBP5 and Dpy30- essential components of the MLL1 complex-, did not have a significant effect on expression of self-renewal and pluripotency genes, unlike knockdown of WDR5 [92]. Furthermore, although WDR5 and Oct4 were found to co-elute with the remaining MLL1 complex members, they were also found to co-elute without the complex members in a lower molecular weight peak. This suggests that WDR5 may complex with Oct4 to regulate transcription in ESC in a manner that is not dependent on MLL1 activity. Or, WDR5 may partition into two separate complexes in ESC with distinct molecular and regulatory functions. How much WDR5 relies on its association with the MLL1 complex to mediate gene regulation is a central question that remains to be addressed. The multitude of WDR5 interaction partners

suggests that WDR5 may be more than just a simple structural scaffold for the MLL1 complex and this idea is supported by the findings in ES cells. The studies in ES cells also show how essential WDR5 function is for maintaining ESC, underlining the importance of WDR5 in regulating mammalian development through transcription.

WDR5 is a regulator of early stage muscle development

Two recent reports have elucidated a new function for WDR5 and the MLL1/2 complexes in Pax7-driven myogenesis [83, 84]. In one study, the MLL1 complex was recruited to Pax7 targets through a methyl-arginine mediated interaction between the MLL2 C-terminus and Pax7 [84]. Methylation of four arginine residues in a conserved domain in Pax7, by the arginine methyltransferase, CARM1, was a prerequisite for this interaction. In the second study, WDR5 was found to interact directly with the Pax3/7_BP through a yeast two-hybrid screen[83]. Taken together, these studies show that Pax7 recruits MLL1/2 complexes through two different mechanisms (1) CARM1-mediated recruitment of MLL1/2 (MLL1 was shown to interact but most of the work focused on MLL2) and (2) CARM1-independent Pax3/7BP-mediated recruitment of WDR5. Biologically, these studies show a role for Pax7-recruitment of WDR5 and two MLL complexes in regulating muscle stem cells and proliferation of myoblast precursors in early post-natal development. This demonstrates an essential role for WDR5 in development in a different system than the hematopoietic system.

WDR5 plays an essential role in the epithelial-mesenchymal transition, an essential process in organ development and metastasis

Recent work also detailed a role for WDR5 in regulating the epithelial-to-mesenchyme transition under hypoxic conditions [81]. EMT is an essential process in organ development, fibrosis and tumor metastasis. Under hypoxic conditions, the transcription factor, Hif1α was found to induce HDAC3, which in turn promotes expression of mesenchymal genes and represses expression of epithelial genes, in a manner that was dependent on its deacetylase activity [81]. Although HDAC activity is traditionally linked to transcriptional repression, HDAC3 was shown to preferentially deacetylate H3K4, clearing the way for methylation of this residue to promote transcription[81]. Indeed, hypoxia was found to decrease H3K4Ac while increasing methylation at this residue. Hypoxia was also found to increase expression of WDR5, but not other MLL complex components, RbBP5 and ASH2L [81]. Examination of the WDR5 promoter found Hif1α and Hif2α response elements in the WDR5 gene [81]. Immunoprecipitation found that WDR5 and HDAC3 could directly interact, but only under hypoxic conditions. This interaction is essential for upregulating expression of mesenchymal genes while downregulating epithelial genes. The existence of a WDR5:HDAC3 interaction is further supported by the identification of both WDR5 and HDAC3 in an MLL1 complex purification although HDAC3 was not detected in later MLL1/WDR5 purifications [86] [50]. The findings of this study are informative about WDR5 biology for two reasons (1) this is the first detailed description of regulation of WDR5 through direct induction of WDR5 expression in response to cellular signaling (2) this is the first study where the ability of WDR5 to interact with another protein is regulated by the cellular status. The activation of the WDR5 gene by an environmentally responsive signaling pathway suggests that WDR5 function may be to integrate information from cellular signaling pathways to regulate function of the MLL1 complex in response to stimuli.

Interestingly, although MLL1-dependent H3K4 methylation was shown to be essential for modulating gene expression in response to Hif1α, of the MLL1 complex members, only WDR5 expression and function was specifically regulated by Hif1α signaling. The upregulation of WDR5 in the absence of concurrent upregulation of MLL1, RbBP5 and ASH2L would not be anticipated to elevate histone methylation. This then raises the question, is WDR5 at suboptimal concentrations for assembling the MLL1 complex in epithelial cells under non-hypoxic conditions? Or is WDR5 functioning in an alternative context than the MLL1 complex in this cell type? Further biochemical studies to address these questions would provide interesting clues as to the function of WDR5 in development.

WDR5 has additional functions in regulating animal development

Functions for WDR5 in development have been identified in multiple organisms and tissues. In bone development, WDR5 is highly expressed in osteoblasts and essential for osteoblast differentiation as well as chondrocyte differentiation in embryonic bone development [93]. It remains to be determined if WDR5 exerts its effects on bone development through the MLL family or by another mechanism. In frogs, WDR5 suppression by morpholino caused defects in skeletal development of frogs and abnormal patterns of *Hox* gene expression, much like MLL1 knockout in mice [94]. These two cases further support the hypothesis that WDR5 is a general regulator of developmental gene expression.

WDR5 possessed multiple protein binding sites and is a structural platform for multiprotein complexes

WDR5 has been shown to possess no intrinisic enzymatic activity, so the question then is how does it execute its multitude of described biological functions? How does WDR5 partition into different multiprotein complexes? Which proteins can WDR5 interact with in the presence of the MLL1 complex and which proteins can it interact with only in the absence of association with MLL1? Finally, how does WDR5 function in other multiprotein complexes, in the absence of MLL1, if it does not function to stimulate methyltransferase activity? These are all important questions to address to understand WDR5 function, and, as biochemistry informs biology, the most obvious starting place to address these questions is to examine the biochemical interactions and functions of the WDR5 protein.

Peptide pulldowns and subsequent crystallographic studies first suggested that WDR5 functions to directly bind to the histone H3 peptide through its central Arg-binding pocket [94]. The reported K_D for this interaction was in the low micromolar range as determined by Isothermal Calorimetry (ITC) [95, 96]. WDR5 was reported to interact with the H3 peptide, primarily through contacts formed between the R2 side-chain and the central channel of WDR5. The primary contact is a "phenylalanine sandwich" formed between F133 and F266 of WDR5 and the guanido group of the R2 side chain [89, 96]. Binding is further stabilized by hydrogen bonding between the guanido group and Ser91 [96]. In these models, binding of WDR5 to H3 R2 was suggested to "present" the critical Lys4 side chain to the MLL1 active site for efficient methylation [94-97].

However, in 2010, two groups suggested that the preferred substrate of the WDR5 Arg binding pocket may be a conserved Arg residue found in the preSET domain of MLL1 [89, 90, 98]. Binding of WDR5 to the conserved MLL1 "WDR5 Interaction" or "WIN" motif was found to be approximately 50-100-fold tighter than binding of WDR5 to the histone H3 peptide,

supporting the idea that WDR5 preferentially binds MLL1 R3765 over Histone 3 R2 [90]. Furthermore, mutation of this interaction interface was shown to disrupt association between MLL1 and WDR5 in *in vitro* biochemical studies [90]. These studies suggest that the key role of WDR5, in the MLL1 complex, may be facilitating complex assembly rather than substrate recognition.

RbBP5 and ASH2L contribute essential catalytic functions to the MLL complex

The remaining members of the MLL1 complex, RbBP5 and ASH2L as well as DPY30 [2]have essential roles in MLL1 complex function as well [92, 99]. RbBP5 and ASH2L form a structurally stable heterodimer and have been shown to have very weak intrinsic histone methyltransferase activity, as well as the capacity to bind SAM [76, 99, 100]. Knockdown of RbBP5 and ASH2L modestly impairs expression of *HoxC8* and *HoxA9,* much like WDR5 [54]. In biochemical studies, a C-terminal fragment of MLL1 demonstrated exceptionally weak monomethyltransferase activity, with a rate constant of 0.003 hr^{-1} [76]. Addition of stoichiometric amounts of WDR5 did not alter the methylation kinetics, while addition of both WDR5 and RbBP5 stimulated the rate of methylation by a factor of 2-fold relative to MLL1 alone [76]. However, addition of equimolar amounts of ASH2L to MWR significantly enhanced complex activity and increased the rate of monomethylation by approximately 400-fold as well as facilitating dimethylation, which had not been observed in the absence of ASH2L [76]. Addition of ASH2L also conferred dimethyltransferase activity on the MLL1 complex [76]. This data suggests that ASH2L may play in an essential, stimulatory role in catalysis, especially of dimethylation, while WDR5 and RbBP5 may serve essential, structural functions.

MLL1 fusion proteins recruit abnormal transcription activities to stimulate overexpression of gene targets in leukemia

Leukemias with MLL1 translocation are haploinsufficient in wild-type MLL1 and yet have elevated H3K4 methylation at and expression of MLL1 target *Hox A* cluster gene s[69]. Taken together, this suggests that MLL1 fusion proteins either recruit or coordinate function with wild-type MLL1 or another HMT to upregulate MLL1-directed H3K4 methylation and subsequent gene expression. The other possibility is that the MLL1 fusion protein bypasses the requirement for MLL1 through recruitment of transcriptional activators/coactivators and chromatin modifiers that act downstream of MLL1/H3K4 methylation in a transcriptional signaling cascade. Indeed, MLL1 fusion proteins have been shown to recruit a host of transcription factors, including members of the fusion protein supercomplex. This supercomplex includes the transcription elongation factors, AF9, ENL, AF4, AFF4, AF5q31p, ELL, which stimulate PolII transcription during the elongation phase. The MLL fusion protein also recruits the PolII-associated complexes pTEFb and PAF1c, which directly stimulate PolII activity through phosphorylation of its C-terminus. The MLL1 fusions also recruit the H3K79-methyltransferase, Dot1L, which is involved in transcription activation. MLL1 and the MLL1 fusion protein for a trimeric complex with the proteins Menin and LEDGF, which are essential for recruitment of both the wild-type and fusion protein to gene targets [70]. Many of the fusion-protein associated factors are essential for gene expression and transformation. However, the essential functions of the different fusion-protein associated transcription coactivators and chromatin regulators do not preclude the possibility that wild-type MLL1 may also be required for fusion-protein-mediated transcription. Indeed, two recent studies have found that MLL-fusion-transformed cells have impaired growth and proliferation as well as downregulated

HoxA9 and *Meis1* expression when wild-type MLL1 is either knocked down or excised [43, 101]. In leukemias with MLL1 translocation, transcription activation of MLL1 targets is facilitated by coordinated action of multiple mechanisms to promote changes in chromatin structure as well as direct stimulation of PolII activity. Targeted disruption of any of these activities, including the MLL1 complex, is hypothesized to impair transformation of leukemia with MLL1 rearrangement.

Targeted therapies to modulate epigenetic regulation have shown promise for leukemia therapy in pre-clinical studies

MLL rearranged leukemias have especially poor prognosis, and despite substantial research, therapeutic outcomes have not improved substantially for this disease since identification of the MLL1 protein. Two therapies have been described in pre-clinical studies, to target epigenetic dysregulation in MLL1 rearranged leukemias. The first of these compounds targets the Menin:MLL1 interaction, which mediates recruitment of both MLL1 and the MLL1 fusion protein to *HoxA9* and *Meis1* in MLL1 rearranged leukemia [102]. The second drug targets the activity of the Dot1L H3K79 methyltransferase [103]. Both of these compounds impair expression of MLL1 targets in leukemia and prevent abnormal establishment of activating histone methylation at MLL1-target genes. These drugs impaired viability and proliferation, specifically of leukemia cells with MLL1 rearrangement and induced differentiation in these cells. Significantly, both Menin and Dot1L have been shown to act in the same pathway regulating chromatin modifications associated with MLL1 translocations. Menin is required for recruitment of MLL1 as well as H3K4me3 and Dot1L at these loci [101]. Whereas Dot1L-mediated H3K79me2 is downregulated in MLL-AF9 cells when MLL1 is knocked down [43].

As these two proteins function upstream and downstream of MLL1 in the same dysregulated chromatin modification pathway, this supports the idea that (1) H3K4 methylation is essential for *HoxA9* expression in leukemia and (2) inhibiting MLL1 H3K4 methyltransferase activity could be a promising strategy for treatment of acute leukemias with MLL1 rearrangement.

HoxA9 and *Meis1* upregulation in MLL1 rearranged leukemias requires activity of the wild-type MLL1 protein. As knockdown of the MLL1 core complex components, WDR5, RbBP5 and ASH2L, has been shown to impair *HoxA9* expression in HeLa, we postulate that the core complex is also essential for facilitating upregulation of *HoxA9* and *Meis1* by MLL1 in these leukemias [54]. Therefore, we hypothesize that interfering with the MLL1 core complex could also interfere with *HoxA9* and *Meis1* overexpression and prove to be a useful strategy for treating leukemias with MLL1 rearrangement or *HoxA9* amplification. WDR5 interacts directly with MLL1 through a small, conserved Arg-binding pocket and facilitates MLL1 core complex assembly [90, 98]. The interaction interface between WDR5 and MLL1 has been detailed by multiple crystal structures and is amenable to small molecule targeting [89, 98]. The MLL1 SET domain structure lacks obvious sites for small molecule targeting which makes it a poor candidate for rational design [75]. Also the previously described, radiometric histone methyltransferase assay is not adaptable to high-throughout screening, which makes this technique for small molecule identification a poor option for this enzyme complex, at present. Therefore, we propose to use rational design to target the WDR5:MLL1 interaction to inhibit MLL1 complex activity for drug development in leukemia with MLL1 rearrangement.

In addition to targeting MLL1 complex activity for leukemia therapy, a drug-like WDR5 inhibitor could also have relevant use for probing the function of WDR5 in different cellular contexts. WDR5 has important functions in development in a multitude of systems, including

embryonic stem cells, muscle development, and the epithelial-to-mesemchyme transition in addition to the hematopoietic system [81, 83-85]. WDR5 has also been found to interact with several other transcription cofactors and chromatin modifiers besides MLL1, but both the regulation of these interactions and their functions remain unclear. Furthermore, it is unknown if these interactions take place in the context of WDR5 function in the MLL1 complex or if they compete for WDR5 association and block its function in the MLL1 complex. To further flesh out our understanding of WDR5 in development and gene regulation, we will need chemical tools to modulate its interaction with different partners. We propose that the WDR5 Arg-binding pocket inhibitor will aid the exploration of WDR5 function in different contexts by allowing us to define functions for WDR5 that are independent of WDR5 binding to MLL1. This chemical tool will also allow us to explore which interaction partners bind specifically to the WDR5 Arg-binding pocket. Finally, this compound will theoretically allow us to establish which of WDR5-dependent histone modifications and gene targets require the Arg-binding pocket activity for activation. These studies would not be possible with standard genetic techniques as (1) no WDR5 knockout model exists at present and (2) genetic knockout or knockdown studies interfere with the function of the entire protein, rather than just one interaction interface. In summary, we propose to use rational design to develop an inhibitor to the conserved WDR5 Arg-binding pocket. This compound should have important utility for both disruption of MLL1 complex activity to treat leukemias with MLL1 rearrangement and exploration of WDR5 function in different biochemical contexts and cell types.
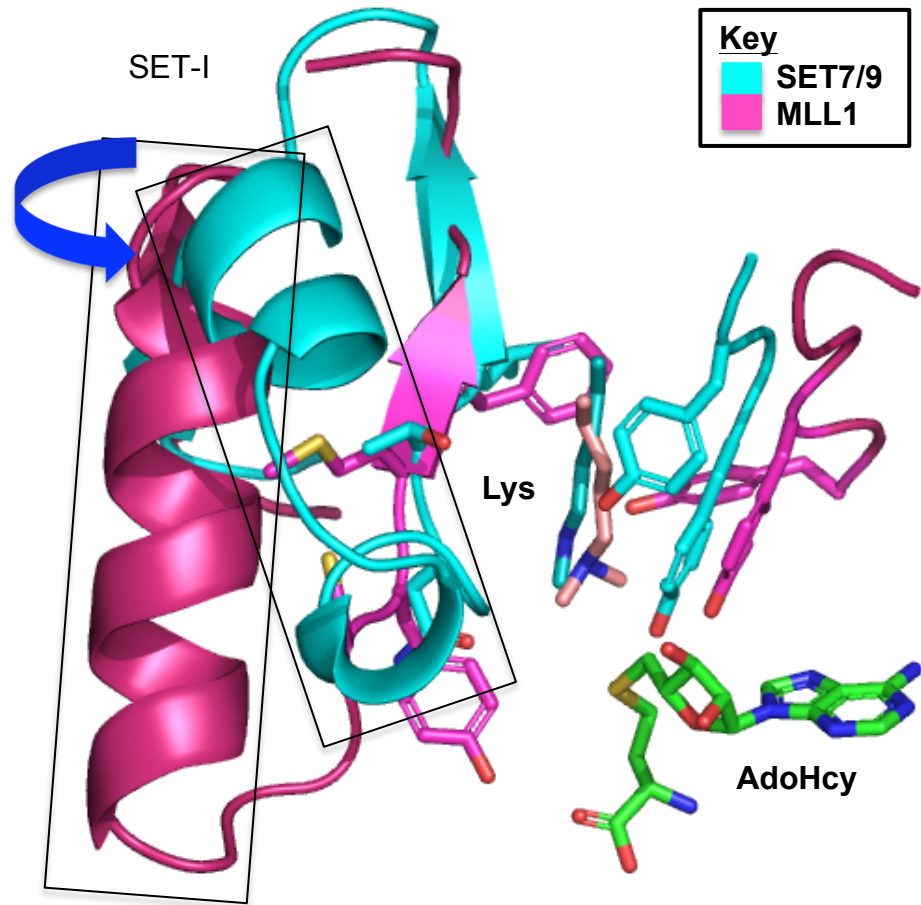
Figure 1.1. Structure of the MLL1 and SET7/9 SET domain active sites, highlighting the i-SET helix and its orientation relative to the active site, and its influence on active site organization. MLL1 is rendered in magenta while SET7/9 is rendered in cyan. This figure was generated with assistance from Michael Lofgren.

Diagram of MLL1 Interactions
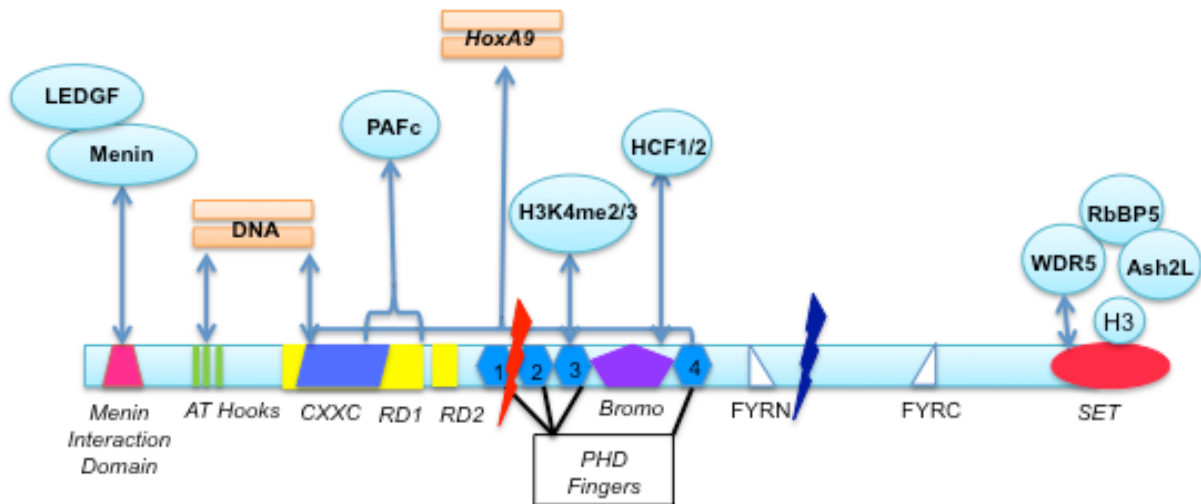
Figure 1.2. Diagram of conserved domain structure and protein-protein interactions in the MLL1 protein. Colored shapes indicate conserved domains, blue arrows depict interactions with other proteins (cyan circles) or genes (beige rectangles). The breakpoint for MLL1 translocation is shown in red and the Taspase1 cleavage site for MLL1 processing is shown in dark blue.

CHAPTER II

Development of Potent Peptidomimetic Inhibitors to Block Interaction of MLL1 and

WDR5 for Inhibition of MLL1 Complex Activity

Abstract

MLL1 is an H3K4 methyltransferase with essential functions in a subset of acute leukemias with genetic translocation of MLL1 [69, 70]. MLL1 interacts with three, highly-conserved partners, WDR5, RbBP5 and ASH2L (WRA) to form a stable multiprotein complex [53, 54]. ~~Interestingly,~~ MLL1 alone has very weak histone methyltransferase activity that is significantly stimulated by interaction with the WRA subcomplex [53, 90, 100]. MLL1 interacts directly with WDR5 and several lines of evidence have pointed to a crucial role for this interaction in facilitating both MLL1 complex formation and catalysis [54, 89, 98]. We hypothesize that chemically inhibiting the interaction between MLL1 and WDR5 can impair MLL1 complex formation and methyltransferase function. To test this hypothesis, we demonstrate that a previously defined MLL1 WDR5-interaction or "WIN" motif is essential for MLL1 complex assembly and activity both *in vitro* and in cells. We show that excess WIN peptide can inhibit MLL1 complex function *in vitro*. We identify a minimal sequence in the WIN motif that can interact with WDR5 and use this sequence as a lead for inhibitor

development. Using the published crystal structure of WDR5, in complex with the WIN peptide, as a guide, we perform structure-function studies to optimize the binding and pharmacological properties of WIN-derived inhibitors.

Introduction

Translocation of MLL1 is found in approximately 10% of all cases of acute leukemia and is particularly resistant to treatment with conventional chemotherapies [69, 70]. In these leukemias, transformation is driven by overexpression of *HoxA9* and *Meis1*, which is facilitated by MLL1 fusion protein binding at *HoxA9* and *Meis1* promoters. In these cases of leukemia, there are two copies of the MLL1 gene, the translocated copy and the wild-type copy. While the translocated copy of MLL1 has been shown to drive overexpression of *HoxA9* and *Meis1*, it lacks the methyltransferase activity that is conventionally thought to stimulate gene activation in wild-type MLL1. Recent work has established that wild-type MLL1 cooperates with the MLL1 fusion protein to upregulate gene expression in leukemia with MLL1 rearrangement [43, 101]. Therefore, we hypothesize that pharmacologically inhibiting the activity of wild-type MLL1 in patients with MLL1 rearranged leukemias could selectively target transformed cells and serve as an effective treatment for this disease.

In humans, MLL1 is the founding member of a family of six related proteins including MLLs 1-4, SET1A and SET1B [50, 86, 104, 105]. The MLL family members associate with a conserved set of three proteins, WDR5, RbBP5 and Ash2L to form a stable multiprotein complex [54]. Structure-function studies of the MLL1 complex have shown that MLL1 must associate with these proteins to efficiently catalyze histone lysine methylation [53, 86, 94]. The remaining MLL family members have also been shown to interact with WRA, but the functions of WRA in

facilitating histone methylation and gene expression by other MLL family members have not been specifically investigated. Assembly of the MLL1 complex is facilitated by a set of direct, pair-wise interactions found between WDR5 and MLL1, WDR5 and RbBP5 and RbBP5 and Ash2L [100]. Biochemical and structural studies have detailed a direct interaction between a conserved motif, located N-terminal to the SET domain of MLL1 and the Arg binding pocket of WDR5 [89, 90, 98]. The RbBP5/Ash2L heterodimer possesses weak, intrinsic methyltransferase capacity and can bind both substrate and cofactor in the absence of MLL1 and WDR5 [99, 100]. Taken together, this information suggests a model where RbBP5/Ash2L contributes essential residues for substrate and cofactor binding to the MLL1 active site and aids in methyltransfer. WDR5 serves as a structural platform to bridge the interaction between MLL1 and the RbBP5/Ash2L heterodimer, intergrating and orienting the complex appropriately for catalysis.

Given, one, the requirement for wild-type MLL1 in driving transformation in leukemia with MLL1 rearrangement and, two, the essential role the WRA subcomplex plays in facilitating histone methylation catalyzed by wild-type MLL1, we hypothesize that chemically interfering with recruitment of WRA to MLL1 could prove to be a promising strategy for treating leukemia with MLL1 rearrangement [43, 54, 100, 101]. In this chapter, we will functionally dissect the WDR5:MLL1 interaction and describe the development of small molecule inhibitors that target this interface. We will demonstrate a specific requirement for binding of a conserved motif within MLL1 to the Arg-binding pocket of WDR5 and then use this motif as a template for development of potent, specific, modestly cell-permeable inhibitors to the MLL1:WDR5 interaction.

Results

Development of a robust, quantitative assay for histone methyltransferase activity

In order to quantitatively evaluate the activity of the MLL1 complex, with a specific utility for inhibitor testing, we needed to first develop a practical, reproducible and quantitative assay for assessing the histone methyltransferase. In previous work, MLL1 complex activity has been tested by combining purified MLL1 complex with recombinant H3 and tritium-labelled SAM [54]. In this protocol, the reaction products are separated on an SDS-PAGE gel and incubated with radiography film to detect the ^{3}H-methyl incorporation into H3. While this method is effective for relative, qualitative assessment of MLL1 complex inhibitors, it is not suitable for quantitative evaluation of candidate MLL1 complex inhibitors or determination of IC50 values.

A quantitative, radiometric assay for histone methyltransferase activity was described where radiolabelled reaction products are precipitated onto P81 phosphocellulose paper with 20% TCA and then scintillation counted to assess histone methylation [106]. To evaluate the suitability of this technique for assaying the MLL1 complex, we TCA-precipitated a reaction mixture of H3$_{1-10}$ and tritium-labelled SAM incubated in assay buffer with, or without, the MLL1 complex, onto phosphocellulose. We also performed this assay with a 50mM sodium bicarbonate, pH 9.0, precipitation method that had recently been reported in the literature [107]. As shown in figure 2.1A, both the TCA precipitation method and the bicarbonate precipitation method yielded expected results, with no activity detectable in the absence of the MLL1 complex and robust activity in the presence of the MLL1 complex. However, the TCA precipitation method had a standard deviation 1.5-fold higher than the signal, which made it unattractive for quantitative assay development, while the bicarbonate precipitation method gave reproducible

results with low standard deviation, making it an attractive method for further, quantitative assay development.

After establishing a precipitation method, we sought to optimize the reaction conditions for the histone methyltransferase assay. The established protocol calls for 20mM HEPES pH 7.8, 5mM DTT, 0.5mM EDTA, 10% glycerol 100mM KCl. To optimize the assay, we varied the pH from 7.8 to 10.0, [KCl] from 100mM to 500mM, assay temperature from 4°C to 25°C, as shown in figure 2.1B. We observed that the MLL1 complex displayed optimum activity at 100mM KCl and increasing the concentration of salt to 200mM decreased the activity approximately 3-fold while increasing [KCl] to 500mM almost completely abolished MLL1 complex activity. We also found that the MLL1 complex exhibited 2-fold higher activity at 16° and 4°C relative to room temperature. From this data, we established assay conditions of Tris pH 8.0, 10% glycerol, 100mM KCl, 5mM DTT and 0.5mM EDTA for subsequent experiments.

As the main utility for this assay was to assess the activity of WDR5 inhibitors, we next sought to determine the proper conditions to observe maximum inhibitor function in our assay.

For inhibitor optimization, we used the compound **MM-101**, described later in this chapter. As we had previously established, the MLL1 complex exhibits optimal activity at 4°C. However, when we tested the inhibitor **MM-101** at 4°C, we observed no inhibition at concentrations where inhibition was robust at room temperature, (figure 2.1C). This data led us to conclude that inhibitor binding to the WDR5 Arg-binding pocket was temperature sensitive. We also tested the activity of the inhibitor when it was pre-incubated with the WRA subcomplex (Method 1) in the reaction mixture or added to the fully reconstituted MLL1WRA complex (Method 2). Method 1, gave an IC50 value equal to 4.2μM while method 2 gave an IC50 = 26.4μM (figure 2.1D), suggesting pre-incubation of the inhibitor was necessary to observe

optimal inhibition. This finding suggests that the kinetics of inhibitor binding may be slower than the kinetics of methyltransfer. From this data, we established assay conditions of pH 8.0, 100mM salt, 10% glycerol with reactions carried out at room temperature after pre-incubation of the inhibitor with the WRA subcomplex.

Kinetic Analysis of Histone Methylation by the MLL1 Complex

After establishing appropriate assay conditions, we set out to determine the steady-state kinetic parameters of the MLL1 complex. To establish kinetic parameters set up the reactions with varying concentrations of our substrate 10mer N-terminal H3 peptide, from 4-500μM, and quenched reactions at 4 minutes, within the linear range of MLL1 complex enzyme activity. We determined the *kcat* value for the complex, at pH 8.0, at room temperature, was 0.186/hr, while the Km was 72.0μM, as shown in figure 2.1E. The kcat/Km was 2.6×10^3 $(M^{-1}hr^{-1})$. For ideal enzyme assay conditions, it is optimal to have a substrate concentration that is lower than the Michaelis constant for that substrate. Based on the kinetic parameters of the MLL1 complex, we chose 50μM as the substrate concentration for our assay.

In summary, we have developed a sensitive, reproducible and quantitative assay for MLL1 complex activity. We have found that assaying the complex at equimolar amounts of all components at 0.5μM yields sufficient signal for robust inhibitor testing. We established assay conditions of pH 7.8, 10% glycerol and 100mM KCl, running the assay at room temperature. We established the kinetics of the MLL1 complex at this concentration and determined the K_D for $H3_{(1-10)}$ is 72.0 ± 23.5μM in our assay conditions. From this information, we set the concentration of $H3_{(1-10)}$ at 50μM, lower than the K_D value, for inhibitor testing. In summary, for

inhibitor testing, we used an assay buffer of tris pH 8.0, 10% glycerol, 100mM KCl; we will use concentrations of 0.5μM for all four MLL1 complex components and 50μM for H3$_{(1-10)}$.

The WIN motif of WDR5 facilitates direct interaction with MLL1 and is required for MLL1 complex activity

Previously, WDR5 has been shown to interact directly with MLL1 in *in vitro* interaction studies. The interaction between the MLL1 WIN peptide and WDR5 has also been detailed by crystallographic studies. The methyltransferase activity of MLL1 is found in the highly conserved SET domain, spanning amino acids 3829-3951. The WIN motif is found N-terminal to the SET domain, spanning residues 3762-3774 of the MLL1 protein (figure 2.2A). To validate the importance of the MLL1 WIN motif in MLL1 complex function, we generated two fragments of MLL1, MLL1^{3762}, which includes both the WIN motif and the SET domain and MLL1^{3800}, which begins at the N-terminus of the SET domain and excludes the WIN motif (figure 2.2A). We also generated an R3765A point-mutation in the MLL1^{3762} fragment to specifically examine the role of the essential Arg residue in MLL1 complex function. We then reconstituted the MLL1 complex with these three MLL1 fragments and assayed the methyltransferase activity using the liquid scintillation assay. The WIN-deficient fragment, MLL1^{3800} exhibited no detectable activity under our assay conditions, in the presence or absence of the WRA subcomplex (figure 2.2B). However, the WIN-containing fragment MLL1^{3762} exhibited robust activity in the presence of WRA but point mutation of the WIN motif Arg residue almost completely abolished this activity (figure 2.2B). This finding supports the hypothesis that the MLL1 WIN motif is essential for interaction of MLL1 with the WRA subcomplex and the WIN motif Arg3765 is crucial for mediating this interaction. This finding

32

also supports the idea that MLL1 must interact with the WRA subcomplex via direct contacts with WDR5 to function as a methyltransferase.

All studies on the MLL1 WIN:WDR5 interaction, to date, have strictly looked at this interaction *in vitro.* To determine if the MLL1 WIN:WDR5 interaction is observed and is required for MLL1:WDR5 interaction in cells, we cotransfected 293T cells with myc epitope-tagged MLL1^{3754}, either wild-type or R3765A, and flag-tagged WDR5, wild-type or with a mutation in the Arg-binding pocket, S91K. We then immunoprecipitated protein complexes using M2 agarose to precipitate the flag-tag on WDR5 and probed for the Myc tag on MLL1^{3754}. In the presence of wild-type, epitope-tagged WDR5, MLL1^{3754} was detected in the immunoprecipitation by western blotting for the myc tag (figure 2.2C). However, when we made mutations to either MLL1 Arg3765 or the WDR5 Arg-binding pocket we were no longer able to detect the MLL1^{3754} construct in the flag immmuoprecipitation (figure 2.2C). This data indicates that the Arg-based WIN:WDR5 interaction described in multiple *in vitro* studies is also required for the interaction of WDR5 and MLL1 in cells.

As MLL1 is a member of a highly conserved family of proteins, including MLL1-4, SET1A and SET1B, we next sought to determine if the remaining MLL family members interacted with the WRA complex through the same binding mode. In all human MLL family members, the Win Arg residue is strictly conserved, as was the N' Ala residue [90]. However, in MLL2 and 3, the C' Ala is replaced with a Ser residue. In a recent paper, the WIN peptide of MLL1 was shown to associate with WDR5 with a K$_D$ value approximately equal to 2.8μM while the K$_D$ values for the interaction of the MLL2, 3 and 4 WIN peptides with WDR5 were found to be approximately 30-50–fold lower [108]. WIN peptides from the final two human MLL family members, SET1A and SET1B also were able to interact with WDR5, and the K$_D$ values for this

interaction were 10-25-fold stronger than the MLL1 WIN peptide[108]. This indicates that not only are other MLL family members capable of interacting with WDR5 by the same mode as MLL1, but the other family members may interact with WDR5 significantly more robustly than MLL1.

To test the functional significance of WDR5 interaction in the other MLL family complexes, we reconstituted MLL1, 2, 3, 4 and SET1A with either the WRA subcomplex, or the RbBP5/Ash2L heterodimer, hereafter referred to as RA, and assayed the histone methyltransferase activity (figure 2.3A). As expected, MLL1 displayed robust activity in the presence of WRA, but in the absence of WDR5, negligible activity was detected. Unexpectedly, all other MLL family members tested showed similar levels of methyltransferase activity, whether or not WDR5 was present in the reaction (figure 2.3A).

In work from our lab, and others, it was observed that the RbBP5/Ash2L heterodimer displays intrinisic low levels of methyltransferase activity, as well as substrate and cofactor binding capabilities [99, 100]. From this information, we reasoned that RbBP5 and Ash2L cooperate with MLL1 to efficiently bind both substrate and cofactor and catalyze methytransfer. Originally, we had hypothesized that WDR5 functioned by interacting directly with both MLL and RbBP5 to integrate and orient the heterodimer in relation to MLL to facilitate methylation. While our data for the MLL1 complex supports this model, the non-requirement for WDR5 observed in the MLL2, 3, 4 and SET1A complexes, suggests that these complexes may use an alternative mechanism for assembly and catalysis than the WDR5-dependent mechanism used by MLL1. We considered two possibilities (1) MLL2, 3, 4 and SET1A do not interact directly with WDR5 and (2) MLL2, 3, 4 and SET1A can interact with WDR5, but this interaction is not required to recruit RbBP5/Ash2L to the complex. The first hypothesis was dismissed based on

the findings that all MLL family WIN peptides interact with WDR5. To test the second hypothesis, we generated GST-tagged fragments of MLL1 and MLL3 that spanned the Win motif and the catalytic SET domain through the C-terminus. We then perfomed GST pulldown experiments with WRA or RA and probed for WDR5, RbBP5 and GST by western blotting (figure 2.3B). We found that at equimolar protein concentrations of 2.5μM, GST-MLL1$^{3762\text{-}C'}$ efficiently pulled down RbBP5 in the presence of WDR5, but could not pull down RbBP5 in the absence of WDR5. This supports our hypothesis that MLL1 depends on WDR5 for complex assembly and activity. However, when we repeated the pulldown experiment with GST-MLL3^{4703}, we found that RbBP5 associates strongly with MLL3 in the absence of WDR5. This suggests a mechanism by which the remaining MLL family members can bypass the requirement for WDR5 in complex formation. More studies would be needed to fully explore the role of WDR5 in other MLL family complexes, as most studies to date have reported that WDR5 is a part of these complexes. However, the conclusion to be drawn from these experiments is that MLL1 is unique amongst the human MLL1 family members in that it requires a direct interaction with WDR5 to assemble with the WRA complex and efficiently catalyze histone methylation. An alternate possibility is that the MLL1:RbBPR5/Ash2L direct interaction is also present, but weaker than the interaction between MLL3 and RbBP5/Ash2L, such that it was not detected under our pulldown conditions. To test this hypothesis, binding studies on the MLL1 and MLL3 complex components, using a quantitative method such as isothermal calorimetry would be required. The data from this experiment suggests a specific mechanism by which the activity of the MLL1 complex can be specifically, chemically modulated without affecting similar methyltransferases.

In summary, we have determined that MLL1 interacts directly with WDR5 through direct contacts between the side-chain of Arg3765, found in the highly conserved Win motif, and the Arg binding pocket of WDR5. This interaction facilitates assembly of the MLL1 complex, which include RbBP5 and Ash2L in addition to MLL1 and WDR5. The MLL1 Win:WDR5 interaction is also essential for the MLL1 complex to effectively methylate histone H3 at lysine 4. The MLL Win motif is strongly conserved across the MLL family and high-affinity interactions between Win peptides derived from MLL2, 3, 4 and WDR5 have been described. Despite the conservation of the Win:WDR5 interaction across the MLL family, MLL1 is unique in its requirement for this interaction in assembling the MLL complex and catalyzing histone methylation. This suggests that the WIN:WDR5 interaction is a promising and specific target for pharmacological inhibition of MLL1 activity.

The WIN peptide inhibits MLL1 complex HMT activity

We had hypothesized that inhibiting the interaction between WDR5 and MLL1 with a small molecule inhibitor could block the interaction between WDR5 and MLL1 and impair MLL1 complex activity. To test this theory, we assayed the MLL1 complex in the presence and absence of excess amounts of a 7-residue MLL1 WIN peptide and qualitatively assessed the effects on MLL1 complex activity by radiography (figure 2.4). As shown in figure 2.4, a robust methylation signal is observed when the MLL1 complex is combined with recombinant H3 and ^{3}H-SAM. However, addition of 3.0mM of a 7mer WIN peptide almost completely abolishes the signal under these assay conditions. This data shows that competitive inhibition of the MLL1 WIN:WDR5 interaction is an effective strategy for interfering with MLL1 complex activity.

This finding also suggests that the MLL1 WIN peptide is a good starting place for inhibitor development for a MLL1 HMT inhibitor.

Ac-ARA-NH₂ is the minimal motif required for binding to WDR5

In order to develop a small, drug-like inhibitor to the WDR5 Arg-binding pocket, we first needed to identify the minimal requirements for peptide binding to WDR5. We employed an optimized fluorescence polarization (FP) assay to test the ability of peptides to disrupt the interaction between WDR5 and a fluorescent-labeled WIN peptide tracer. Starting with the 12 amino acid WIN sequence, Ac-GSARAEVHLRKS-NH$_2$, we systematically truncated the WIN peptide and tested the ability of shorter WIN-derived peptides to interact with WDR5 in this assay. The numbering scheme for the amino acids in the WIN peptide is shown in Table 2.1 for convenient reference. Unless otherwise indicated, all peptides were capped with an acetyl group at the N-terminus and an amide group at the C-terminus. We began by truncating the residues N-terminal to the critical Arg residue and measuring binding with our optimized fluorescence polarization assay. The Ki value for binding of the WIN 12mer to WDR5 was 0.16 μM, in good agreement with the Ki of 0.12μM reported by Patel et al (Table 2.2) [90]. Truncation of this peptide by removal of the N-terminal Gly residue did not significantly impact the binding affinity; the Ki for this peptide was 0.20μM. Interestingly, replacement of the N-terminal acetyl with an amide group, improved binding by a factor of 10. However, removal of the N-terminal Ser to create a 10mer peptide increased binding approximately 50-fold, Ki = 0.003μM. Further N-terminal truncation of WIN by removal of the Ala at +1, reduced binding 2000-fold relative to the 10mer Win peptide suggesting that's Ac-AR- is the minimal sequence needed on the N-terminal side of Arg3765 for effective binding of the peptide to WDR5.

Next, we sought to determine the residues needed on the C-terminus of the Arg residue for effective binding. Starting from the 10mer, Ac-ARAEVHLRKS-NH$_2$, we began by removing the RKS-NH$_2$ sequence at the end of the sequence as these residues are disordered in the crystal structure. The 7mer peptide resulting from this truncation had a Ki = 0.03; while this interaction affinity is 10-fold weaker than the Ki of the10-mer peptide, it is still 5-fold higher than the Ki of the original 12-mer (Table 2.2). This indicates that while the RKS motif stabilizes binding of the WIN-peptide to WDR5, the contacts that these residues form with the protein are not essential for binding. Further C-terminal truncations, down to the 3mer Ac-ARA-NH$_2$ sequence, slightly decreased binding from the 7mer peptide, but not more than the original 12mer peptide. However removal of the C-terminal Ala residue at position +3, reduced binding approximately 200-fold demonstrating the essential role for this residue in binding. This indicates that the Ac-ARA-NH$_2$ sequence is the minimal sequence required for binding to the WDR5 Arg binding pocket (Table 2.2).

Intramolecular hydrogen-bonding is essential for maintaining the appropriate conformation for peptide binding to the Arg-binding pocket

In structural studies of the WIN:WDR5 interaction, two main-chain hydrogen bonds were identified that facilitate a 3_{10} helical secondary structure which is thought to contribute to binding to WDR5. To investigate the role of these hydrogen bonds, depicted in figure 2.6, we made modifications to the chemical groups involved in hydrogen bonding and tested the affinity of these peptides for WDR5 in our assay (Table 2.3). First, we disrupted hydrogen bond #1, by changing the N-terminal acetyl group on both the 3mer and 10mer peptides, described previously. In both cases, the acetyl-to-amide modification, which abolishes hydrogen bonding

with the main-chain Ala3 amide, and reduces binding over 1000-fold. The same effect was observed when the amide hydrogen in Ala3 that participates in this interaction was changed to a methyl group. This indicates that this intramolecular hydrogen bond is essential for establishing the appropriate conformation for binding to WDR5. In order to probe the role of the second hydrogen bond, we made mono- and di-methylated versions of the C-terminal amide. The mono-methylated peptide was able to hydrogen bond and thus maintained a Ki value, 0.15μM, close to that of the 3mer peptide. The dimethylated peptide, Ac-ARA-N(Me)$_2$ was unable to hydrogen bond with the Ala1 carbonyl and had a 50-fold reduced binding affinity relative to Ac-ARA-NH$_2$. While this was a significant reduction in binding affinity, it was not as dramatic an effect as disruption of the first intramolecular hydrogen bond. This indicates that the second hydrogen bond is less essential to maintaining the optimal conformation of WIN for binding to WDR5.

H3 peptides are less potent binders of WDR5 than WIN due to deficiencies in main-chain hydrogen bond formation

WDR5 was originally identified to be a histone H3 binding protein and was postulated to function by binding to the H3 tail and "presenting" it for methylation by the MLL1 complex. However, it was found that the MLL1 WIN peptide can bind to WDR5 with ~150-fold higher affinity than the histone peptide, casting doubt on this model for WDR5 function. Our studies, which show that the N-terminal acetyl-group plays an essential role in peptide binding to WDR5 suggest that the discrepancy between H3 and WIN binding may be due to the presence of the N-terminal acetyl moiety on the latter peptide, but not the former. To test this theory, we examined the binding of the 10mer histone peptide, or a 3mer histone-derived ART peptide, with either the

standard N-terminal amide group, or an acetyl group. In both cases, replacement of the amide with the acetyl, improved binding over 10,000-fold, to better than the WIN peptides of corresponding length (Figure 2.5, Table 2.4). This allows us to draw two conclusions (1) the lack of the N-terminal acetyl on the histone tail impairs its ability to form main-chain hydrogen bonds and thus adopt the appropriate conformation for binding to WDR5 and (2) the Thr side chain at +3 improves binding relative to the Ala side chain, suggesting a method to improve the Ac-ARA-NH$_2$ affinity for WDR5.

Modifications of the Ac-ARA-NH$_2$ residues identified binding requirements of the WDR5 binding pocket and yielded inhibitors with Ki <1nM

After we had determined that Ac-ARA-NH$_2$ was the minimum sequence needed for robust binding to WDR5 we used the published crystal structures to predict a model for binding of this peptide into the WDR5 Arg-binding pocket. We further divided the WDR5 Arg-binding pocket into 5 sub-pockets, identified as pockets P1-5 in figure 2.7. The methyl side-chain of Ala1 residue protrudes into a small pocket formed by WDR5 residues Tyr131 and Phe149 and designated P1 in figure 2.7. To determine what chemical groups could interact optimally with this pocket, we made modifications to the Ala 1 residue in Ac-ARA-NH$_2$ and tested the binding of these peptides in the competitive fluorescence polarization assay (Table 2.5). First, we changed Ala1 to Gly **(1a)** to determine if reducing the side-chain would improve or decrease binding. Mutation of Ala1 to Gly reduces the Ki of binding from 0.12μM to 16.7μM, which is an approximately 130-fold reduction in binding affinity. This suggests that the small methyl side chain on Ala1 makes important contacts with the P1 pocket, which are necessary for robust binding to WDR5. We then sought to explore the size requirements of the P1 pocket by

mutating the Ala1 side-chain to different small, aliphatic residues. Mutation of Ala1 to Val **(1c)** -which has a side-chain isopropyl group, or Abu (2-amino butyric acid) **(1b)** , which has an ethyl side chain, improves the Ki to 0.06μM and 0.05μM, respectively. However, when we increased the size of the side-chain by replacing Ala1 with Leu **(1e)**, binding dropped 20-fold. This indicates that the small P1 pocket is permissive of small aliphatics such as methyl, isopropyl or ethyl, but larger groups, like the isobutyl side-chain of Leu, are not tolerated at this position. We also modified the Ala to cyclohexylgycine, and observed a 5-fold reduction in binding affinity, further supporting the hypothesis that side-chains larger than isopropyl or ethyl sterically hinder interactions with the P1 pocket. To test the electrostatic nature of the P1 pocket, we replaced the Ala1 methyl side chain with small, polar residues, Ser **(1i)** and Thr **(1j)**; these mutations reduced the binding affinity of the peptide 5-fold relative to Ala. Both the polar aromatic His **(1g)** residue and non-polar aromatic Phe **(1h)** residue at the 1 position decreased binding relative to Ala by factors of 3x and 6x, respectively, in support of the idea that P1 is only permissive of small aliphatic groups, such as methyl, isopropyl and ethyl. Systematic modification of the Ala1 position revealed that the side-chain methyl of Ala1 forms important contacts with the small P1 pocket that are essential for strong peptide binding to WDR5. Binding can be slightly improved by changing Ala1 to a residue with a slightly larger, aliphatic side-chain, such as Val or Abu. However, increasing the size of the side-chain beyond isopropyl or ethyl, or adding in a larger cyclic or aromatic side chain is not well tolerated at this position. Furthermore, small, charged residues destabilize binding approximately 5-fold, demonstrating the hydrophobic nature of the P1 pocket.

After determining the requirements for WDR5 binding at the Ala1 position, we systematically modified the Arg2 residue. In previous crystallographic studies as well as our

predicted binding model, the Arg side chain has been demonstrated to insert into the central channel of WDR5, making multiple contacts with residues lining this channel, in what we refer to as the P2 pocket[89, 95-98]. The guanido group of Arg2 forms cation-π interactions between its ω-nitrogens and the aromatic side-chains of Phe133 and Phe266. These nitrogens also form water-mediated hydrogen bonds with the Ser175 and Ser218 side-chain hydroxyls as well as a hydrogen bond with the Ser91 and Cys261 main chain carbonyls. To determine the requirements of this binding pocket, we first altered the Arg2 residue to Norleucine to remove the guanido group and replace it with a methyl (Table 2.5). As expected, this modification led to a complete loss of binding in our assay as it resulted in the loss of multiple different interactions between the P2 pocket and the side-chain. We also made more minimal changes; we changed the Arg2 residue to ornithine, which replaced the guanido with an amide group. This modification also resulted in a complete loss of binding in our assay. We changed the Arg2 residue to the other, natural, nitrogen-containing amino acid, lysine, and observed the same loss of binding. Finally, replacement of the guanido with a urea group also completely disrupted binding. These mutations support the strict requirement for Arg in binding to WDR5.

The Ala3 methyl is predicted to interact with the side-chains of A47 and L321 in the small L4 pocket. As with the Ala1 position, changing Ala3 to Gly substantially decreases binding, approximately 20-fold, showing again that the Ala3 residue also makes essential contacts for WDR5 binding (Table 2.5). As with Ala1, we began our serial modification studies by replacing the Ala3 methyl with other small aliphatic groups, including ethyl (**3b**) and isopropyl (**3c**); both of these modifications substantially improved binding by a factor of 6-10-fold. This indicates that the contacts made between the Ala3 methyl and the P4 pocket, are not optimal and improved contacts can be made by subtly increasing the size of the side-chain.

However, changing Ala to Leu (**3e**) decreases the binding affinity of the peptide by a factor of 60, indicating that the isobutyl group clashes with the P4 pocket and disrupts binding. The effect of replacing the methyl side chain with the larger cyclic groups, cyclohexylglycine (**3f**) or phenyl (**3g**), is even more dramatic and results in a 500-fold reduction in binding affinity relative to the ARA peptide. Interestingly, while mutating the Ala3 position to the charged Ser residue results in a subtle 3-4-fold decrease in binding, mutation to the branched, charged Thr residue actually improves binding 6-fold. This indicates that part of the P4 pocket can accommodate, and even preferentially bind a charged residue. Finally, changing Ala3 to the large, changed Glu residue (**3j**), as expected, completely abolishes binding in our assay. This data gives us a starting point to improve binding of the ARA peptide to WDR5, by mutating the Ala3 residue to small non-polar or charged residues.

To further explore the binding requirements of the P1 and P4 pockets, we tested the binding of 3mer peptidomimetics with a variety of different small aliphatic groups at the +1 and +3 positions in our assay. To improve binding to the P1 pocket, we started with the Ac-ARV-NH₂ peptide, and added different groups to the R1 and R2 (not to be confused with Arg2) positions on the Ala1 Cα carbon, as shown in Table 2.6. We began by replacing Ala with amino acids that have other small aliphatic side chains, *tert*-leucine (**4g**) and norvaline (**4h**). With these modifications, we observed only a slight, 2-fold, decrease in binding affinity. Modification of Ala to an amino acid with small cyclic side chains, cyclopentylglycine (**4i**) or phenylglycine (**4j**) significantly reduces the binding affinity by 15-fold and 50-fold, respectively. Changing the chirality of phenylglycine by putting the phenyl group at the R2 position instead of R1 decreases the binding affinity 10-fold further. Next, we tested the addition of a second group at the R2 position of the Ala residue (**4e**) and observed a 10-fold increase in binding affinity, suggesting

the formation of new contacts between the second methyl group and the P1 pocket. To further probe these contacts, we generated constrained cyclic molecules with 2, 3, 4 and 5-carbon linkers between the R1 and R2 position of Cα. The 2-carbon cyclopropyl (**4a**) decreased binding of the peptide by 3-fold, relative to ARV. However, the 3-carbon cyclovaline (**4b**) improved binding 10-fold relative to the ARV peptide and the 4- and 5-carbon cyclics (**4c**, **4d**). In summary, addition of two methyl groups to the R1 and R2 positions or addition of a 3 carbon linker between these positions improves peptide binding 10-fold relative to ARV. We made similar modifications to the VRA peptide to test the binding requirements of the P4 pocket, summarized in Table 2.7. Only the addition of a 4-carbon linker between R1 and R2, cycloleucine (**5c**), improved binding appreciably, approximately 3-fold. All other modifications tested at the Ala3 position decreased binding by at least 10-fold.

We then combined our findings from the mutagenesis of Ala1 and Ala3 and made peptides with multiple modifications to assess the combinatorial effect on binding of these modifications, as shown in Table 2.8. We started with two methyl side-chains at the +1 position and tested aminobutyl (**6a**), cycloleucine (**6b**) or threonine (**6c**) at the +3 position and compared the binding affinity of these peptides relative to the ARA peptide. Both **6a** and **6c** had binding affinities of less than 1nM, while **6b** was 15-fold better than ARA, with a Ki = 8nM. Next, we tested cyclovaline at the +1 position in combination with the same three amino acids at the +3 position (**6d, 6e, 6f**). The peptide (**6d**) with cyclovaline at +1 and aminobutyl at +3 also had a binding affinity <1nM. **6e** and **6f** had Ki values equal to 6nM and 1nM respectively, indicating these modifications improved binding significantly relatively to ARA but not as well as ARA. By replacing Ala1 and Ala3 with unnatural amino acids that have small, aliphatic side chains, we

were able to improve the binding of the WIN peptide to the WDR5 binding pocket from Ki = 120nM to less than 1nM.

WIN-mimetic inhibitors inhibit MLL1 complex methyltransferase activity

The interaction between WDR5 and MLL1 has been previously shown to be essential for MLL1 complex activity. Disrupting this interaction with excess amounts of the Win peptide can impair MLL complex activity (Figure 2.4). In order to test the ability of the WDR5 inhibitors to block complex activity, we reconstituted the MLL1 complex (MLL1, WDR5, RbBP5 and Ash2L) and assayed it under the conditions previously described with inhibitors at concentrations ranging from 0.1 to 400μM. As described by Patel et al, the K_D for the interaction between WDR5 and MLL1 is 120nM. In our fluorescence polarization assay, both WDR5 and the WIN peptide are held at concentrations below the K_D value for this interaction, as is standard for inhibitor studies; WDR5 is tested at 30nM while the WIN tracer is 4nM. In our methyltransferase assay, we had to use concentrations of WDR5 and MLL1 well above the K_D value for this interaction, 0.5μM for both, in order to achieve sufficient signal. Due to this, the IC50 values established with the methyltransferase assay are anticipated to be well above the IC50 values established with the fluorescence polarization assay.

To begin with, we chose to assay several of the 3mer peptides that were representative of the 3mers tested in the FP assay. We tested the GRA, FRA, VRA, ACitA and ARAbu peptides, which represented both different types of modifications made to the ARA backbone as well as a range of different inhibitory potencies(Figure 2.8). As in the FP assay, the GRA, FRA and ACitA peptides were the weakest inhibitors, with no inhibition observed at concentrations up to 400μM. Although GRA and FRA had lower IC50 values in the FP assay, 16.7 and 0.7μM,

respectively, this discrepancy is accounted for by the much higher protein concentrations used in the methyltransferase assay. In the fluorescence polarization assay, the VRA peptide showed improved activity over the ARA peptide, with a Ki=0.05μM compared to the Ki=0.12 μM for ARA. While, ARAbu showed 8-fold better binding to WDR5 than VRA, with Ki=0.006μM. In the methyltransferase assay, ARAbu had a 7-fold better IC50 relative to VRA showing comparable results to the FP assay. We then tested our best peptidomimetic inhibitors, **6a** and **6c**, in the methyltransferase assay. **6a** and **6c** demonstrated IC50s of 0.5μM and 0.9μM, 2-3-fold better than ARAbu, which is comparable to the results obtained from the FP assay. These results show that inhibitors of the WDR5:WIN interaction inhibit MLL1 complex methyltransferase activity and the relative potency is in good agreement with the data obtained from the FP assay. This data showed us that (1) the methyltransferase assay is a quality secondary assay to use for inhibitor development and (2) WDR5 inhibition, as expected, is a good strategy for MLL1 complex inhibition.

Addition of hydrophobic groups to the peptidomimetic improves permeability of WIN mimetic inhibitors

One disadvantage to using peptidomimetics as drug candidates is the low cellular permeability conferred by the polar amide bonds in the peptide backbone. To determine if our most potent inhibitors (**6a, 6b, 6e** and **6g**) could be used for cell-based studies, we used the parallel artificial membrane assay (PAMPA) to measure the passive diffusion permeability *in vitro* and reported the data in Table 2.8. Our data showed that all peptides tested, including ARA, have a permeability coefficiency (P_e) value <0.01 in our assay, which indicates poor cell permeability.

To improve the permeability of these compounds, we sought to add hydrophobic groups to the peptide. As shown in Figure 2.7, the N-terminus of the 3mer peptide is projected into a hydrophobic P5 pocket; we hypothesized that we could add larger hydrophobic groups to this position of this peptide to (1) make hydrophobic contacts with the P5 pocket and (2) improve permeability. As described in Table 2.9, we added aliphatic groups, isopropyl (**7a**), propyl (**7d**), butyl (**7e**) and isobutyl (**7f**) and compared the binding of these compounds to the ARA peptide. The addition of the isopropyl group at the N-terminus (**7a**) improved binding 3-fold relative to ARA, while addition of the linear propyl group (**7d**) had little effect on binding. The larger butyl (**7e**) and isobutyl (**7f**) groups impaired binding by approximately 40-fold, indicating that the larger groups impede binding. We also experimented with small cyclics, cyclopropyl (**7b**) and cyclobutyl (**7c**); the addition of the epoxide ring (**7b**) did not improve or impair binding relative to ARA, but the cyclobutyl ring (**7c**) impaired binding by a factor of 10-fold.

The C-terminal amide of Ac-ARA-NH2 is surrounded by a small hydrophobic P4 patch (Figure 2.7). We hypothesized that we could improve both binding and permeability by adding hydrophobic groups at the N-terminus to make additional contacts with the P4 patch. To test this hypothesis, we substituted the amide hydrogen with hydrophobic groups ranging from methyl up to biphenylmethyl. The majority of these modifications improved binding by factors ranging from 2- (**8b, 8d, 8e**) to 20-fold (**8g**).

As addition of biphenylmethyl improved both binding and the hydrophobicity of the peptidomimetic most dramatically, we chose to work with this modification for further studies. We generated peptidomimetics with the diethylglycine of (**4f**) at position A1 and cycloleucine from (**5c**) at position A3. We capped the peptidomimetic with isopropyl at the N-terminus, as in (**7a**) and biphenylmethyl at the C-terminus (**8g**) to generate molecule **MM-101.** We also

experimented with fluoro- and chloro-substitutions on the biphenyl methyl group (**MM-102, MM-103**). In the fluorescence polarization assay, all of these molecules had Ki < 1nM. To determine the effect these modifications had on cell permeability, we used the PAMPA assay to measure permeability and found that **MM-101** and **MM-102** had improved permeability over compounds **6a-6g**, but the permeability was still modest. We chose to proceed with functional analysis of these compounds, both in our *in vitro* biochemical studies and selected cell-based studies.

To confirm that the binding mode of the heavily-modified **MM-102** peptide was comparable to the WIN peptide, we co-crystalized **MM-102** and WDR5 and generated a structure. As shown in Figure 2.9A and B, **MM-102** binds to the WDR5 Arg binding pocket by insertion of the Arg side chain. Hydrogen bonding, as shown in Figure 2.9C and D creates the 3_{10} helix. Many of the contacts identified between the binding pocket and the MLL1 WIN peptide are identified in binding of **MM-102**. We also demonstrated the ability of **MM-102** to inhibit interaction between purified WDR5 and the MLL1^{3762} SET-domain proteins (Figure 2.2A) in a surface plasmon resonance assay. In this assay format WDR5 was able to bind the MLL1 fragment with a $K_D = 55 \pm 0.8nM$; **MM-102** inhibited this interaction with an IC50 = 20 $\pm$ 3nM. The K_D of the WDR5:MLL1 interaction was approximately 2-fold stronger than the WDR5:WIN interaction reported in the fluorescence polarization assay. This, minor, discrepancy may be due to slight differences in the assay format, assay buffers or additional contacts formed by the larger MLL1^{3762} protein with WDR5. Despite the slightly improved binding, **MM-102** was able to disrupt the interaction between the two proteins, with a low nanomolar IC50 value. This data demonstrates that the inhibitor, MM-102 can potently bind the Arg-binding pocket of WDR5 and block its interaction with the MLL1 protein.

Cyclization of MLL1 Peptidomimetics constrains structure to enhance hydrophobicity and improve binding

To further improve permeability and enhance binding, we experimented with cyclizing the peptides using carbon linkers of 4-6 carbon length. We hypothesized that this would enhance the hydrophobicity through addition of alkyl groups, improve protease resistance and improve binding to WDR5 by constraining the peptide in a 3_{10} helical conformation that is optimal for binding. The binding of cyclized peptidomimstic, **MM-401** to WDR5 in the FP assay was comparable to the **MM-101** and **MM-102** compounds and the permeability was slightly improved.

Discussion

WDR5 is a conserved protein with essential functions in developmental gene regulation [94]. WDR5 has been identified in complex with MLL family members, MLL1, 2, 3 and 4, as well as other proteins with functions in gene regulation. WDR5 disruption has been demonstrated to impair expression of MLL1 targets *HoxA9, HoxC8* and *Meis1* as well as retinoic-acid-induction of MLL3/4 targets, which shows that it has an essential function in other MLL family complexes, as well[55]. Biochemical and genetic studies were carried out to attempt to determine the function of WDR5 in the MLL family complexes.

Initial work on WDR5 suggested that WDR5 functioned in complex with MLL family members to bind the histone tail and "present" it to the associated MLL for efficient histone methylation[94]. This interaction is accomplished by insertion of the Arg2 side chain of histone 3 in a conserved arginine-binding pocket of WDR5. This hypothesis was developed based on

findings that (1) the histone H3 tail peptide pulled down WDR5 in a GST pulldown study (2) WDR5 co-crystalized with an H3 tail peptide and bound it with an affinity of approximately 10μM in ITC and SPR binding studies and (3) knockdown of WDR5 impaired H3K4 methylation at and expression of key *MLL1* gene targets[94]. However, this hypothesis was called into question by data demonstrating a high-affinity interaction between a conserved motif in MLL1 and the WDR5 binding pocket that was previously reported to bind H3. This interaction had a reported K_D of 120nM in sedimentation studies and was demonstrated to be essential for WDR5:MLL1 interaction *in vitro*[90]. Despite the approximately 50-fold higher affinity for MLL1 than H3, there has still been debate about the substrate specificity of the WDR5 Arg binding pocket, in part, based on the fact that the nuclear concentration of the H3 tail is expected to be significantly higher than the nuclear concentration of MLL1. While the relative amounts of these proteins have not been specifically quantified, the histones are some of the most abundant cellular proteins.

In order to resolve the issue of substrate specificity for WDR5, we performed a co-immunoprecipitation with WDR5 and a C-terminal fragment of MLL1 that contained both the SET domain and the reported WDR5 interaction motif. We made mutations to both the essential Arg residue in the WIN motif of MLL1 and the Arg-binding and found that disrupting either abolished the ability of these two proteins to interact in cells. While this does not rule out the possibility that WDR5 interacts with H3, it does clearly demonstrate that MLL1 must interact with WDR5 through the Arg binding pocket in order for the MLL1 complex to assemble. In further support of this notion, GST pulldown of the MLL1 complex demonstrated that in the absence of WDR5, MLL1 cannot interact with RbBP5/Ash2L either. MLL1 has been shown previously to require association with the remaining core complex components to catalyze

histone methylation efficiently. To determine the specific role of the MLL1 WIN:WDR5 role in histone methylation, we tested the activity of the MLL1 SET domain with no WIN motif, an intact WIN motif or a WIN motif with a point mutation of the critical Arg residue. We found that without the wild-type WIN motif, MLL1 could not catalyze detectable levels of histone methylation, even in the presence of the remaining complex components. This finding further supports the notion that, at least in the MLL1 complex, the WDR5 Arg binding pocket functions to bind MLL1, nucleating assembly of the complete MLL1WRA complex for histone methylation. While there is still a possibility for some sort of dynamic association between WDR5 and both MLL1 and H3, it seems unlikely given the both requirement for all complex members in regulating expression of MLL1 target *Hox* genes, and the essential role WDR5 play in assembling the MLL1 complex. Based on these findings, we hypothesize that in the context of the MLL1 complex, WDR5 functions as an essential structural platform to construct the multiprotein complex. We further postulate that the Arg-binding pocket of WDR5 plays a needed function in complex assembly and is likely not important for direct histone binding.

The essential role that a structural, non-catalytic protein plays in contributing to enzyme activity highlights another compelling of MLL1 function and regulation. That is, MLL1 has a conserved SET domain, with all sequence motifs that have been found to be essential for catalyzing histone methylation conserved in this domain[75]. However, despite the conservation of these elements, MLL1 possesses negligible methyltransferase activity unless associated with WDR5, RbBP5 and Ash2L (figure 2.2B) [90]. Furthermore, even association of the remaining complex proteins confers relatively weak methyltransferase activity to the complex, based on the catalytic parameters reported in this chapter. Of the human histone methyltransferases with reported kinetic parameters, MLL1 is by far the weakest enzyme, with a catalytic efficiency

(*kcat/Km*) that is 3-4 orders of magnitude lower than other methyltransferases SET7/9, SUV39H1 and G9A[16, 109, 110]. Of the other enzymes studied, the data on SET7/9 is most directly comparable as the buffer pH is the same in both studies and the cofactor concentration is consistent[16]. Furthermore, SET7/9 is also specific for H3K4, so both enzymes recognize the same substrate[16]. When the kinetic parameters are compared, SET7/9 is found to possess relatively similar substrate affinity with only 2.5-fold stronger binding to the H3 peptide than M1WRA. However, the catalytic turnover is approximately 350-fold slower in MLL1WRA than SET7/9 and the catalytic efficiency is 3 orders of magnitude poorer than SET7/9. This demonstrates that while MLL1 has reasonable substrate binding capacity, the rate of methyltransfer proton abstraction and subsequent methyltransfer from the cofactor to the substrate ε-nitrogen is significantly slower. A rationale for the slow rate of methyltransfer catalyzed by MLL1WRA can be found by comparing the structures of SET7/9 and MLL1. In the SET7/9 structure, the lysine side chain is bound tightly in a solvent free environment with the ε-amino nitrogen positioned at the entrance to a small, solvent restricted pore that connects to the methyl-donating cofactor[16, 111]. Methyltransfer is hypothesized to occur through this pore. In the MLL1 SET domain, the lysine side-chain is not constrained in optimal conformation for methyltransfer and is solvent-exposed[75]. The MLL1 structure hypothesized that the remaining MLL1 complex members act to move two domains of the MLL1 active site into a "closed" conformation to restrict solvent accessibility to the lysine and optimize geometry for methyltransfer. Further structural and biochemical studies would be needed to support this claim.

While this discussion offers some answers to the question of "how" MLL1 activity is stimulated by associated proteins, the question of "why" remains. The need for additional

proteins to perform its basic catalytic functions suggests that the default state for MLL1 is non-functional. This suggests that it is preferable for cellular function for MLL1 to not function, than to function promiscuously. This befits the role of MLL1 as a regulator of developmental gene function. Biologically, MLL1 has been shown to maintain expression of a small subset of *Hox* genes in stem cells and early progenitors [112]. This suggests that MLL1 activity is needed in only a few of cell types at a relatively small percentage of PolII genes to do its job. Over-stimulation of MLL1-directed gene expression, as in the case of MLL1 rearrangement, leads to transformation and leukemia [69, 113]. While deletion of the MLL1 SET domain has a relatively weak phenotype [69]. This suggests that it is better for MLL1 to be inactive than hyperactive, which gives some clue as to why MLL1 must associate with, at minimum, three additional proteins to activate its methyltransferase capabilities. Essentially, evolution is not taking any chances with MLL1 activity.

One of the more interesting findings from these studies was the information that WDR5 is not required to mediate association of MLL3 with RbBP5/Ash2L and is not essential for catalysis in the MLL2, 3, 4 or SET1A complexes. This is surprising because WDR5 has been found to interact with these complexes by immunoprecipitation and it has been demonstrated to play an important role in MLL3-dependent gene expression by knockdown[54, 55, 114]. This suggests that WDR5 may play an alternate role in the other MLL family complexes, perhaps by mediating interaction with an additional factor that is important for regulation or recruitment. Further studies would be needed to flesh out our understanding of WDR5 function in other MLL family complexes. Perhaps, the first experiment that would be needed would be a biochemical mapping of direct WDR5 interaction partners that are part of the MLL2, 3 and 4 complexes.

Understanding which proteins interface directly with this protein would give some clues as to the function of WDR5 in other complexes.

After establishing that WDR5 is essential for assembly and activity of the MLL1 complex, we sought to develop pharmacological inhibitors to WDR5 for therapeutic use in acute leukemia with MLL1 rearrangement. As no assay for histone methyltransferase activity has yet been described that is readily adaptable for high-throughput screening and there are several crystal structures of WDR5 in complex with the MLL1 WIN peptide, we chose to use rational design for inhibitor development. We began by truncating the MLL1 WIN sequence to determine the minimal motif required for binding, which was Ac-ARA-NH$_2$ (Table 2.5). We then made systematic modifications to different parts of the Ac-ARA-NH$_2$ peptide to probe the binding requirements of each individual sub-pocket in the WDR5 structure (Figure 2.7). We validated the ability of these compounds to inhibit the MLL1:WDR5 interaction using a secondary histone methyltransferase assay, which we established in this chapter, as well (Figure 2.1, 2.8). We combined the modifications, which yielded optimum binding and permeability into peptidomimetics **MM-101** and **MM-102**. We characterized the binding of MM-102 to WDR5 in a crystal structure, and assessed the ability of this compound to disrupt the interaction between the MLL1 SET domain and WDR5 by surface plasmon resonance. We then generated a cyclic derivative of **MM-101, MM-401**, that has a 4-carbon linker connecting the N- and C-termini of the peptidomimetic. **MM-401** was anticipated to have equivalent binding and improved pharmacological properties, relative to **MM-102.** We then ascertained the cell permeability of **MM-101**, **MM-102** and **MM-401** in a PAMPA assay to be sufficient for cell-based studies, going forward. This describes the rational design of a potent, cell-permeable, peptidomimetic

inhibitor to the MLL1:WDR5 interaction. Further studies will be done to determine the biological mechanism of action for these compounds.

(A)

MLL1: -- +   -- +

% Activity

2.5
2.0
1.5
1.0
0.5
0.0

☐ TCA
■ NaHCO₃

TCA   NaHCO₃

Precipitation Method

(B)

CPM

10000

5000

0

7.8 8.5 9.0 10.0

pH

CPM

6000

4000

2000

0

100mM 200mM 500mM

[KCl]

CPM

10000

5000

0

22°C 16°C 4°C

T

(C)

% Activity

100

50

0

0   1   2   3

log₁₀[MM-101]µM

● RT
■ 4°C

(D)

% Activity

100

50

0

-2 -1 0 1 2 3

log₁₀[MM-101]µM
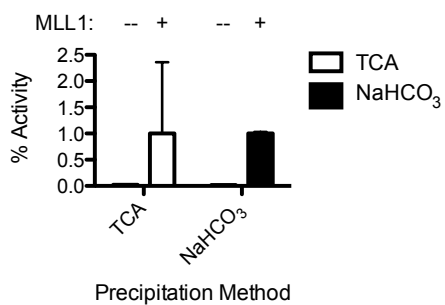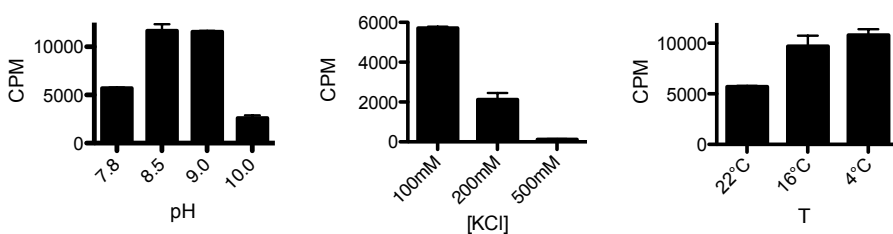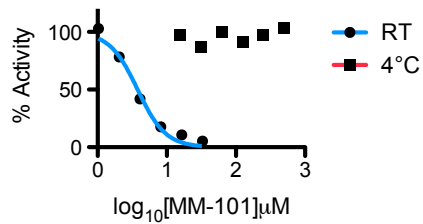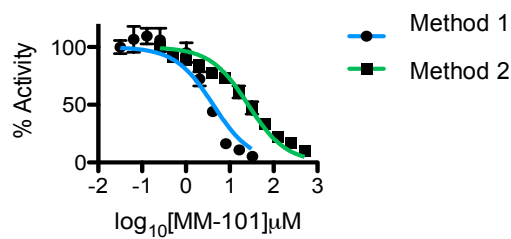
● Method 1
■ Method 2

	Method 1	Method 2
IC50	4.199	26.36

(E)

$kobs_{(min^{-1})}$

0.0015

0.0010

0.0005

0.0000

0   200   400

[H3₁₋₁₀]µM
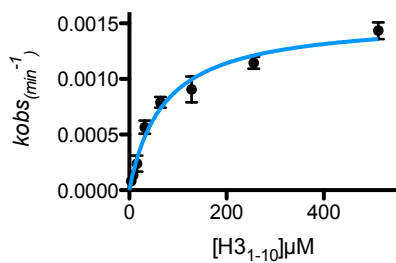
kcat (hr⁻¹)	Km(µM)	kcat/Km (M⁻¹hr⁻¹)
0.186 ± 0.02	72.010±23.448	2.58 x 10³

Figure 2.1. Optimization of a quantitative assay for MLL1 complex histone methyltransferase activity. **(A)** H3 peptide that was ^{3}H-methylated by incubation with the MLL1 complex, followed by precipitation with 20% TCA or 50mM NaHCO$_3$, pH 9.0 to establish a method for scintillation counting that could yield reproducible activity measurements. Standard deviation is determined from two experiments. **(B)** MLL1 complex activity was tested at varying [KCl], T°C and pH to determine optimal reaction conditions. Standard error calculated from two experiments. **(C)** MLL1 complex activity was tested in the presence of an inhibitor, **MM-101**, at 4°C and RT to determine the temperature dependence of WDR5 inhibitor binding. Error bars represent standard error from two replicates **(D)** MLL1 complex was assayed in the presence of **MM-101** after pre-incubation to determine the order of operations for inhibitor testing. **(E)** Steady-state kinetic analysis of the MLL1 complex at standard reaction conditions to evaluate MLL1 complex function and establish peptide concentration for inhibitor testing. Error bars represent standard error from two replicates.
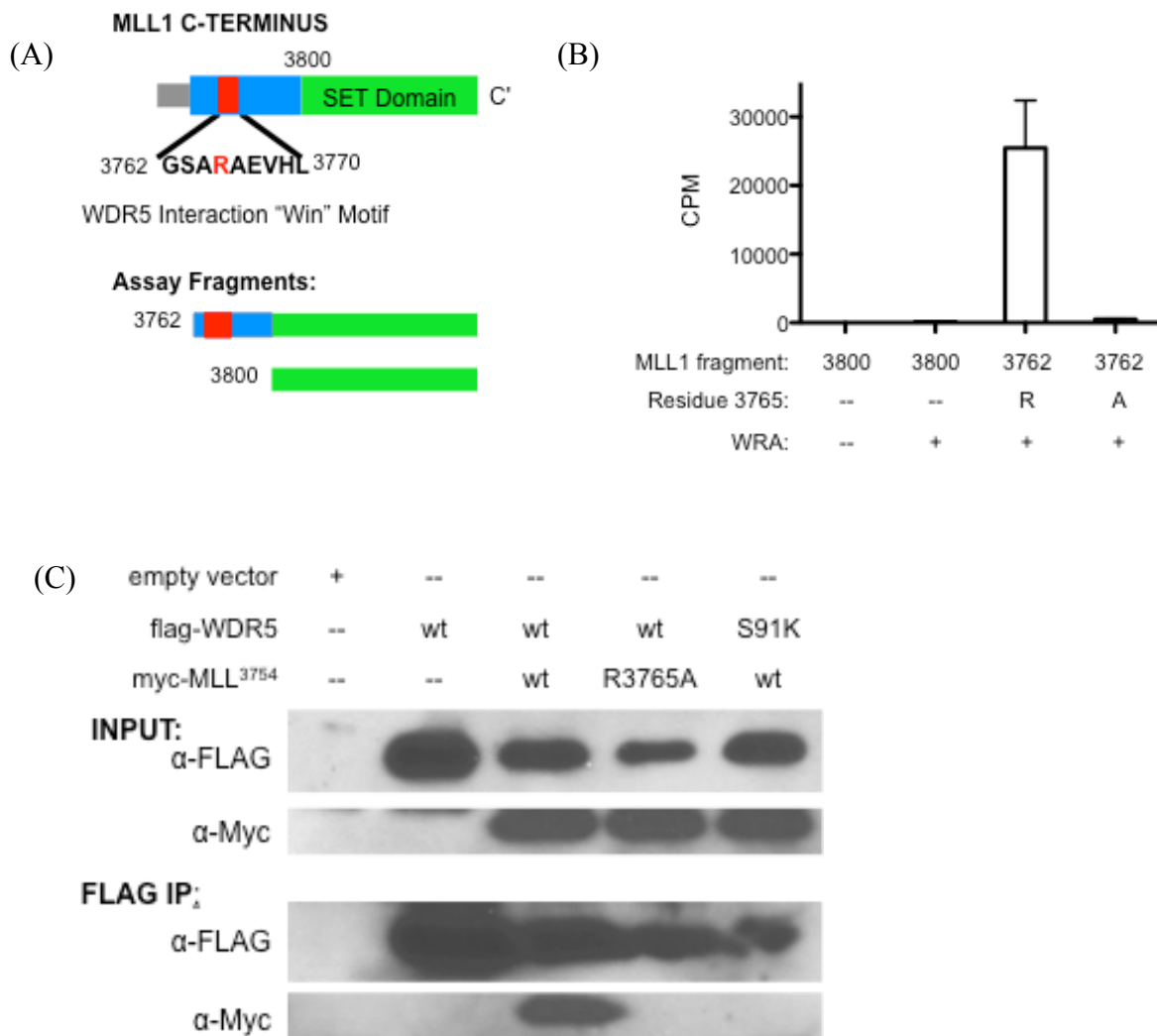
Figure 2.2. MLL1 WIN Motif interaction with the WDR5 Arg-binding pocket is essential for MLL1:WDR5 interaction and MLL1 complex activity.
(A) Schematic of MLL1 C-terminus, including SET domain and WIN motif including a depiction of the assay fragments **(B)** MLL1 activity was measured (1) without WRA, subcomplex, (2) with WRA but without WIN (3) with WRA and wild-type WIN or (4) with WRA and a point-mutant WIN motif to test the requirement for WIN in MLL1 complex activity. Error bars represent standard error from two separate experiments **(C)** MLL1, wt or R3765A, were co-expressed with epitope-tagged WDR5, wt or Arg-pocket mutant and co-precipitated to determine the requirement for the WIN:WDR5 interaction in mediating association between WDR5 and MLL1 in cells. Western results are representative of 3
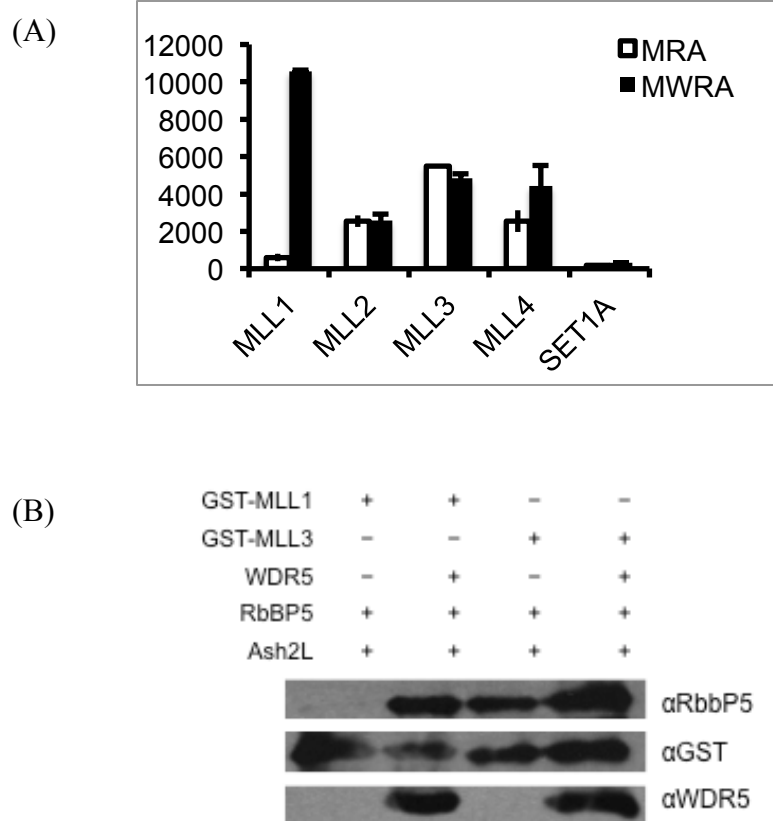
Figure 2.3. **MLL1, but not MLL2, 3 and 4, require WDR5 for mediating association with RbBP5/Ash2L and stimulating catalysis. (A**) Methyltransferase activity of MLL1-4 members, was tested in the presence of RbBP5 and Ash2L, with or without WDR5 to determine the requirement for WDR5 in the MLL family complexes. **(B)** The association of GST-MLL1^{3969} and GST-MLL3^{4703} with RbBP5/Ash2L was tested in the presence and absence of equimolar amounts of WDR5 by GST pulldown to test the requirement for WDR5 in complex formation. Western is representative of 3 experiments.
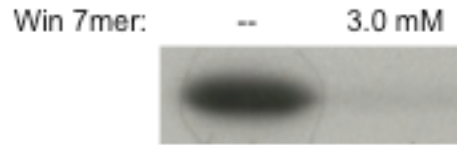
Figure 2.4. Excess WIN Peptide inhibits methylation of H3 by the MLL1 complex.
The ability of the MLL1 complex to incorporate ^{3}H-CH$_3$ into recombinant H3, in the presence or absence of the WIN peptide was analyzed by autoradiography.
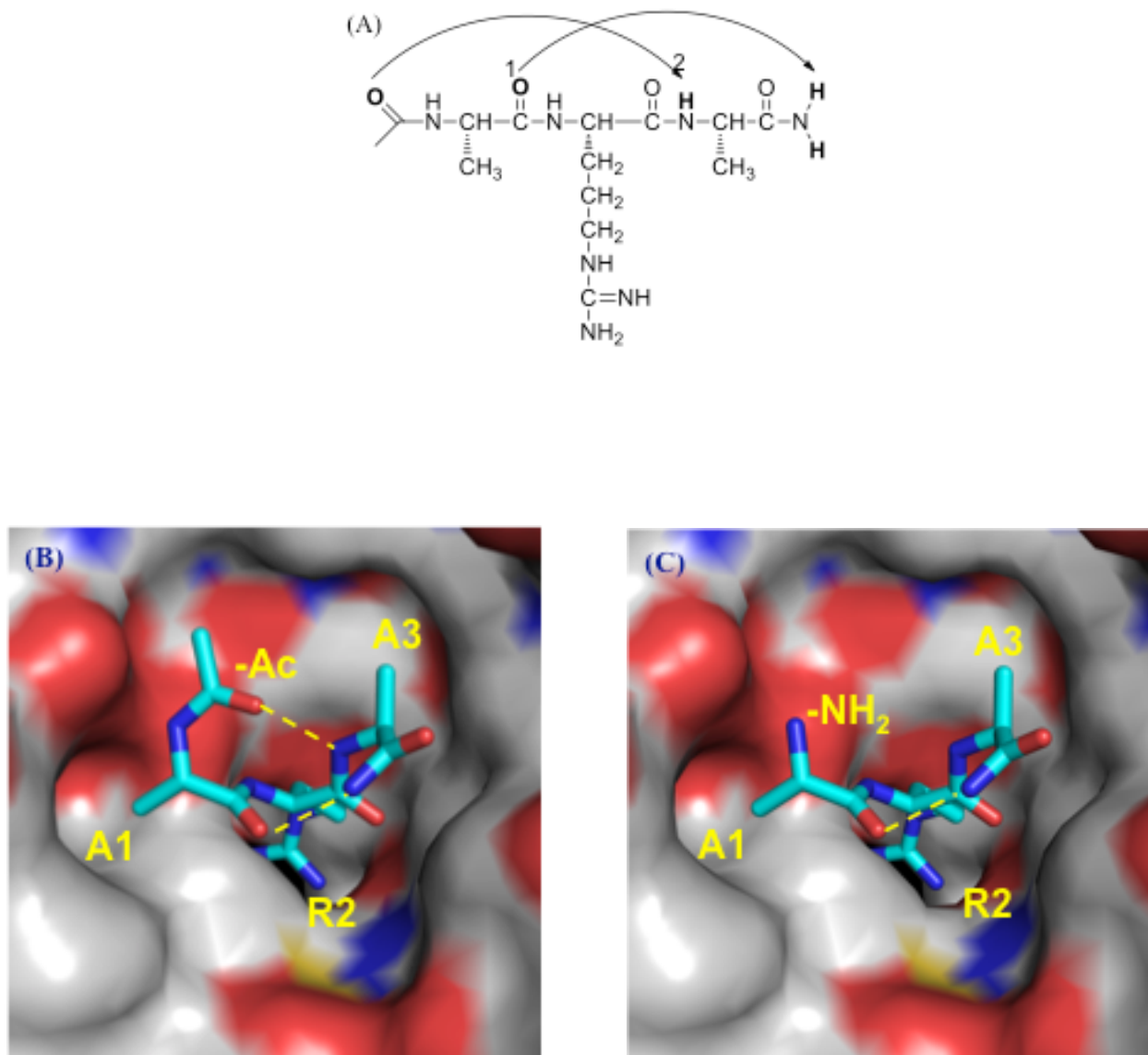
Figure 2.5. Intramolecular hydrogen bonds establish the 3_{10} helix structure of the WIN and ARA peptides and help adopt optimal conformation for binding to WDR5.
(A) Schematic of hydrogen bonds in the Ac-ARA-NH_2 peptide depcts hydrogen bond #1 between the N-terminal carbonyl and the main-chain amide on Ala3 and hydrogen bond #2 between the Ala1 carbonyl and the C-terminal amide. **(B)** Hydrogen bond #1 is shown to facilitate 3_{10} helix formation in a molecular model of Ac-ARA-NH_2 in complex with WDR5 **(C)** Hydrogen bond #1 is not formed in a molecular model of NH_2-ARA-NH_2 **.** Molecular modeling based on PDB entry 3EG6. Intramolecular hydrogen bonds are shown as yellow dots. Carbon atoms are shown in cyan in the peptide and grey in WDR5. The nitrogen and oxygen atoms are colored in blue and red, respectively. This figure was prepared by Dr. Hacer Karatas, molecular modeling was done by Dr. Denzil Bernard.

(A)

Inhibitor	IC50(µM)
ACitA	≥400µM
FRA	≥400µM
GRA	≥400µM
VRA	12.1±0.6µM
ARAbu	1.8±0.18µM
6a	0.5±0.1µM
6c	0.9±0.05µM

(B)

--   ARA   ARAbu   VRA   GRA
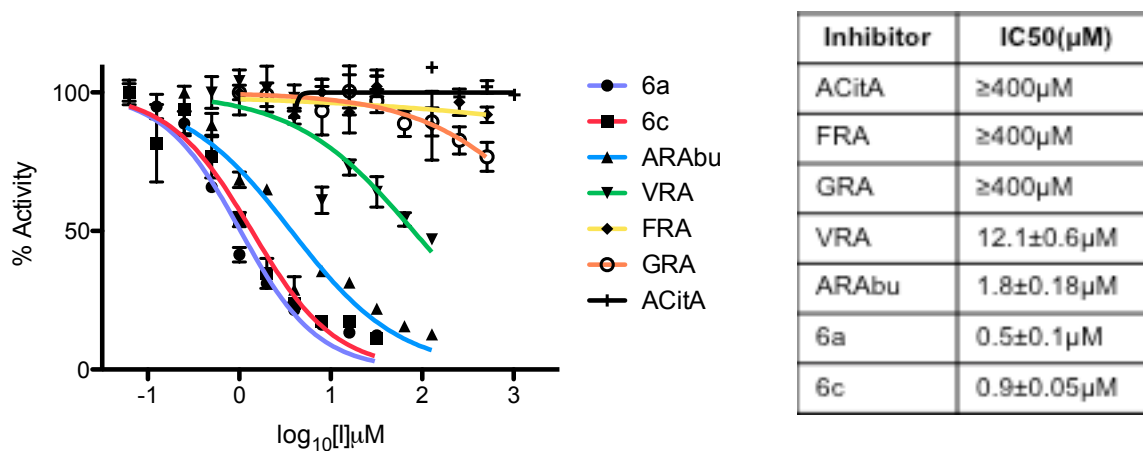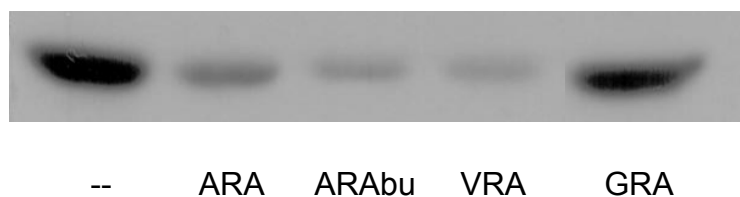
Figure 2.6. WIN-derived peptides inhibit MLL1 complex activity.
Representative WIN-derived peptides, with a wide range of activities in the fluorescence polarization assay, were selected from each step of peptide optimization and tested in the MLL1 complex activity assay and scintillation counted to test the ability of WDR5 Arg-pocket inhibitors to block MLL1 complex activity. Standard deviations were calculated from duplicate or triplicate experiments.
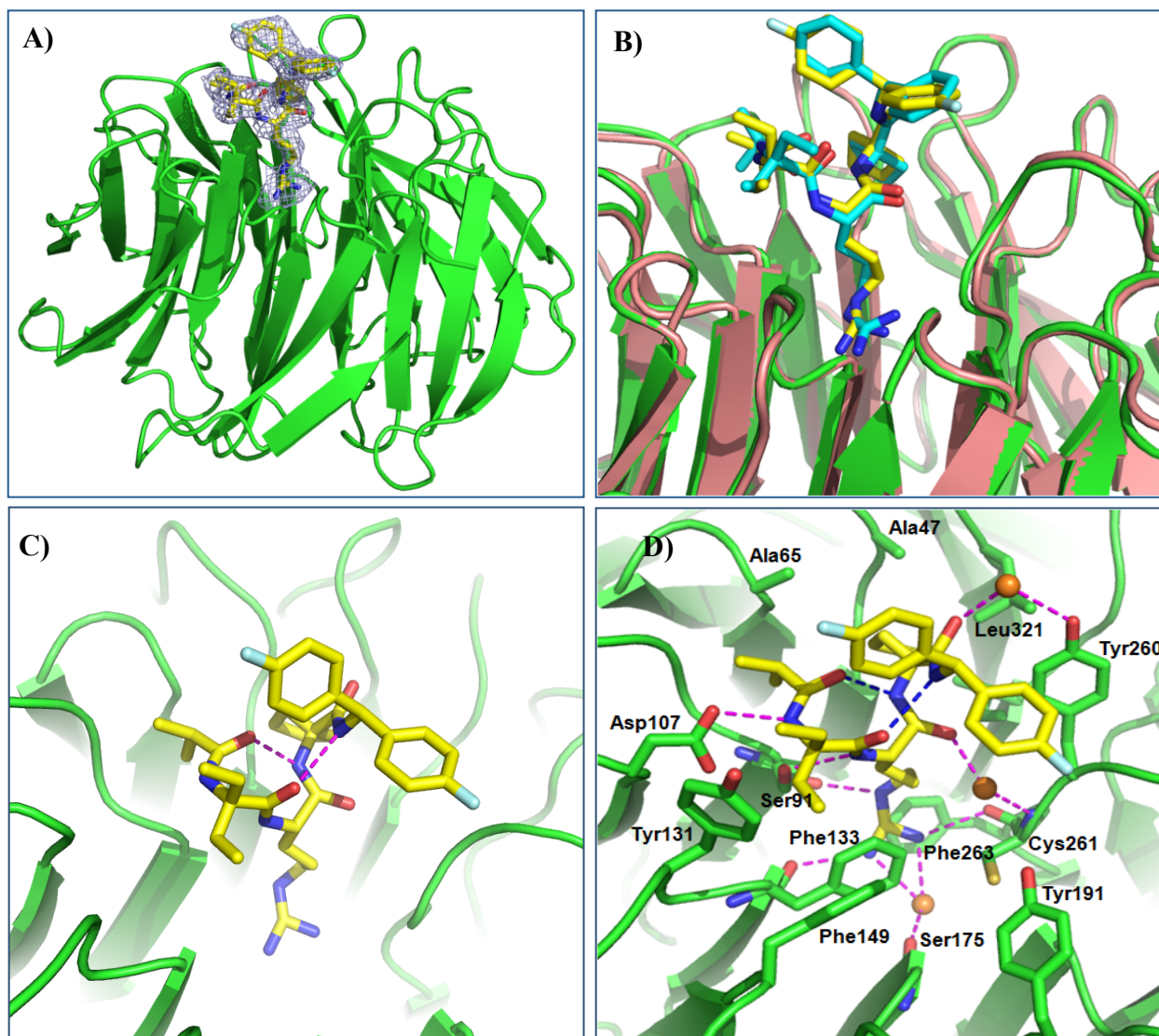
Figure 2.7. Crystal structure of WDR5-MM-102 complex.
WDR5 is colored in green and MM-102 is colored in yellow. **(A)** The electron density (2Fo-Fc) map, contoured to 1δ is shown for MM-102; **(B)** The comparison of MM-101 and MM-102 in WDR5 complexes. In WDR5-MM-101 complex, WDR5 is colored in salmon and MM-101 is in cyan; **(C)** MM-102 exhibits a 3_{10}-helical configuration. The intramolecular hydrogen bonds in MM-102 are shown in magenta dotted lines; **(D)** The interface between compound MM-102 (yellow) and WDR5 (green). MM-102 and WDR5 pack across an extensive interface, involving both hydrophobic packing and hydrogen bonds (magenta dotted lines). Intramolecular hydrogen bonds and water molecules are shown as blue dotted lines and orange spheres, respectively. Crystal structure prepared by Dr. Yong Chen.

(A)

KD (nM)= 54.5 ± 0.78

(B)
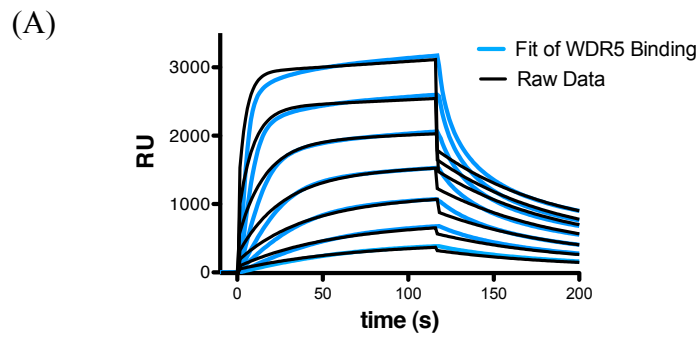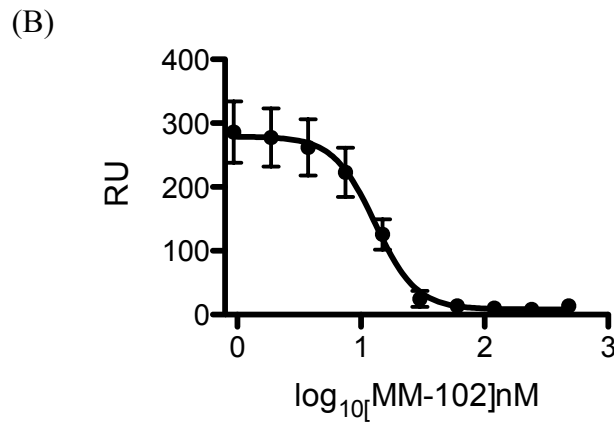
Figure 2.8. MM-102 potently disrupts the association of WDR5 with MLL1[3762] .
(A) Association between WDR5 and MLL1[3762] proteins was determined by surface plasmon resonance. K_D is representative of two separate experiments. **(B)** Ability of **MM-102** to disrupt the association between MLL1 and WDR5 proteins was tested by surface plasmon resonance, standard deviation is representative of two separate experiments.

WIN			G	S	A	R	A	E	V	H	L	R	K	S
N-term of H3					A	R	T	K	Q	T	A	R	K	S
Numbering used here			-2	-1	1	2	3	4	5	6	7	8	9	10

Table 2.1. Sequence of WIN peptide and N-term of H3 peptide. Residues 1-10 in H3 and 3762-3773 in MLL1 are shown. Numbering assigned here compares the residues in these two peptides.

Peptide	Formula	$IC_{50} \pm SD$ (μM)	$Ki \pm SD$ (μM)
WIN	Ac-GSARAEVHLRKS-NH$_2$	0.75 ± 0.10	0.16 ± 0.02
Ac-11mer	Ac-SARAEVHLRKS-NH$_2$	1.04 ± 0.14	0.20 ± 0.03
Ac-10mer	Ac-ARAEVHLRKS-NH$_2$	0.02 ± 0.004	0.003 ± 0.001
H$_2$N-11mer	H$_2$N-SARAEVHLRKS-NH$_2$	0.08 ± 0.01	0.02 ± 0.002
Ac-9mer	Ac-RAEVHLRKS-NH$_2$	29 ± 4	6.30 ± 0.80
Ac-7mer	Ac-ARAEVHL-NH$_2$	0.16 ± 0.03	0.03 ± 0.01
Ac-6mer	Ac-ARAEVH-NH$_2$	0.40 ± 0.10	0.09 ± 0.02
Ac-5mer	Ac-ARAEV-NH$_2$	0.75 ± 0.10	0.16 ± 0.03
Ac-4mer	Ac-ARAE-NH$_2$	0.40 ± 0.05	0.08 ± 0.01
Ac-3mer	Ac-ARA-NH$_2$	0.54 ± 0.03	0.12 ± 0.01
Ac-2mer	Ac-AR-NH$_2$	125 ± 6	27 ± 1.4

Table 2.2. Binding affinities of truncated MLL peptides to WDR5.
Binding affinities for peptides to WDR5 were determined by a competitive fluorescence polarization assay for this and all subsequent tables. Fluorescence polarization data in this table and all subsequent tables generated by Dr. Hacer Karatas.

Peptide	Formula	$IC_{50} \pm SD$ (µM)	$Ki \pm SD$ (µM)
Ac-10mer	Ac-ARAEVHLRKS-NH$_2$	0.02 ± 0.004	0.003 ± 0.001
H$_2$N-10mer	H$_2$N-ARAEVHLRKS-NH$_2$	34 ± 3	7.30 ± 0.70
Ac-3mer	Ac-ARA-NH$_2$	0.54 ± 0.03	0.12 ± 0.01
H$_2$N-3mer	H$_2$N-ARA-NH$_2$	> 300	ND*
CHO-3mer	CHO-ARA-NH$_2$	14.9 ± 1.4	3.20 ± 0.3
Δ1	Ac-AR-(N-Me)A-NH$_2$	> 300	ND*
Δ2a	Ac-ARA-CONHMe	0.70 ± 0.14	0.15 ± 0.03
Δ2b	Ac-ARA-CONMe$_2$	30 ± 5	6.50 ± 1.20
Δ2c	Ac-ARA-COOCH$_3$	7.30 ± 0.80	1.60 ± 0.20

* Not determined under the conditions tested.

Table 2.3. Removal of intramolecular hydrogen bonds in Ac-ARA-NH$_2$.
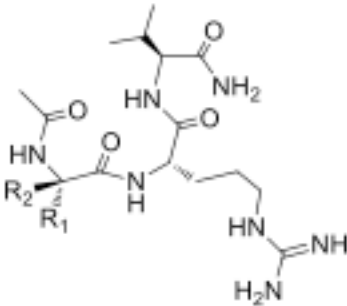
Peptide	Formula	$IC_{50} \pm SD$ (µM)	$K_i \pm SD$ (µM)
H3-10mer	H$_2$N-ARTKQTARKS-NH$_2$	70 ± 6	15.10 ± 1.30
Ac-H3-10mer	Ac-ARTKQTARKS-NH$_2$	0.006 ± 0.002	< 0.001
H3-3mer	H$_2$N-ART-NH$_2$	127 ± 12	27.30 ± 2.50
Ac-H3-3mer	Ac-ART-NH$_2$	0.08 ± 0.003	0.02 ± 0.001
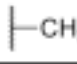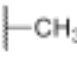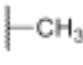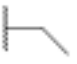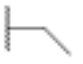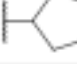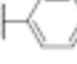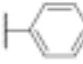
Table 2.4. H3 binding to WDR5. Binding data and peptide synthesis by Dr. Hacer Karatas.

| ARA IC_{50} = 0.54 ± 0.03 µM K_i = 0.12 ± 0.01 µM | | | | | | | | |
| A1 Modifications | | | | R2 Modifications | | | A3 Modifications | | |
Peptide		IC_{50}	K_i	Peptide		IC_{50}	K_i	Peptide		IC_{50}	K_i
1a	GRA	77.4 ± 13.2	16.7 ± 2.8	2a	ANleA	> 300	> 65	3a	ARG	10.3 ± 1.2	2.2 ± 0.3
1b	AbuRA	0.28 ± 0.02	0.06 ± 0.001	2b	AOrnA	> 300	> 65	3b	ARAbu	0.03 ± 0.008	0.006 ± 0.002
1c	VRA	0.24 ± 0.03	0.05 ± 0.005	2c	AKA	> 300	> 65	3c	ARV	0.11 ± 0.02	0.02 ± 0.003
1d	CRA	1.83 ± 0.30	0.4 ± 0.6	2d	ACitA	> 300	> 65	3d	ARC	0.08 ± 0.01	0.02 ± 0.003
1e	LRA	10.8 ± 0.40	2.3 ± 0.3					3e	ARL	34 ± 6	7.3 ± 1.2
1f	ChgRA	8.7 ± 0.60	1.9 ± 0.1					3f	ARChg	280 ± 70	61 ± 16
1g	HRA	1.7 ± 0.3	0.4 ± 0.03					3g	ARF	280 ± 40	60 ± 8
1h	FRA	3.1 ± 0.3	0.7 ± 0.07					3h	ARS	1.8 ± 0.03	0.4 ± 0.07
1i	SRA	2.9 ± 0.61	0.6 ± 0.1					3i	ART	0.08 ± 0.003	0.02 ± 0.001
1j	TRA	2.9 ± 0.4	0.6 ± 0.09					3j	ARE	> 100	> 20

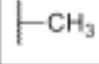2-Abu (2-amino butyric acid), Chg (cyclohexylglycine), Nle (Nor-leucine), Orn (Ornithine), Cit (citrulline)
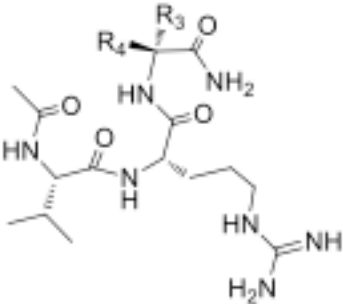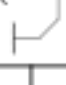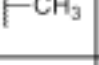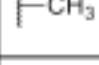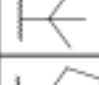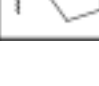
Table 2.5. Binding affinities of Ac-ARA-NH₂ analogues designed to investigate WDR5-ligand interaction through the P1, P2 and P4 sites. Binding data and peptide synthesis by Dr. Hacer Karatas.
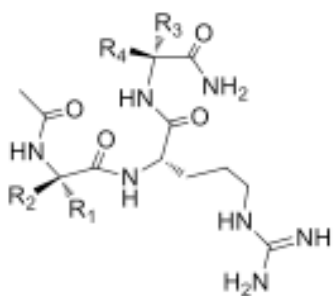
	Compound	R_1	R_2	$IC_{50} \pm SD$ (µM)	$K_i \pm SD$ (µM)
3c	ARV	—CH$_3$	-H	0.11 ± 0.02	0.02 ± 0.003
4a	ACPC-RV			0.26 ± 0.06	0.06 ± 0.013
4b	CycVal-RV			0.01 ± 0.008	0.002 ± 0.001
4c	CycLeu-RV			0.04 ± 0.003	0.009 ± 0.001
4d	homocycloLeu-RV			0.04 ± 0.01	0.007 ± 0.002
4e	α-MeAla-RV	—CH$_3$	—CH$_3$	0.01 ± 0.002	0.002 ± 0.0005
4f	Deg-RV			0.02 ± 0.01	0.004 ± 0.002
4g	Tle-RV		-H	0.18 ± 0.04	0.04 ± 0.005
4h	Nva-RV		-H	0.18 ± 0.01	0.04 ± 0.002
4i	Cpg-RV		-H	1.56 ± 0.30	0.34 ± 0.06
4j	Phg-RV		-H	5.40 ± 1.10	1.20± 0.25
4k	D-Phg-RV	-H		68 ± 4	14.6 ± 0.80
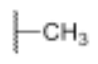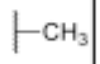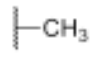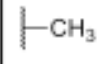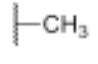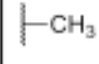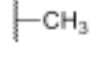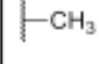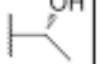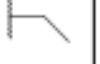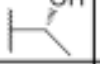
Table 2.6. Binding affinities of Ac-XRV-NH$_2$ analogues designed to further investigate the P1 pocket. Binding data and peptidomimetic synthesis by Dr. Hacer Karatas.

68

	Compound	R_3	R_4	$IC_{50} \pm SD$ (µM)	$K_i \pm SD$ (µM)
1c	VRA	-H	—CH$_3$	0.24 ± 0.03	0.05 ± 0.005
5a	VR-ACPC			2.71 ± 0.34	0.6 ± 0.07
5b	VR-CycVal			2.43 ± 0.55	0.52 ± 0.12
5c	VR-CycLeu			0.09 ± 0.01	0.018 ± 0.001
5d	VR-homocycloLeu			2.23 ± 0.67	0.48 ± 0.14
5e	VR-α-MeAla	—CH$_3$	—CH$_3$	7.44 ± 0.15	1.6 ± 0.15
5f	VR-Tle	-H		41 ± 7	8.7 ± 1.5
5g	VR-Cpg	-H		41 ± 5	8.8 ± 1.1
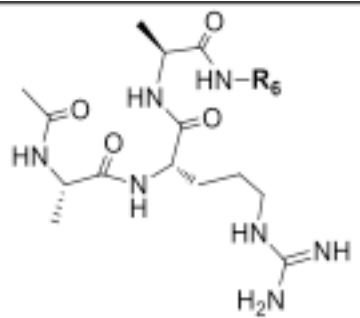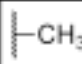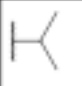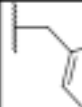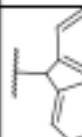
Table 2.7. Binding affinities of Ac-VRX-NH$_2$ analogues designed to further investigate the P4 pocket. Binding data and peptidomimetic synthesis by Dr. Hacer Karatas.
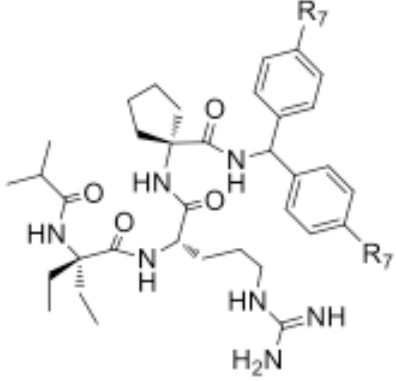
Compound	R_1	R_2	R_3	R_4	$IC_{50} \pm SD$ (nM)	$K_i \pm SD$ (nM)	P_e ($\times 10^{-6}$ cm^2/s)
ARA	—CH$_3$	-H	-H	—CH$_3$	540 ± 30	120 ± 10	< 0.01
6a	—CH$_3$	—CH$_3$	-H	(structure)	5 ± 1	< 1	< 0.01
6b	—CH$_3$	—CH$_3$	(structure)	(structure)	36 ± 5	8 ± 2	< 0.01
6c	—CH$_3$	—CH$_3$	-H	(structure, OH)	6 ± 0.4	< 1	ND*
6d	(structure)		-H	(structure)	5 ± 1	< 1	< 0.01
6e	(structure)		(structure)	(structure)	32 ± 7	6 ± 2	ND*
6f	(structure)		-H	(structure, OH)	9 ± 1	1 ± 0.3	< 0.01
6g	(structure)	(structure)	(structure)		80 ± 14	16 ± 3	< 0.01

*ND. Not Determined.
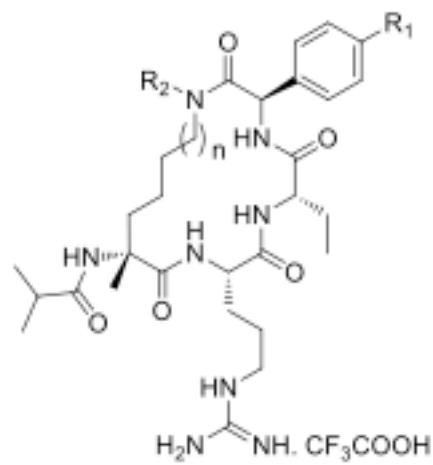
Table 2.8. Binding affinities of peptidomimetics combining favorable groups at the Ala1 and Ala3 positions. Binding data and peptidomimetic synthesis by Dr. Hacer Karatas.

70

Compound	R_6	$IC_{50} \pm SD$ (µM)	$K_i \pm SD$ (µM)
ARA	-H	0.54 ± 0.03	0.12 ± 0.01
8a	—CH₃	0.70 ± 0.14	0.15 ± 0.03
8b		0.16 ± 0.1	0.05 ± 0.01
8c		0.10 ± 0.06	0.02 ± 0.01
8d		0.28 ± 0.06	0.06 ± 0.01
8e		0.34 ± 0.08	0.06 ± 0.02
8f		0.12 ± 0.02	0.03 ± 0.004
8g		0.04 ± 0.01	0.007 ± 0.002

Table 2.9. **Binding affinities of ARA peptide analogues with C-terminal amide modifications.** Binding data and peptidomimetic synthesis by Dr. Hacer Karatas.

71

Compound	R_7	$IC_{50} \pm SD$ (nM)	K_i (nM)	P_e ($\times 10^{-6}$ cm^2/s)
MM-101	-H	2.9 ± 1.4	< 1	0.52 ± 0.14
MM-102	-F	2.4 ± 1.7	< 1	0.05 ± 0.01
MM-103	-Cl	4.5 ± 0.6	< 1	Precipitated under the assay conditions

Table 2.10. **Structures and binding affinities of MM-101 and analogs.** Binding data and peptidomimetic synthesis by Dr. Hacer Karatas.

Compound	R₁	R₂	Linker size (n+3)	Pe (10⁻⁶ cm/s)
MM-401	-H	-H	4	0.08±0.07

Table 2.11. **Structure of cyclic-derivative of MM-101.** Binding data and peptidimimetic synthesis by Dr. Hacer Karatas.

CHAPTER III

Disruption of the MLL1:WDR5 Interaction Impairs a Leukemia-Causing Epigenetic Program in Acute Leukemia with MLL1 Rearrangement

Abstract

Leukemia with MLL1 translocation is characterized by the overexpression of common gene targets of the wild-type MLL1 protein, including *HoxA9* and *Meis1*[69, 113]. In normal blood cell development, these genes play an essential role in maintaining the proliferative and self-renewal properties of hematopoietic stem cells (HSCs) and early progenitor cell types [68]. Overexpression of these genes by MLL1 fusions blocks normal differentiation and drives an abnormal program of rapid proliferation and self-renewal,that is characteristic of these leukemias. We hypothesize that interfering with the elevated expression of these genes through disruption of wild-type MLL1 activity, could prove to be an effective means to block transformation and promote cell-death of leukemias with MLL1 rearrangement. To this end, we utilized the cell-permeable MLL1:WDR5 inhibitors, developed in the previous section, and demonstrate that these compounds can specifically interfere with the enzymatic action of the MLL1 complex. We then demonstrate that these compounds can downregulate expression of *MLL1* targets in leukemia and induce differentiation and cell death.

Introduction

MLL1 translocation is found in over 70% of acute leukemias in infants (<18 months) and in 10% of AML in adults [70]. Both infant and adult leukemias with MLL1 translocation have generaly poor outcomes [70]. Leukemias with MLL1 rearrangement are characterized by elevated expression of *HoxA9* and *Meis1*. *HoxA9* and *Meis1* expression is facilitated by a set of transcription factors and cofactors, which, are recruited to these loci to activate gene expression by the MLL1 fusion protein. *HoxA9* and *Meis1* overexpression are found in other types of leukemia besides just leukemias with *MLL1* translocation. High expression of *HoxA9* is associated with 10-15% patient survival after 5 years compared to 40% survival in AML patients with low *HoxA9* expression [74]. Given the poor outcomes of patients with MLL1 translocation and/or elevated *HoxA9* expression in response to conventional therapy, it is apparent that new and improved therapies are needed to treat these leukemias.

Targeted therapy has shown promise for treatment of leukemias with BCR-ABL translocation [115]. Complete cytogenetic remission is observed in 90% of CML patients with BCR-ABL translocation, treated with the targeted ABL-kinase inhibitor, imatinib or Gleevec, after 18 months [116]. This suggests that specifically targeting the translocated protein could be a promising strategy for targeted therapy. With this in mind, we sought to explore the possibility of targeting MLL1 function for treatment of MLL1 rearranged leukemias.

The majority (over 70%) of leukemias with MLL1 translocation have been found to recruit a common set of factors that promote transcription elongation by both altering the chromatin structure to a more permissive state and directly stimulating elongation by PolII [70]. These factors act, in concert, to drive abnormal upregulation of *HoxA9* and *Meis1,* which is necessary and sufficient for leukemogenesis [117]. In MLL1 translocated leukemias, the MLL1

fusion protein recruits multiple factors, to promote transcription through multiple mechanisms. These factors include (1) transcription elongation factors, such as ELL, which facilitate promoter clearance and transcription elongation [118, 119] (2) the PolII-specific kinase and elongation factor, pTEFb, which phosphorylates PolII to promote transition to productive elongation [120], (3) the polycomb group protein, CBX8, which, in the context of these leukemias, recruits the HAT, Tip60, to create a hyperacetylated, transcriptionally-permissive chromatin environment [121] (4) Dot1L cooperates with MLL1 fusion proteins to promote transcription through H3K79 methylation at target loci [122] (5) the tumor suppressor, Menin, which is required to recruit both wild-type and translocated MLL1 to target loci in leukemia and normal gene expression [123-125] (6) wild-type MLL1, which is recruited to the *HoxA9* locus independently of the fusion protein, but must bind to promote stable binding of the fusion protein and critical epigenetic alterations at the *HoxA9* locus [43, 101]. Knockdown and rescue studies have shown that interference with any one of these mechanisms is sufficient to block transformation and promote apoptosis of leukemia cells transformed with the MLL1 fusion protein. Therefore, we hypothesize that pharmacologically interfering with any of these essential factors could impair viability of transformed cells and prove to be a useful method to treat this disease. In support of this hypothesis, two promising pre-clinical studies have been published which demonstrate that inhibiting the activity of either Menin or Dot1L, prevents leukemic gene activation and transformation [102, 103]. Both Menin and Dot1L activity are linked to activity of the wild-type MLL1 complex through recruitment and cross-talk, and thus, we hypothesize that MLL1 complex inhibition will specifically target the mechanisms driving gene-expression, transformationand proliferation of leukemias with MLL1 rearrangement.

While recruitment of wild-type MLL1 was found to be essential for changes in chromatin structure and gene expression at the *HoxA9* and *Meis1* loci, the contributions of both MLL1 H3K4 methylation activity and MLL1 complex members to epigenetic dysregulation and transformation has not been investigated. However, as H3K4 methylation is so strongly correlated with gene activation and WDR5, RbBP5 and Ash2L are necessary for H3K4 methylation byMLL1-directed H3K4 methylation, we anticipate that these proteins will be required for *HoxA9* overexpression MLL1-rearranged leukemias. Another key question is how the MLL1 complex is involved in recruitment of MLL1, wild-type and fusion, to target loci.

To test this hypothesis, we created tight-binding, cell-permeable inhibitors to the MLL1:WDR5 interaction, **MM-102** and **MM-401,** and demonstrate that these compounds could specifically interfere with both assembly and activity of the MLL1 methyltransferase complex. We then show that treating MLL1-AF9-transformed mouse leukemia cells with **MM-102** and **MM-401** specifically induces growth arrest and cell death of leukemia cells with MLL1 translocation, but does not interfere with growth of normal bone marrow. We then demonstrate that **MM-401** specifically relieves the differentiation block in MLL1-AF9 transformed cells and promotes differentiation along the myeloid lineage. Finally, we show that **MM-401** treatment blocks expression of *HoxA9* and *Meis1* in both MLL1-AF9 transformed cells and MLL1 wild-type mouse embryonic fibroblasts and downregulates MLL1 recruitment and activating chromatin modifications at these genes. The action of the MLL1:WDR5 inhibitor, **MM-401**, is consistent with the activity of previously characterized targeted therapies to MLL1 translocation leukemias and shows promise for clinical utility for treating these leukemias.

Results

MLL1 WIN peptidomimetics inhibit MLL1 complex activity

In chapter II, we describe the creation of peptidomimetic inhibtors of WDR5, **MM-101**, **MM-102**, **MM-401**. These compounds were demonstrated to have Ki values of <1nM and modest to moderate cell permeability (Table 2.10, 2.11). Further characterization of **MM-102** found that this compound binds the WDR5 Arg-binding pocket in crystallographic studies and disrupts the interaction between the MLL1 SET domain and WDR5 in a surface plasmon resonance assay. To determine if these compounds can inhibit MLL1 complex activity, we reconstituted the MLL1 complex, and tested its activity in our HMT assay at concentrations ranging from 0.03 μM to 30 μM. For **MM-101**, **MM-102** and **MM-401,** the IC50 values were 3.3μM, 0.82μM and 0.32μM, respectively, as shown in figure 3.1A. While these IC50 values are well above the Ki values for these compounds in our FP assay, they are in line with the HMT IC50 values for the previously tested compounds (Figure 2.7). These compounds compare well to the activity of compounds **6a** and **6c** in the HMT assay (Figure 2.7), which also have reported Ki values <1nM. In the PAMPA assay, the cell permeability of **MM-101** was slightly better than **MM-102** and **MM-401**, however, the IC50 value for this compound in the HMT assay is one order of magnitude lower than **MM-401** and 4-fold lower than **MM-102** (Table 2.10, 2.11). Furthemore, the PAMPA assay is generally considered to give a reasonable approximation of cell-permeability but is not a rigorous quantitative determinant of this pharmacological property. For these reasons, we chose to focus our functional studies on **MM-102** and **MM-401**.

Inhibiting the WDR5 binding pocket specifically inhibits activity of the MLL1 complex but not other SET-domain histone methyltransferases

WDR5 has been found in complex with MLL1, 2, 3 and 4. The interaction interface between MLL and WDR5 is highly conserved across the human MLL family, as described previously [90]. However, in chapter 2, we show that only the MLL1 complex requires WDR5 for methyltransferase activity and interaction with the remaining core components, RbBP5 and Ash2L. In order to determine if the specific requirement for WDR5 in MLL1 complex activity translates to specific inhibition of the MLL1 complex by our WDR5 inhibitor, we tested the activity of the MLL1, 2, 3 and 4 complexes in the presence of **MM-401** and assessed the activity of the different complexes by scintillation counting. **MM-401** inhibits the MLL1 complex with an IC50 of 0.32 ± 0.13, as shown in figure 3.1B. However, MLL2, 3, 4, in complex with WRA, were not detectably inhibited by **MM-401** at concentrations up to 250μM. This pattern of inhibition is in good agreement with our data that only MLL1, of the MLL family members, must associate with WDR5 for function.

WDR5 inhibition blocks complex assembly differentially in MLL1 and MLL3 complexes

To determine the effects of WDR5 inhibition by **MM-102** and **MM-401** on MLL family complex assembly, we performed GST pulldowns of the MLL complex components using GST-MLL^{3762} and GST-MLL3^{4703} as bait. In order to get efficient formation of the MLL complexes, 5-fold higher complex concentration was used than in the methyltransferease assays, with 2.5μM of each component. We performed each pulldown with increasing concentrations of **MM-102**, (2.0, 10 and 50μM) and **MM-401** (0.04, 0.2, 1.0, 5.0 and 25μM) as well as **MM-NC-401** (25μM). Both **MM-102** and **MM-401** disrupted association of WDR5 and RbBP5 with GST-MLL1 in a concentration-dependent fashion (Figure 3.2A). **MM-102** disrupted WDR5 association with MLL1 mildly at 2.0μM, moderately at 10μM and completely at 50μM. 50%

disruption of the MLL-WDR5 association, with both proteins at 2.5μM occurred between 2 and 10μM, which is in good agreement with the HMT IC50 of 0.8μM for inhibition of a 0.5μM MLL1 complex. In this particular interaction study, complete disruption of RbBP5 interaction was not observed. However, partial disruption was observed with 10 and 50μM of compound. In previous experiments to optimize this pulldown, complete disruption of RbBP5 had been observed at equivalent concentrations, so the appearance of fainter bands of RbBP5 is likely due to overloading of the protein and high antibody concentrations. **MM-401** had a similar effect to **MM-102** on complex assembly, but its effects were observed at lower concentrations (Figure 3.2A). **MM-401** blocked association of both WDR5 and RbBP5 with GST-MLL1 in a concentration-dependent fashion, with an estimated IC50 between 1.0 and 5.0μM.

MM-102 also disrupted association of WDR5 with GST-MLL3 but did not alter the association of RbBP5 with MLL3 (as shown in figure 3.2B). Half-maximal disruption of the WDR5:MLL3 interaction occurred between 10 and 50μM, so the inhibitor was slightly less potent in its effect on MLL3 than on MLL1. **MM-401** only disrupted association of WDR5 with GST-MLL3 at the concentrations tested and did not impair association between RbBP5 and MLL3. The estimated IC50 for MLL3:WDR5 was between 1.0 and 5.0μM, with negligible WDR5 being pulled down at 5.0μM **MM-401** or greater. It should be noted that Ash2L was included in all pulldown experiments, but as (1) Ash2L has previously been shown to associate strongly with RbBP5 and the two proteins generally migrate at the same molecular weight on a gel and (2) Ash2L has no direct interaction with WDR5 and the association is mediated by RbBP5 we did not specifically look for this protein on western blot.

This data supports our previous observation that MLL3 can associate directly with the RbBP5/Ash2L heterodimer in the absence of WDR5. Interestingly, this data suggests that the

RbBP5/Ash2L heterodimer has a unique binding site for MLL3, and possibly other MLL family members such as MLL2 and 4, that cannot interact with MLL1, or interacts with MLL1 much more weakly. The nature of this interaction interface and the functional significance for this interaction in regulating H3K4 methylation remains to be determined. However, the specific requirement for the WIN:WDR5 interface in the MLL1 complex demonstrates that this is a highly specific inhibitor, a property which is beneficial for clinical utility with minimal side effects.

MM-401 inhibits growth and proliferation of MLL1-AF9 transformed mouse leukemia cells

First, we established that our inhibitors, **MM-102** and **MM-401**, had sub-micromolar IC50 values, specificity for our target, and reasonable cell permeability. Next, we sought to test the ability of **MM-401** and **MM-102** to inhibit growth of leukemia cells, transformed with MLL1 fusion proteins. We chose to begin our studies with mouse MLL1-AF9 transformed bone marrow cells as this is a convenient model system to study the detailed mechanism of inhibitor action, and will inform us as to the utility of mouse MLL1-AF9 leukemia cells for drug testing relative to future application of a mouse model for inhibitor testing. We treated MLL1-AF9 transformed bone marrow cells with varying concentrations of **MM-401**, from 5-40μM, along with 40μM of the **MM-NC-401** control compound and 0.2% DMSO and monitoring the number of live cells by standard cell counting with Trypan Blue staining over the 4 days (Figure 3.4A). DMSO was used to solubilize **MM-401** at the concentrations required for our experiments; the DMSO concentration in each treatment sample was held consistent at 0.2%. We also treated untransformed bone marrow with 40μM **MM-401** and 160μM **MM-NC-401** to test the effects of our inhibitor on untransformed hematopoietic tissue (Figure 3.4). We found that over the course of 4 days, our control-treated MLL-AF9 transformed bone marrow grew from 2 x 10^5 cells to 2-

2.5 x 10^7 under our culture conditions. The lowest concentration of **MM-401** used in this experiment, 5μM, permitted similar levels of growth as the control samples. However, doubling the inhibitor concentration to 10μM slowed the rate of cell growth by nearly half, such that there were only 1.3 x 10^7 live cells after 4 days treatment. Treating the MLL1-AF9 transformed bone marrow cells with 20μM inhibitor halved the growth rate such that there were 6.6 x 10^6 cells after 4 days treatment. With 40μM treatment an initial 5-fold increase was observed in cell number after the first 2 days of treatment compared to the 20-fold increase in cell number observed in the DMSO treated cells. However, no further growth was observed after 2 days, holding at around 1 x 10^6 cells. Visual inspection of the cells under 10x magnification with Trypan Blue staining revealed that the majority of cells in the 4 day, 40μM **MM-401** treated samples were small and somewhat irregular in appearance rather than large and round with well defined boundaries. This suggests that most of the cells in the 40μM **MM-401** treatment were unhealthy or dying.

In order to quantitate the effects of the inhibitor, we treated both MLL1-AF9-transformed and wild-type bone marrow with **MM-401** for 4 days and measured cellular proliferation by the Cell Titre Glo assay (Promega) (Figure 3.4A). We also measured the proliferation of MLL1-AF9-transformed bone marrow treated with **MM-NC-401** for 4 days. During this treatment, we passaged each sample to a density of 1 x 10^5 at day 2 to prevent cell proliferation from being inhibited by high cell density in cultures. We found that after 4 days, **MM-401** inhibits cellular proliferation of MLL1-AF9-transformed bone marrow with an IC50 of 14.4μM, but it has no effect, up to 160μM, on growth of untransformed bone marrow. **MM-NC-401** does not inhibit growth of the transformed cells at any of the concentrations tested, up to 40μM. One important finding to point out is that **MM-401** inhibited cell growth with a 50-fold higher IC50 than was observed in our methyltransferase assay. This finding is not entirely unique to the WDR5

82

inhibitor, as the recently published Dot1L inhibitor was shown to inhibit Dot1L-catalyzed histone methylation with an IC50 of 0.4nM yet its cellular effects were observed at concentrations ranging from 0.05-3.0μM[103]. The Dot1L inhibitor is hypothesized to work by a similar mechanism to our MLL1:WDR5 inhibitor and thus it is relevant to compare the activities of the two compounds. Cellular permeability of **MM-401** has been shown to be modest, at best (Table 2.11). Therefore, we anticipate that only a fraction of **MM-401** is able to penetrate the cellular membrane the nucleus to target the MLL1:WDR5 interaction. Thus, even though the cells are treated with 40μM **MM-401**, at the site of the interaction, the concentration is likely much lower.

In order to determine the mechanism of growth arrest in **MM-401** treated MLL1-AF9 cells, we stained cells from each treatment sample with propidium iodide and monitored cell cycle progression by cell sorting (Figure 3.4B). We found that **MM-401** arrested cells in G1 in a concentration dependent fashion.

MM-102, 401 induce differentiation of MLL-AF9 transformed bone marrow cells

MLL fusion proteins have been postulated to act by abnormally upregulating a program of *HoxA9* and *Meis1* expression, to drive proliferation and self-renewal in HSCs and early progenitors. This prevents MLL-AF9-transformed progenitors from differentiating down their myeloid and lymphoid lineages to generate functional blood cells. Blocking the function of the MLL1 fusion protein is anticipated to down-regulate this genetic program and allow for, or promote, normal hematopoietic differentiation. In general, MLL1-rearranged leukemias are characterized by having a regular, blast-like morphology with small round cells characterized by large, round nuclei. As differentiation proceeds, the cells tend to increase in size, becoming more irregularly shaped with smaller nuclei, relative to the cytoplasm. Many later hematopoietic

precursors and differentiated cell types are also characterized by having irregular or multi-lobed nuclear structures. In order to test the ability of WDR5 inhibitors to differentiate leukemia cells, we treated MLL1-AF9-transformed bone marrow cells with either **MM-102**, **MM-401** and **MM-NC-401** for 4 days and then analyzed cellular morphology by cytospin with Wright-Giemsa staining. As 4 days treatment with these compounds had previously been demonstrated to slow cell proliferation, it is a reasonable possibility that this slowing of cell growth is a consequence of differentiation.

In vehicle- or control-treated cells, the majority of cells are small and regular shape with comparatively large nuclei relative to the overall cell size (Figure 3.5A,B). There are some hallmarks of early differentiation, including many cells with irregularly shaped nuclei and some cytoplasmic vacuolization, however, these cells have, primarily blast-like morphology. Cells treated with **MM-NC-401** closely resemble the DMSO-treated cells (Figure 3.5B). However, cells treated with either **MM-102** or **MM-401** exhibited substantial changes in morphology. Cells treated with 50μM **MM-102** (Figure 3.5C) had substantial cell death and the remaining viable cells had larger cytoplasm relative to the nucleus and more irregular-shaped nuclei than the control treated cells, indicating that there was some differentiation. However, we observed no cells in this sample that exhibited morphology consistent with terminally differentiated macrophages or neutrophils. In contrast, both 20μM and 40μM **MM-401** treated samples had a significant population of large, flattened-looking cells with small round nuclei and large cytoplasm, consistent with differentiated macrophages (Figure 3.5 D,E). The cells in the 40μM **MM-401** treated sample almost uniformly exhibited this morphology. However, in the 20μM **MM-401** treated sample, a number of the observed cells were smaller with irregular shaped nuclei and comparatively smaller cytoplasms, suggesting these might be myeloid precursors. It

should be noted that in a study where Dot1L was excised from MLL1-AF9 leukemia cells, cells differentiated almost exclusively into macrophages [103]. While concentration-dependent cell death was observed in MLL1-AF9 cells treated with both **MM-401** and **MM-102**, only **MM-401** induced obvious differentiation of cells down the myeloid lineage. This suggests that **MM-102** may act by some non-specific mechanism to induce death. However, the evidence showing that **MM-401** induces differentiation supports the hypothesis that inhibiting MLL1 complex activity, through blocking the interaction between MLL1 and WDR5, impairs the cascade of epigenetic dysregulation that results in abnormal *HoxA* cluster activation. This downregulates *HoxA9* expression and induces differentiation. This is the first piece of data demonstrating the mechanism of action of the WDR5 inhibitor in MLL1 fusion-transformed cells.

MM-401 impairs viability of human leukemia cells with MLL1 rearrangement

To determine if **MM-401** could specifically induce death in human leukemia cells as well as mouse leukemia cells, we cultured several human leukemia cell lines with different fusion proteins in the presence of **MM-401** over the course of 8 days. We treated human cells for twice as long as mouse cells because the human leukemia cell lines had a slower rate of growth and we sought to treat all cells for a similar number of cell divisions (Figure 3.6). After 8 days treatment, we measured cell growth by the Cell-Titre Glo assay. We found that the MLL1-AF4-transformed AML cell line, MV4:11, was most sensitive to growth inhibition by **MM-401,** with an IC50 = 9.5μM. MV4:11 was also observed to be highly sensitive to the Menin inhibitor, MI-2 [81, 102]. The next most responsive leukemia cell line was the ALL cell line, KOPN8, which had an IC50 of 36.5μM. This result demonstrates that WDR5 inhibition can target both AML and ALL, with MLL1 rearrangement. The BCR-ABL-transformed cell line, K562, does not

have MLL1 rearrangement or *HoxA9* amplification and was not inhibited detectably at any tested concentrations of **MM-401**. This suggests that, with one notable exception, **MM-401** can kill leukemia cell lines with MLL1-rearrangement but not other leukemias without MLL1 translocation or normal levels of *HoxA9* expression. The one notable exception is the MLL1-AF9-transformed human leukemia cell line, MOLM-13, which is inhibited minimally, with an IC50 of 140μM with **MM-401.** It should be noted that in our initial tests with this cell line, we did not culture these cells with insulin, however, in most studies, this is an important component of the culture media. It is possible that insulin promotes the growth mechanisms that confer sensitivity to **MM-401.** To draw further conclusions about the utility for **MM-401** for treating different human leukemias, it will be relevant to expand the panel of cell lines to include *HoxA9^{high}* cells without MLL1 translocation as well as multiple cells lines for each different MLL1 fusion protein. However, from the cell lines tested, we can tentatively draw the conclusion that WDR5 is a relevant target for human leukemias with MLL1 rearrangement.

MM-401 inhibitors block expression of HoxA9 in MLL1-AF9 transformed bone marrow

Next, we sought to determine if the growth inhibition and differentiation observed in the **MM-401**-treated MLL1-AF9 bone marrow cells was a result of reduction in *HoxA9* expression through inhibition of MLL1 complex activity, as hypothesized. To test this hypothesis, we examined the expression of *HoxA9* and *Meis1* in these cells. We treated cells with either 40μM **MM-401** or 40μM **MM-NC-401** for 4 days and then harvested the cells, and analyzed mRNA levels by RT-PCR. We observed that at 4 days, there was an approximately 50% reduction in *HoxA9* expression after treatment with **MM-401** (Figure 3.7). As **MM-401** treatment at this concentration over 4 days highly cytotoxic, it remains to be determined if the cells that are viable

86

in this treatment sample are representative of the response to the inhibitor, or if they are some unique, drug-resistant population. It also remains to be determined if the inhibitor can elicit a similar response on a wide range of MLL1 targets, or if it only alters expression select MLL1 target genes.

Given the reduction in *HoxA9* and *Meis1* expression in **MM-401**-treated MLL1-AF9 cells, we tested the levels of H3K4me3 at these loci in treated cells. After 4 days treatment with 40μM MM-401, we observed an approximately 30% reduction in H3K4me3 at *HoxA9* and a 60% reduction at *Meis1* by chromatin immunoprecipitation [126]. This indicates that **MM-401** interferes with H3K4me3 at MLL1 targets in MLL1-AF9-tranformed leukemia cells. This data supports our hypothesis that the MLL1:WDR5 interaction is needed for methylation at and expression of *HoxA9* and *Meis1* in MLL1-rearranged leukemias. This also informs us as to the mechanism of action of **MM-401** in these leukemia cells.

Given that MLL1 has been reported to regulate a small subset (<5%) or genes with enriched H3K4me3 and given that our inhibitor is specific for MLL1 complex function, we anticipate that **MM-401** treatment will not elicit a global defect in H3K4me3. To test this idea, we harvested MLL1-AF9 cells that had been treated for 4 days with **MM-401** or controls and tested global H3K4me3 levels by western.

When we attempted to characterize additional histone post-translational modifications in these cells by ChIP, we were unable to obtain sufficient cells to generate a quality signal for ChIP analysis. This is likely due to the significant cell death observed after 4 days treatment with **MM-401**. Histone H3 K4 methylation is one of the more abundant post-translational modifications and thus is likely to be significantly enriched by immunoprecipitation. We hypothesize that this is likely why we were able to ChIP for H3K4me3, but no other post-

translational modifications or proteins in *MLL1-AF9*-transformed cells. However, we were still interested in examining the effects of WDR5-MLL1 interaction inhibition on chromatin modifications and protein recruitment to the MLL1 target loci. We decided to proceed with further experiments in immortalized mouse embryonic fibroblasts (MEFs), which we hypothesized would be insensitive to **MM-401** treatment. This would allow us to treat cells with **MM-401** without worrying about substantial cell death interfering with our ability to harvest sufficient numbers of cells for ChIP.

We treated immortalized MEF cells with 40μM **MM-401** or **MM-NC-401** for 4 days and looked at MLL1 recruitment to the *HoxA9* locus by ChIP. We observed a 50% reduction in MLL1 recruitment to *HoxA9* after **MM-401** treatment, indicating that the interaction with WDR5 is required for MLL1 recruitment to its targets. This was surprising; given the multitude of DNA- and chromatin-binding domains (Figure 1.1) found within the MLL1 protein, we anticipated that MLL1 would facilitate recruitment of the MLL1 complex to target genes rather than driving WRA recruitment of MLL1 to target genes. Two possibilities are (1) the WRA complex does, indeed mediate binding to target loci through described interactions between Ash2L and DNA or interaction between the complex and other chromatin-binding factors, such as MOF[127] (2) MLL1 possesses the necessary information to recruit to target loci, but its recruitment is stabilized by the WRA subcomplex. Further experiments would be needed to test these hypotheses.

We also examined H3K4me3, H3K79me2 and H3 at the *HoxA9* locus. We found, as expected that H3 did not change at the HoxA9 locus in the presence of MM-403. This is a good control for chromatin immunoprecipitation in the treated versus control samples. We observed an approximately 30-40% reduction in H3K4me3 at *HoxA9* loci in the MEF cells, similar to the

MLL1-AF9 transformed leukemia cells. We also observed a comparable reduction, approximately 30%, in H3K79me3 at the *HoxA9* locus in **MM-401** treated cells relative to control treated cells. This suggests that H3K79me3 at *HoxA9* in untransformed cells is dependent on H3K4me3. It should be noted that in Dot1L knockout studies, Dot1L was significantly enriched, with a broader localization pattern at the *HoxA9* locus in transformed cells. It was hypothesized that MLL1 fusion proteins recruit Dot1L to the *HoxA9* locus through some abnormal mechanism in these cells. This mechanism is likely not recapitulated in our MEFs, therefore, we cannot necessarily assume that H3K79 methylation is disrupted by MM-403 treatment of MLL1-AF9 transformed cells. However, the differentiation data showed earlier shows that **MM-401** causes cellular differentiation, very similar to the Dot1L inhibitor, in MLL1-AF9 transformed. Indeed, in both our **MM-401** treated cells and the Dot1L inhibitor treated cells, differentiated macrophages were observed. While this does not conclusively demonstrate that **MM-401** alters Dot1L-mediated H3K79 methylation in transformed cells, it certainly supports this hypothesis.

Discussion

In this chapter, we have described the mechanism of action of a small molecule inhibitor of the MLL1 complex in leukemias with MLL1 rearrangement. We have established that this compound is a specific inhibitor of the MLL1 complex activity but has no effect on activity of other MLL family members. We have established that this specificity is due to a unique interaction between other MLL family members and the RbBP5/Ash2L heterodimer, that allows these enzymes to bypass the requirement for WDR5 in complex assembly. We have determined that this compound blocks the growth and proliferation of leukemia cells with MLL1-AF9

89

transformation. We demonstrate that in MLL1-AF9 transformed cells, inhibitor treatment downregulates expression of *HoxA9* through inhibition of H3K4 methylation at this locus; we postulate that this is the primary mechanism of action for this inhibitor. We go on to show that in MEF cells (*MLL1^{wt/wt}*), inhibition of the WDR5:MLL1 interaction blocks efficient MLL1 recruitment to MLL1 target loci and interferes with H3K79 methylation as well as H3K4 methylation. Finally, we demonstrate that this inhibitor can interfere with growth and viability in a variety of human cell lines with MLL1 rearrangement, pointing to a utility for this compound in treatment of MLL1 rearranged leukemias in humans.

The specific, concentration-dependent, inhibition of MLL1 complex assembly and activity by **MM-401** indicates that the WDR5:MLL1 interaction is essential for MLL1 complex function. In further support of this concept, biological functions that are mediated by the MLL1 core complex, including *HoxA9* and *Meis1* upregulation and H3K4 methylation at these loci, are impaired in cells treated with **MM-401**. H3K4 methylation and gene expression were disrupted in both *MLL1^{wt/wt} cells and MLL1^{wt/MLL1-AF9}* cells indicating that the MLL1 complex acts both in the wild-type pathway for *HoxA9* activation and the mutant pathway driven by fusion protein activity. This finding points to a broader utility for our inhibitor, as *HoxA9* and *Meis1* are upregulated in multiple forms of leukemia, with and without the *MLL1* fusion protein. As our findings have shown that **MM-401** can block *HoxA9* and *Meis1* upregulation in the absence of the fusion protein indicating that this compound could prove useful for treating all leukemias with *HoxA9* and *Meis1* amplification. This is a particularly noteworthy finding, as leukemias with *HoxA9* and *Meis1* upregulation are generally, poorly-responsive to conventional therapies.

The effects of **MM-401** are similar to the effects observed in MLL1 rearranged leukemias after treatment with the Dot1L inhibitor, EPZ00447 and the Menin inhibitor, MI-2. These compounds act on transcription cofactors that either recruit, or are recruited by the MLL1 fusion protein. Specifically, **MM-401** causes downregulation of H3K4me and H3K79me at *HoxA9* and *Meis1*, which are also downregulated by EPZ00447 and MI-2. The overlapping effects of MM-401, EPZ00447 and MI-2, suggest that these compounds all act in the same pathway of epigenetic dysregulation that drives abnormal chromatin modification and gene expression in MLL1 rearranged leukemias. This idea is supported by the finding that Menin mediates recruitment of both wild-type and translocated MLL1 and wild-type MLL1, in turn, facilitates H3K4 methylation and H3K79methylation at target genes [101]. Disruption of this epigenetic signaling cascade is a promising method for treating acute leukemia with MLL1 rearrangement.

Another promising utility of this compound is its potential as a chemical tool to study the role of WDR5 in regulation of developmental gene expression in different systems. Despite having a multitude of described functions, specifically in embryonic stem cell maintenance and regulation of stem cell and early progenitor phenotypes, the detailed mechanisms of WDR5 action in different systems remain to be elucidated. The strict conservation of WDR5 as well as the essential function of WDR5 in ES cell maintenance suggests that genetic ablation of this gene might have such a severe phenotype and early embryonic lethality as to be minimally useful. Therefore, a strategy to chemically interfere with select interaction interfaces on the WDR5 protein has the potential to be very informative about the regulation of WDR5 in different biological systems.

Thus far, our inhibitor has demonstrated that, at a molecular level, WDR5 interaction with MLL1 is essential for recruitment of MLL1 to or stabilization at its gene targets. This shows that the WDR5 inhibitor is not only an promising therapeutic compound, but also an effective tool for understanding the molecular regulation of multiprotein complexes with WDR5.

(A)

Inhibitor	IC50(µM) ± SD
MM-101	3.3 ± 0.28
MM-102	0.82 ± 0.08
MM-401	0.32 ± 0.10
MM-NC-401	>250

(B)

HMT	IC50(µM) ± SD
MLL1 + WRA	0.32 ± 0.10
MLL2 + WRA	>250
MLL3 + WRA	>250
MLL4 + WRA	>250
SET7/9	>250
EZH2	>250
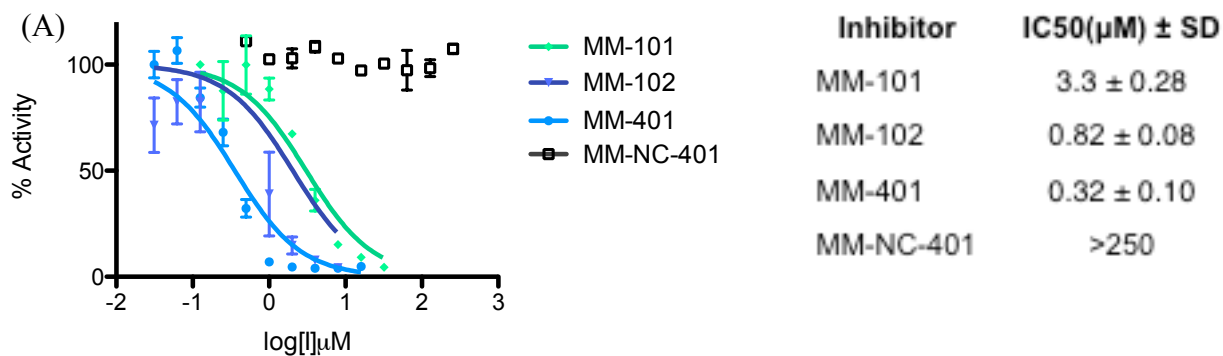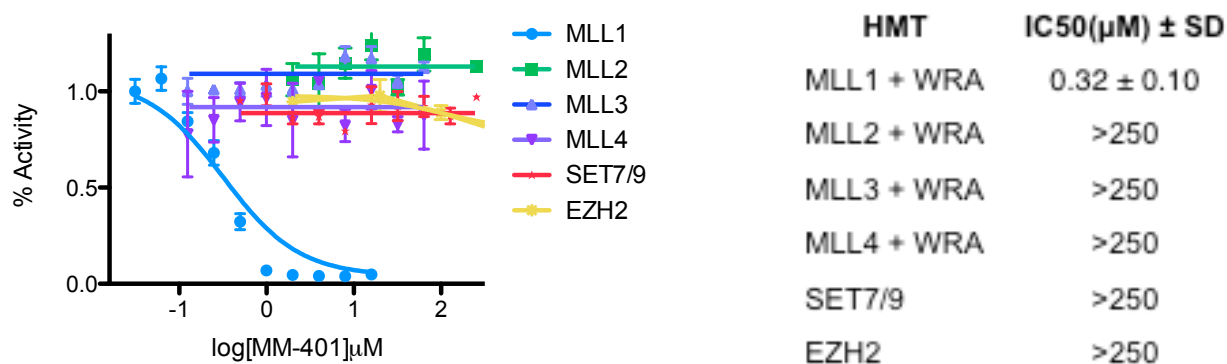
Figure 3.1   MLL WIN Peptidomimetics, MM-101, MM-102 and MM-401 specifically impair the methyltransferase activity of the MLL1 complex. **(A)** To test the activity of cell-permeable inhibitors, **MM-101, MM-102** and **MM-401**, we titrated these compounds, as well as a non-binding control, **MM-NC-401**, into the MLL1 complex HMT assay at concentrations ranging from 0.03-32µM **(B)** To test the specificity of our inhibition strategy, we titrated **MM-401** into HMT assays with MLL family complexes, MLL2, 3 and 4, as well as SET7/9 and EZH2. Error bars are representative of standard error from two replicates.

(A) **GST-MLL1^{3762}**

MM-102(µM)   --   2.0   10.0   50

RbBP5   αRbbP5

MLL   αGST

WDR5   αWDR5

GST-MLL1^{3762}

MM-401(µM)   --   --   0.04   0.2   1.0   5.0   25
MM-NC-401(µM)   --   25   --   --   --   --   --

RbBP5   αRbBP5

MLL   αGST

WDR5   αHis

(B) **GST-MLL3^{4703}**

MM-102(µM)   --   2.0   10.0   50

RbBP5   αRbbP5

MLL   αGST

WDR5   αWDR5

GST-MLL3^{4703}

MM-401(µM)   --   --   0.04   0.2   1.0   5.0   25
MM-NC-401(µM)   --   25   --   --   --   --   --

RbBP5   αRbBP5

MLL   αGST

WDR5   αHis
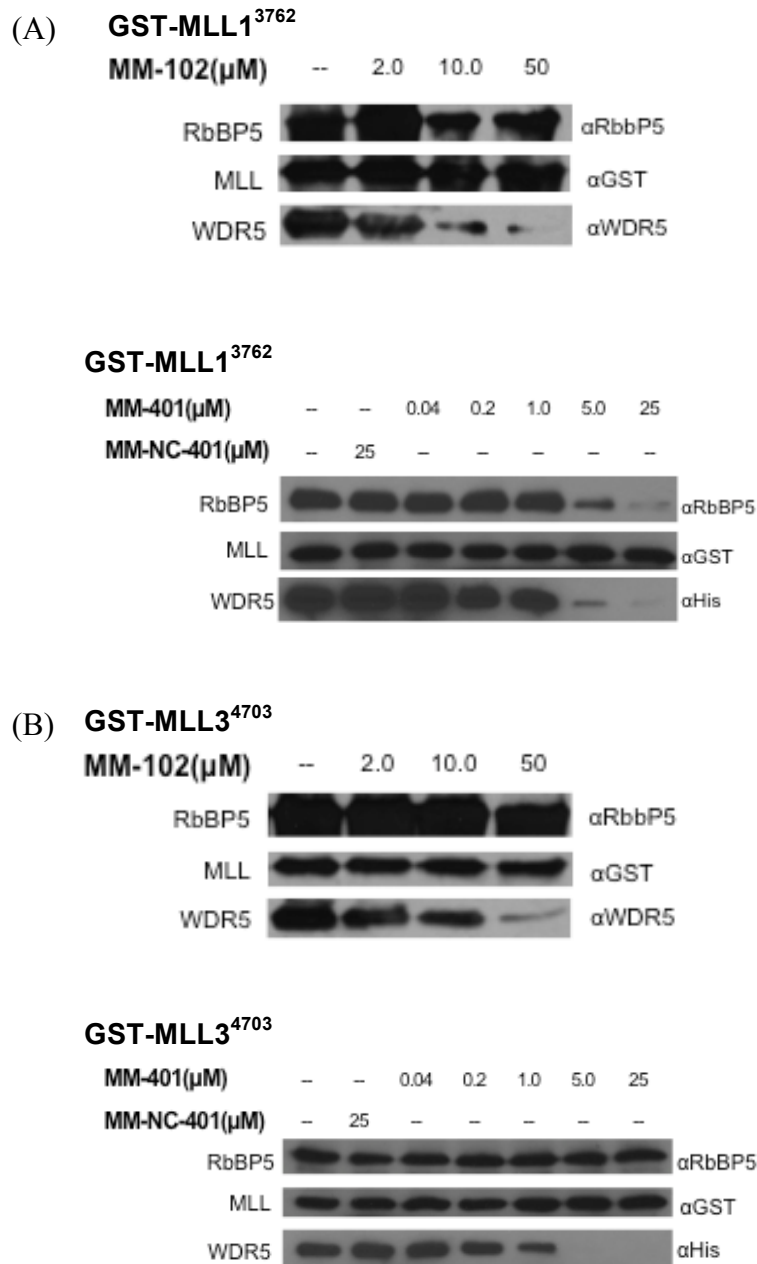
Figure 3.2. MLL peptidomimetics completely disrupt association of complex with MLL1 but only disrupt the MLL3:WDR5 interaction in the MLL3 complex (A) To test MLL1 complex assembly, we assembled the MLL1 complex at 2.5µM by GST pulldown and titrated in **MM-102** and **MM-401** at 2-50µM, and 0.04-25µM, respectively. Higher inhibitor concentrations were used than in the HMT assay reflective of higher protein concentration. Westerns are representative of 3 experiments. (**B**) We repeated the experiment from (A) with GST-MLL3 to test the effect of **MM-102** and **MM-401** on assembly of another MLL family member
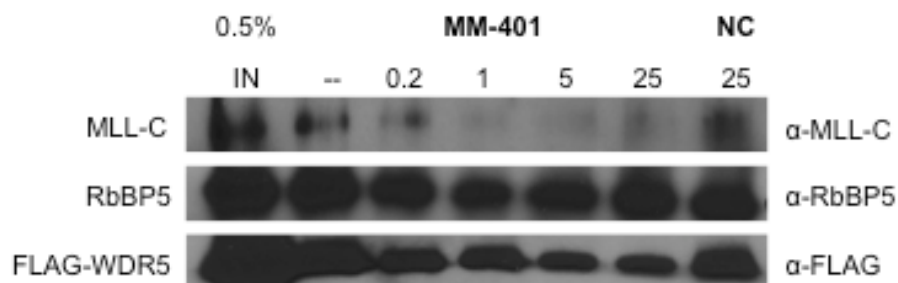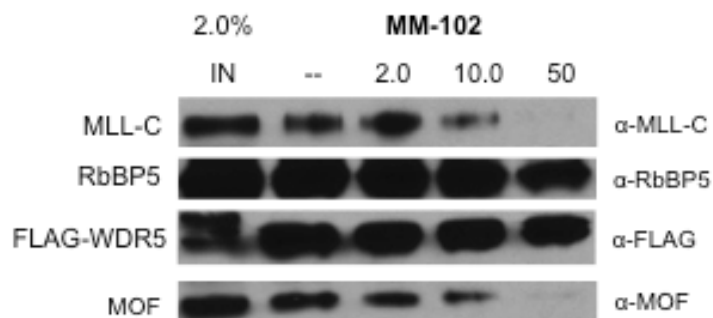
Figure 3.3. MLL peptidomimetics, MM-102 and MM-401 prevent association of MLL1 with WDR5 in cells. We examined the ability of inhibitors to block association of RbBP5 and MLL1 with WDR5 in a FLAG immunoprecipitation of WDR5 from nuclear extract of a stable cell line. Westerns are representative of 3 experiments.

(A)

(B)
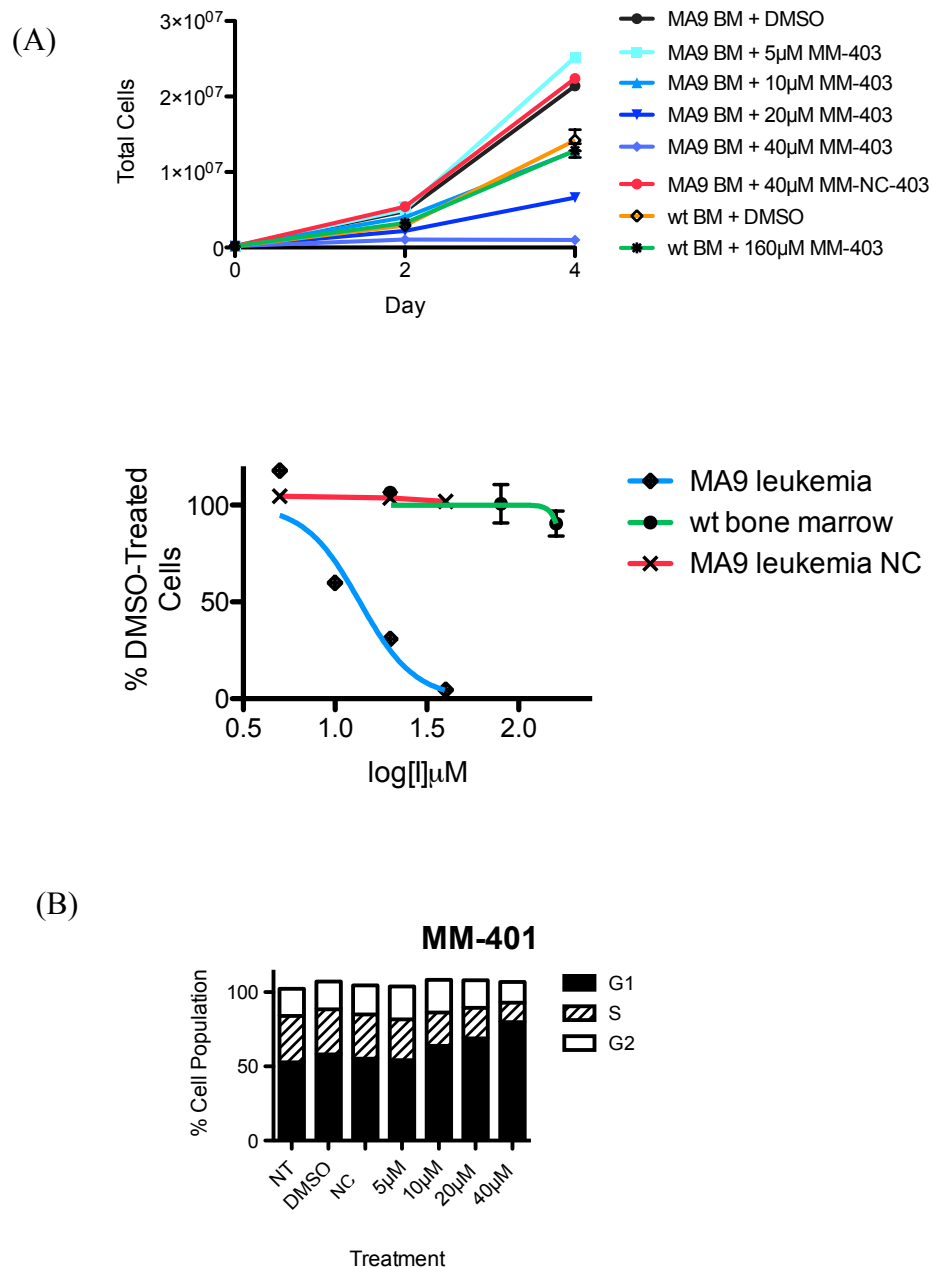
Figure 3.4. MM-401 specifically impairs growth and viability of MLL-fusion transformed mouse bone marrow. (A) Cell growth curve of wild-type and MLL1-AF9 transformed bone marrow treated with MM-401 over 4 days shows to test the effect of **MM-401** on proliferation specifically of transformed cells. **(B)** Cell cycle progression of MLL1-AF9 bone marrow, in the presence of **MM-401** is monitored by propidium iodide staining with flow cytometry

(A)

(B) 40μM MM-NC-401

(C) 50μM MM-102

(D) 20μM MM-401

(E) 40μM MM-401

(F)
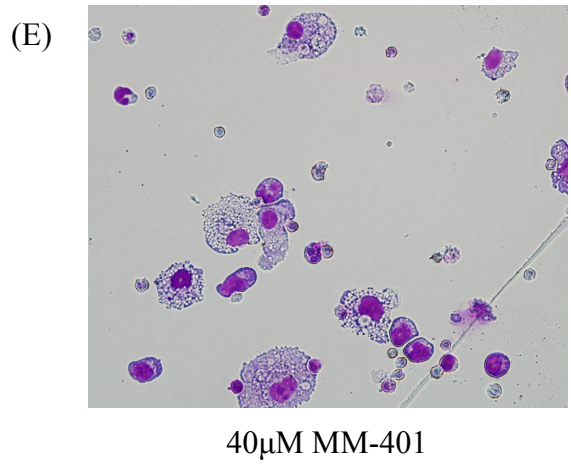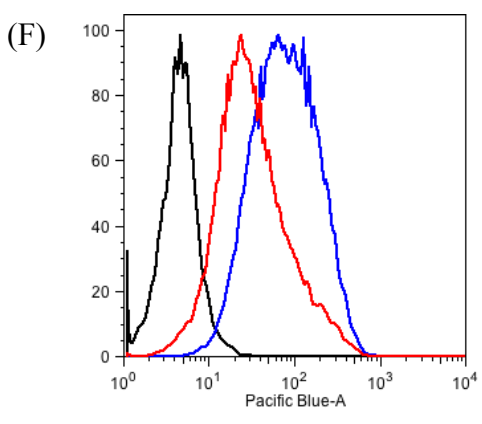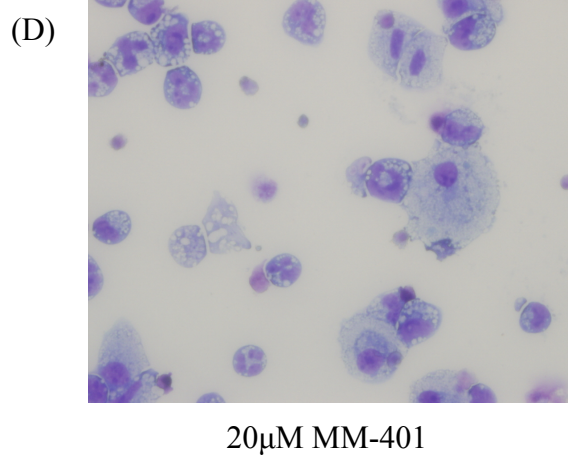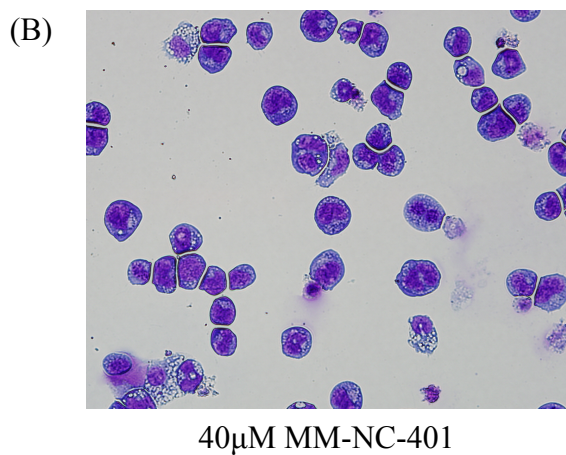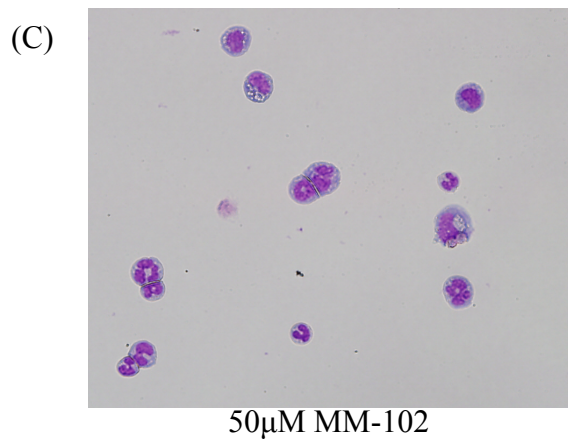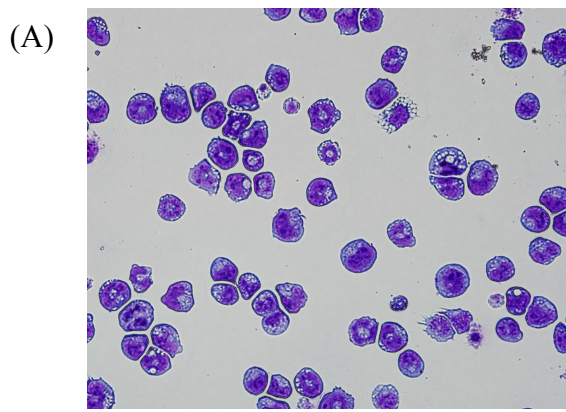
Figure 3.5. Treatment of MLL1-AF9 bone marrow cells with MM-401 specifically induces differentiation in the myeloid lineage. (**A-B)** MLL1-AF9 transformed cells were treated with DMSO or **MM-NC-401** with 4 days and then cytospinned with Wright-Giemsa staining to analyze morphology (**C)** Morphology of **MM-102** treated cells after 4 days treatment **(D-E)** Morphology of MLL1-AF9 bone marrow cells treated with two concentrations of **MM-401**. Cytospins are representative of two separate experiments. **(F)** Flow cytometry for the myeloid-surface marker, CD11b+ of 20µM **MM-401** treated cells to quantitatively evaluate differentiation.
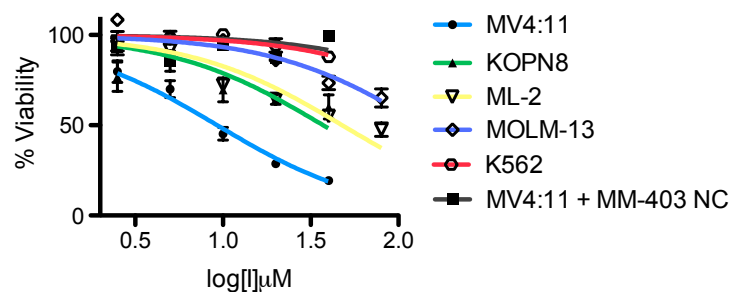
Cell Line	Leukemia	MM-403 IC50(μM)
MV4:11	MLL-AF4 (AML)	9.54 ± 1.66
KOPN8	MLL-AF6 (ALL)	36.4 ± 1.26
MOLM-13	MLL-AF9 (AML)	139
ML-2	MLL-AF9 (AML)	47.8
K562	BCR-ABL (AML)	No Inhibition

Figure 3.6. MM-401 specifically inhibits growth of acute leukemia cell lines with MLL1 rearrangement.
Human leukemia cell lines were treated with varying concentrations of **MM-403** from 2.5-80μM over 8 days and growth was monitored by the Cell-Titre-Glo assay. Standard deviation is representative of two experiments.
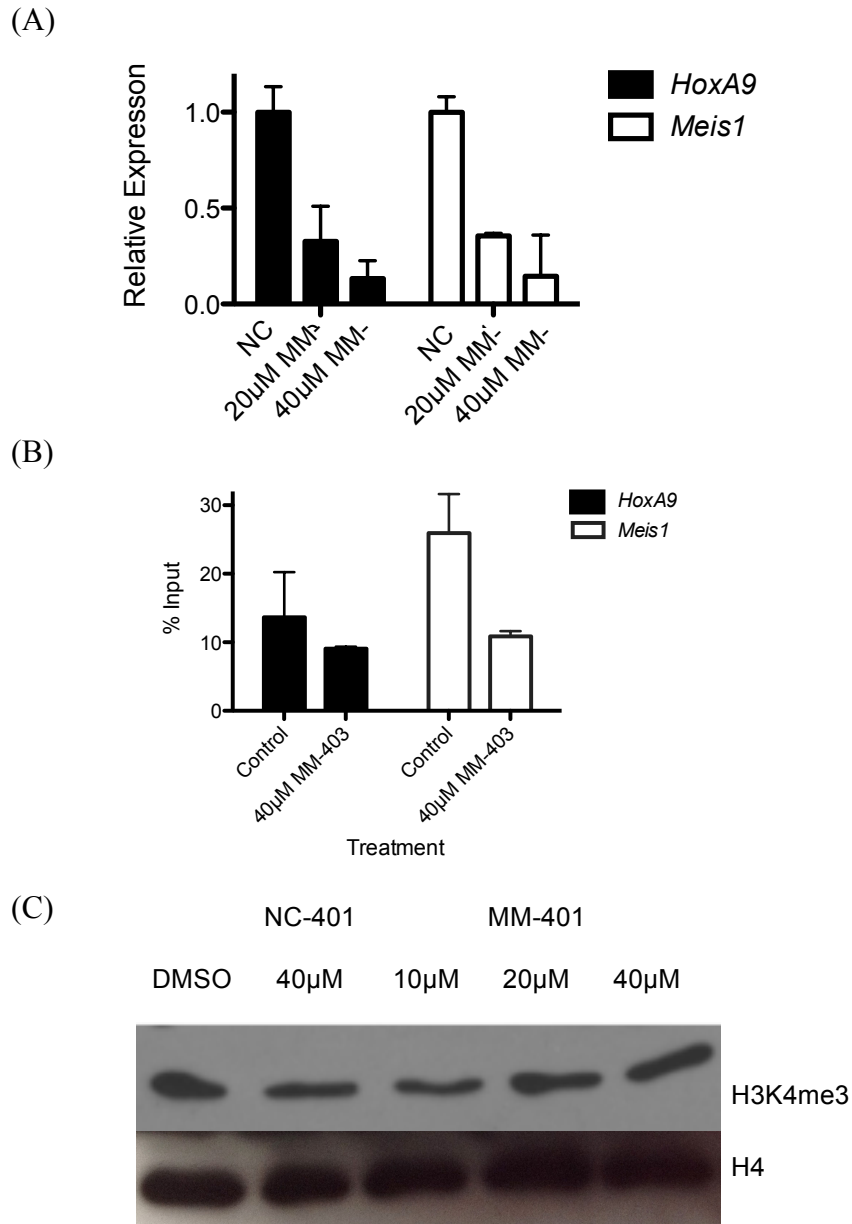
Figure 3.7. Treatment of MLL1-AF9 bone marrow cells with MM-401 downregulates MLL1 target gene expression and H3K4me3 at these loci (A) MLL1-AF9 transformed cells treated were treated with negative control, or MM-401 (20μM and 40μM) for 6 days and *HoxA9* and *Meis1* expression was assessed by RT-PCR **(B)** MLL1-AF9 transformed cells were treated with 40μM negative control or MM-401 for 4 days and harvested for chromatin immunoprecipitation with antibodies for H3K4me3. Gene association was determined by qPCR. **(C)** Global H3K4me3 in MLL1-AF9-transformed cells was examined after 4 days treatment with **MM-401**.
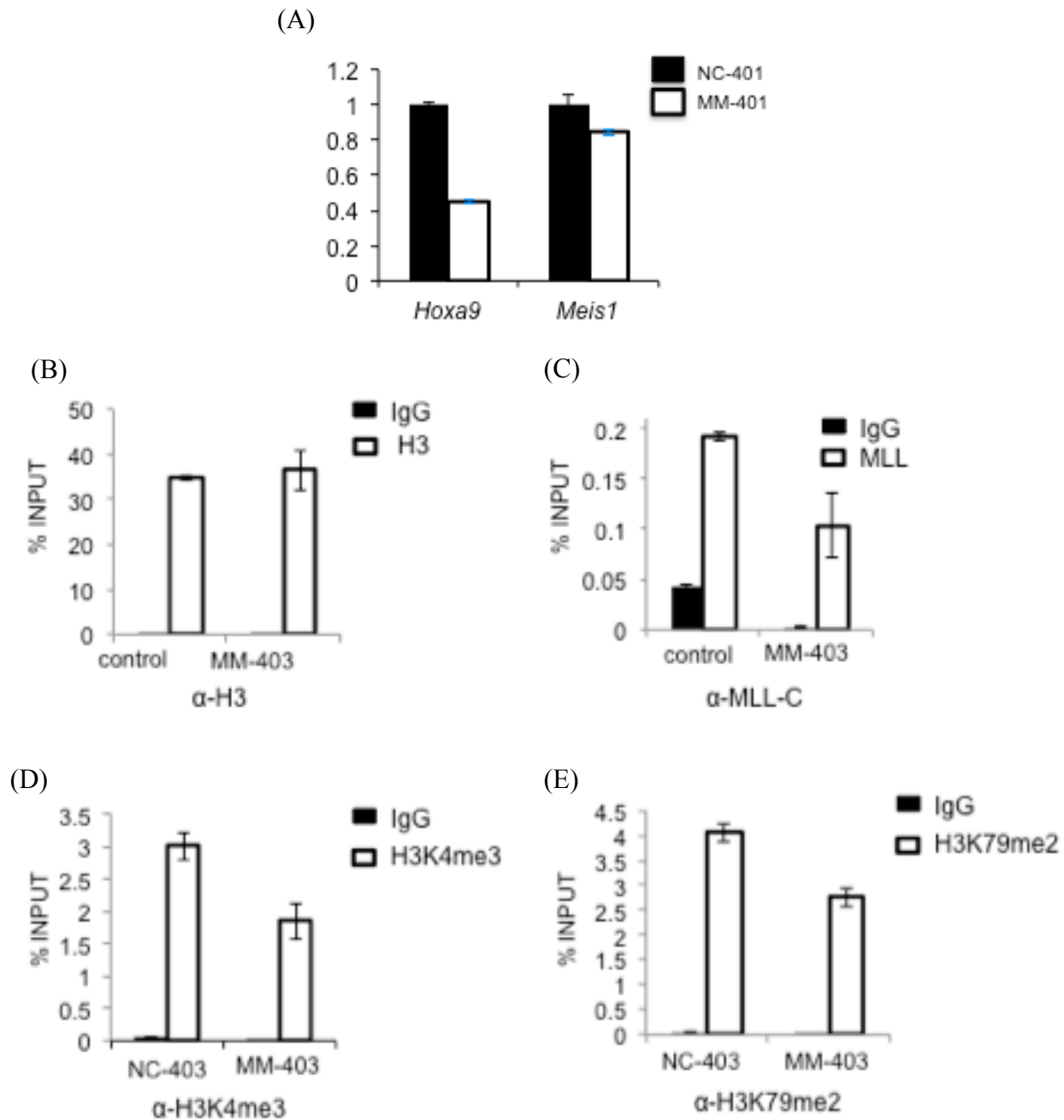
Figure 3.8. Treatment of *MLL1^{wt/wt}* MEF cells with MM-401 downregulates MLL1 target gene expression and activating histone methylation at these loci (**A**) To determine *HoxA9* and *Meis1* expression levels, we treated immortalized MEFs with **40μM MM-401** or **MM-NC-401** and analyzed *HoxA9* and *Meis1* expression after 4 days (**B**) H3K4me3 levels in **40μM MM-401** or **MM-NC-401**-treated MEFs (**C**) As a control for chromatin immunoprecipitation, we harvested cells for ChIP and IPed for H3 after 4 days treatment with **40μM MM-401** or **MM-NC-401 (D)** H3K4me3 levels in **40μM MM-401** or **MM-NC-401**-treated MEFs (**E**) H3K4me3 levels in **40μM MM-401** or **MM-NC-401**-treated MEFs. This data was prepared by Dr. Fang Cao.

CHAPTER IV

Discussion

Research into the molecular mechanisms of leukemia has identified different genetic events, typically translocations, that drive development of the disease. Common translocations include NPM1 translocation, MLL1 fusions, BCR-ABL, NUP98 and many others. Patients with a specific genetic translocation often exhibit consistent genetic signatures and common molecular mechanisms driving their disease as well as similar prognosis. For instance, patients with NPM1 or MLL1 translocations often have elevated expression of *HoxA9*, which is associated with low long-term survival rates [68]. This raises the possibility of developing drugs to target the particular molecular mechanism involved in leukemia with a common translocation, either through interfering with the action of the fusion protein or blocking the elevated gene target.

In the last decade, the tyrosine kinase inhibitor, imatinib of Gleevec, has been implemented for treatment of CML and ALL in adults with BCR-ABL translocation, also known as the Philadelphia chromosome [115]. The drug specifically targets the leukemia-causing genetic translocation through inhibition of the ABL kinase. Where CML with the Philadelphia chromosome was previously fatal in over 50% of patients, over 90% of patients treated with

imatinib/Gleevec have achieved complete hematological remission and many have lived without relapse for up to a decade [115]. In patients who have developed resistance to Gleevec, second generation drugs designed to target the mechanisms of resistance have been effective. This drug has also been approved for other kinds of cancers and the clinical data on alternate uses is now coming available. The success of Gleevec points to the potential of targeted therapies to other leukemic translocations, such as the MLL1 translocations found in the majority of infant leukemias. As patients with this disease have a bleak prognosis and low rates of long-term event-free survival, it is especially imperative to improve on the currently available treatments for this disease [70].

Significant research has already done detailing the molecular mechanisms driving abnormal gene expression and transformation in leukemias with MLL1 rearrangement [70]. This work has described the abnormal recruitment of a multitude of transcription factors, cofactors and chromatin modifiers, that act, in concert to establish a transcriptionally active chromatin state and directly stimulate transcription at target genes. We hypothesize that blocking either the establishment of a transcriptionally permissive chromatin state or inhibiting transcription by PolII could be a promising route for treatment of leukemia with MLL1 rearrangement.

To this end, we have sought to further our understanding of the basic mechanisms that promote transcription activation by MLL1 fusions through chromatin-based mechanisms. MLL1 rearranged leukemias are heterozygous for wild-type MLL1. Wild-type MLL1 is a histone methyltransferase with essential functions in *Hox* gene activation in normal hematopoiesis [50, 51]. Wild-type MLL1 cooperates with a conserved complex of proteins, WDR5, RbBP5 and ASH2L to catalyze histone H3K4 methylation at target loci [53, 86]. While H3K4 methylation is associated with PolII transcription and gene activation, it is not known if this activity is

essential for gene activation in MLL1 rearranged leukemias. Furthermore, the unique molecular functions of the MLL1 complex components in MLL1 rearranged leukemias are not well understood.

MLL1 core complex assembly is nucleated by interaction between WDR5 and MLL1, which, in turn, recruits RbBP5/ASH2L for complete complex assembly. The interaction interface between WDR5 and MLL1 is highly conserved and well described in crystallographic studies [89, 90]. We hypothesized that interfering with the WDR5:MLL1 interaction would completely disrupt assembly of the core complex and block its function in hematopoiesis and leukemia. In support of this hypothesis, knockdown of WDR5 was found to interfere with expression of the MLL1 target gene, *HoxA9* [54]. To further test this hypothesis, we sought to develop a small-molecule inhibitor to the WDR5:MLL1 interaction. We chose to use small molecule targeting as opposed to genetic techniques to study this protein:protein interaction as an inhibitor would allow us to disrupt the interaction of interest without interfering with the stability or function of other important domains and molecular structures in the complex. Furthermore, if the WDR5:MLL1 inhibitor was found to interfere with MLL1 target gene expression in leuekmia, this compound could prove to be a promising lead for development of novel therapies to acute leukemia with MLL1 rearrangement.

In addition to having functions in MLL1 complex assembly, hematopoiesis and leukemia, WDR5 also has many described functions in regulating gene expression in important developmental and disease proceses [81-86]. WDR5 also has many described interaction partners with essential functions, including MOF, HDAC3, Oct4 and Nanog [81, 83, 84]. The mechanisms, which regulate WDR5 interactions and functions in different cell types and developmental processes, as well as the extent to which these functions involve MLL1, are

incompletely understood. An inhibitor to a specific protein-binding pocket, such as the MLL1 interaction pocket, on WDR5 could be a powerful tool to begin addressing some of these questions.

To validate our inhibitor strategy, we first prove that WDR5 and MLL1 interact in cells through the biochemically described interface. The WDR5 Arg-binding pocket described to mediate interaction with MLL1 was initially identified to bind the N-terminus of H3, albeit with 100-fold lower affinity than it binds MLL1 [90, 95, 96]. To demonstrate the WDR5 binding partner in cells, we mutated both components of the MLL1:WDR5 interaction interface and expressed these proteins in cells. We found that mutations to these interaction sites abolished the association between these two proteins [128]. While this does not rule out the possibility that WDR5 can bind histone tails, especially given that the abundance of the histone proteins in the nucleus, it does prove that WDR5 must interact with the conserved Arg-containing WIN motif on MLL1 to associate with this protein. We also established that WDR5 and the WIN motif must be present for MLL1 to efficiently methylate H3, but was not required for MLL2, 3 or 4 to catalyze histone methylation. This unique requirement for WDR5 in MLL1 complex function bodes well for our inhibitor strategy as it suggests that the inhibitor will be highly specific for MLL1. However, it calls into question the function of WDR5 in other MLL family complexes. WDR5 has been found in other MLL family complexes and in these complexes, the WIN motif is conserved and WDR5 has been found by immunoprecipitation [55]. Furthermore, knockdown of WDR5 has been shown to interfere with expression of MLL3 gene targets [55, 129]. However, our data suggests that WDR5 does not function in these complexes to integrate the complex and facilitate catalysis. We suggest that in other MLL family complexes, WDR5 may instead serve to mediate interaction of the complex with additional factors for regulation.

However, further studies would be required to (1) rule out the possibility that the non-requirement for WDR5 observed in our assay is simply an artifact of our assay conditions and (2) determine additional proteins that WDR5 can interact with in the context the MLL2-4 complexes.

To develop the WDR5 inhibitor, we used the conserved sequence on MLL1, the WIN motif, that interacts with WDR5, with high affinity, as our template. Using the co-crystal of WDR5 in complex with the WIN peptide as a guide, we made systematic truncations and modifications to different positions in the WIN sequence to generate cell-permeable inhibitors. We were able to improve binding as well as the pharmacological properties of the minimal Ac-ARA-NH$_2$ sequence by (1) substituting the Ala side chains with small aliphatic side-chains (2) adding bulky hydrophobics to the C-terminus of the peptide and (3) connecting the peptide termini with a 4-carbon linker to improve hydrophobicity and binding to generate two lead candidates, **MM-102** and **MM-401**. Despite the improvements, the cell-permeability of the compounds generated was still modest, complicating the functional analysis of these compounds in cells. Optimizing cell permeability is a common problem with rational drug design based on peptide templates. For further development of this drug candidate, we will either need to find ways to significantly enhance cell permeability of our existing peptidomimetic template or identify a different lead molecule that has more amenable pharmacological properties However, despite the permeability issues, we proceeded with biochemical and cell-based proof-of-concept studies with **MM-102** and **MM-401.**

In biochemical studies, we determined that both **MM-102** and **MM-401** could specifically inhibit assembly and activity of the MLL1 complex in a concentration-dependent fashion with sub-micromolar IC50 values. These two compounds disrupted WDR5 association

with MLL3 as well, but did not also block the recruitment of RbBP5 and Ash2L to MLL3. This suggests that the other MLL family members can interact directly with WDR5 and this interaction is mediated by the same interaction interface as the WDR5:MLL1 interaction, but this interaction is not required to recruit RbBP5 and Ash2L to augment catalysis. This further supports our idea that WDR5 interacts directly with the MLL2-4 complexes, but the function of this interaction is not for catalytic stimulation.

In cells, we found that both **MM-401** and **MM-102** could specifically interfere with growth and proliferation of leukemia cells, from both humans and mice, with MLL1 fusion proteins. However, only **MM-401** could relieve the differentiation block in leukemic blasts and generate differentiated cell-types. As other inhibitors of MLL1 fusion-associated factors, EPZ004777 and MI-2 also induce differentiation of MLL1 fusion-transformed cells, we postulate that the differentiation observed with **MM-401** treatment points to its specific action in this pathway[102, 103]. In hematopoiesis, both *MLL1* and *HoxA9* expression are elevated in progenitor cell types and downregulate during differentiation. The elevated expression of these genes is thought to promote self-renewal and proliferation in undifferentiated progenitor or leukemia cell types in both normal hematopoiesis and leukemia. As our inhibitor is expected to block the expression of *HoxA9* it is anticipated to promote differentiation. This action is observed, supporting our hypothesis for the mechanism of action of our inhibitor strategy.

We found that **MM-401** could specifically interfere with (1) the establishment of activating histone modifications associated with MLL1 fusion protein action and (2) expression of *HoxA9* and *Meis1* in both MLL1-AF9 transformed mouse cells and MEFs. This suggests that the WDR5:MLL1 interaction is essential for maintaining *HoxA9* expression driven by normal MLL1 activity and abnormal MLL1 fusion proteins. This points to the potential utility for this

inhibitor as both a leukemia therapeutic and a research tool for investigating the role of WDR5 in normal gene expression. This information also suggests that this inhibitor could impair normal hematopoiesis in patients receiving it for therapy. However, compared to the severe illness caused by the general cytotoxic effects of traditional chemotherapies, impaired immune system development during treatment seems like an acceptable risk relative to fatality from leukemia or the severe side-effects from conventional therapies.

One interesting finding from the chromatin studies in inhibitor-treated cells was the finding that wild-type MLL1 recruitment was impaired with **MM-401** treatment. This suggests that interaction with the WDR5/RbBP5/Ash2L sub-complex is needed for MLL1 recruitment to or stabilization at gene targets. This finding also supports the utility of this inhibitor as a chemical tool for studying the role of different protein interactions within the MLL1 complex, as this novel finding would be challenging to recapitulate with genetic tools. We had originally hypothesized that recruitment of MLL1 to *HoxA9* and other targets is facilitated by MLL1 interaction with DNA, histone modifications and transcription factors through the multitude of conserved nucleic acid and protein-binding domains identified in the MLL1 protein. However, the reduction of MLL1 binding to *HoxA9* in the presence of **MM-401**, suggests that the WDR5/RbBP5/Ash2L complex drives recruitment of the MLL1 protein, or at least stabilizes its binding to target loci. One possible mechanism by which the WRA subcomplex could drive MLL1 recruitment to *HoxA9* is through a direct interaction between WDR5 and a non-coding RNA involved in Hox gene expression. WDR5 can interact directly with the lincRNA, HOTTIP, which binds to the Hox loci and promotes recruitment of the MLL1 complex through its interaction with WDR5[80]. Another possibility is that the WRA subcomplex does not facilitate recruitment of MLL1, but, rather, promotes its stability and prevents degradation. To check this

possibility, we would have to examine the protein levels of MLL1 in the presence and absence of **MM-401.**

Activation of transcription, especially of developmental factors, such as the *Hox* genes is a complex, highly-regulated process that involves a multitude of factors to alter chromatin structure, recruit the transcription machinery to the promoter and allow it to progress through the nucleosomes in the coding region. In order to better understand the coordinated recruitment of some of these factors in response to environmental or developmental stimuli, we must first understand the biochemical mechanisms that facilitate recruitment. As many of the factors involved in gene activation, such as MLL1, are large, multidomain proteins with a wealth of interactions, simple genetic ablation will not clarify the issue of recruitment. To make further inroads into understanding the processess that drive transcription activation, we must rigorously characterize the protein-protein interactions that govern these processes and develop novel methods to study their function.

Chromatin modification is an important means by which cellular phenotype is regulated, especially during development. For example, histone H3K4 methylation by MLL1 permits and/or promotes the expression of *HoxA9* in hematopoietic stem cells and progenitors. This promotes the proliferating, self-renewing phenotype that is essential for the function of these cell types. However, as development proceeds, *MLL1* is downregulated, resulting in downregulation of H3K4 methylation at the *HoxA9* locus. This results in a loss of *HoxA9* upregulation, which impairs self-renewal and proliferation. This is important because differentiated hematopoietic cell types cannot grow and proliferate, unchecked. The abnormal expression of *HoxA9* in differentiated cell types, leads to abnormal self-renewal and proliferation, resulting in cancer. This highlights the need for appropriate regulation of chromatin modification in cells to promote

appropriate development and prevent transformation. While this concept is illustrated with an example from the hematopoietic system, there are many other cases where epigenetic dysregulation results in cancer. New methods to study both normal and abnormal epigenetic regulation will enhance our understanding of how epigenetic dysregulation can lead to disease. These new methods can also provide promising clues as to how to interfere with epigenetic dysregulation in cancer for development of improved therapies.

Materials and Methods

Chemistry

See Karatas et al. 2011

Fluorescence Polarization (FP) Based Experiments. All the fluorescence polarization based experiments were performed in Microfluor[®] 2 Black, "U" Bottom, 96-well Microtiter Plates (ThermoSci.) and FP was measured as millipolarization units (mP) in a microplate reader (Tecan Ultra) with excitation at 485 nm and emission at 530 nm. The K_d of the tracers and the IC_{50} value of the inhibitors were calculated using GraphPad Prism 4 software.

Saturation binding experiment to determine dissociation constant (K_d) of the tracers: To dilutions of WDR5Δ23 (2.2-0 μM) in 100 μl assay buffer (0.1M Phosphate, 25mM KCl, 0.01% Triton, pH 6.5) 20 μl of a fixed concentration of the tracer in the assay buffer was added, followed by an addition of 5 μl DMSO to give 125 μl of total volume. Each assay has two controls; blank (without protein and tracer) and tracer only (without protein). The plates were incubated on a shaker at room temperature to reach the equilibrium and mP values were measured at the 3 h time point.

Competitive Binding Experiments. The binding affinities of the synthetic peptides were measured in a competitive binding assay. A pre-incubated complex solution of WDR5Δ23 and the tracer in 120 μl assay buffer were added to dilutions of the test compound in 5 μl DMSO,

giving final concentrations of WDR5Δ23 and the tracer of 4 nM and 0.6 nM, respectively. Three control wells are included in each plate; blank (without protein and tracer), 100 % inhibition (tracer only), and 0 % inhibition (complex solution only). The plates were incubated with shaking at room temperature. The mP values were measured after five hours of incubation and K_i values were calculated using the equation described by Nikolovska-Coleska et.al. and provided on the web.

Protein Purification

Protein expression and purification for the binding assay. N-terminal His-tagged WDR5Δ23 (24-334) was expressed from the pET28-MHL vector in Rosetta2(DE3) pLysS cells (Novagen). Cells were grown to OD_{600}= 0.4-0.6 in 4L 2XTY at 30°C, induced with 0.1mM IPTG at 16°C for 16 h and harvested in 20mM HEPES pH 7.5, 500mM KCl, 10% glycerol, 0.1mg/ml PMSF, 0.05% NP40. Cells were lysed by addition of 0.2mg/ml hen egg white lysozyme followed by sonication and clarification by centrifuging for 30 min at 15,000 rpm. The supernatant was combined with 5.0mM imidazole at pH 7.5 and 4ml of pre-equilibrated Ni^+NTA resin (Qiagen) and rotated at 4°C for 4 h. The resin was washed 3 times for 10 min with 40 ml lysis buffer. His-WDR5Δ23 was eluted from the resin by 3×15min elutions with 20mM HEPES pH 7.5, 100 mM KCl, 10% glycerol, 250mM imidazole pH 7.5. Elutions were clarified by centrifugation at 2000 rpm for 1 min and syringe-filtered through a 0.45 μM membrane (Millipore). The eluate was loaded onto two 5 ml SP-Sepharose Hi-Trap columns using the AKTApurifier (GE Healthcare). Fractions were eluted in 20mM HEPES pH 7.5, 10% glycerol with a KCl gradient from 0-1000 mM and peak fractions were pooled and concentrated to 64 μM using a Amicon Ultra centrifugal filter, 10,000 MWCO (Amicon). Concentrated protein was aliquoted and samples were frozen on dry ice and stored at -80°C.

For Enzymatic Assays MLL1$^{3762-C'}$, WDR5$^{23-C'}$, RbBP5 and ASH2L^{SPRY} were expressed as His-SUMO fusions from the pET28A-SUMO vector. Proteins were expressed from BL21 DE3 pLyss codon (+) at 16 °C overnight after induction with 0.1 mM IPTG in the mid-log phase of bacterial growth. Cells were harvested and protein was purified by the His-tag on Ni-NTA resin (Qiagen). The SUMO tag was removed from RbBP5, ASH2L and MLL1 by incubation with the ULP1 protease at 4 °C overnight. The protease and cleaved SUMO-His tag were collected by batch binding with the Ni-NTA resin for 1h.

For GST Pulldown MLL1$^{3762-C'}$ and MLL3$^{4703-C'}$ were cloned into pGEX6P1 and expressed and lysed as described above. Proteins were lysed and purified in 50mM NaPi, pH 7.8, 400mM KCl and 10% glycerol, with 0.1mM PMSF, 0.1mM benzamidine for protease inhibition. GST fusion proteins were collected by batch-binding with 1mL glutathione 4B sepharose (GE Healthcare) and eluted according to the manufacturer's directions.

Histone Methytransferase Assays

Radiography. MLL1$^{3762-3969}$,WDR5, RbBP5 and Ash2L were combined in storage buffer (20mM tris, pH 8.0, 500mM KCl, 10% glycerol at 5μM) at a concentration of 5.0μM and then diluted 1:10 into the reaction for a final concentration of 0.5μM. 1.0μg recombinant H3 and 1.0μCi ^{3}H-S-adenosyl methionine were added and the reaction was incubated at room-temperature for 60 minutes. Reaction products were combined with SDS loading dye and separated on a 15% acrylamide SDS-PAGE gel before staining, treatment with Amplify (GE Healthcare) for 30 minutes and drying. SDS-PAGE gel was combined with film for 4 days before development.

Kinetic Assays. The HMT assay was performed in 50 mM HEPES pH 7.8, 100 mM NaCl, 1.0 mM EDTA and 10% glycerol at room temperature (approximately 22 °C). Each reaction contained 1.0 μCi of the co-factor, ^{3}H-*S*-adenosyl methionine (Perkin Elmer). 0.5μM (final concentration) WDR5-RbBP5-Ash2L subcomplex was added to the reaction buffer with substrate and cofactor and reactions were initiated by addition of MLL1^{3762} at a final concentration of 0.5μM. Reactions were quenched after 4 minutes by addition of β-mercaptoethanol (Fisher) at a final concentration of 178μM. Reactions were then spotted onto 15mm x 15mm squares of P81 phosphocellulose (Whatman) and submerged in 50-100ml 50mM bicarbonate, pH 9.0 and washed 3 x 10 minutes at RT, dried at 60°C, vortexed in Ultima Gold scintillation fluid and counted.

Inhibitor Assays. H3 10-residue peptide was used as the substrate at 50 μM. Compounds were added at concentrations, as indicated in the text, 0.125-128 μM and incubated with the pre-assembled WDR5-RbBP5-ASH2L complex at a final concentration of 0.5 μM for each protein for 2-5 min. Reactions were initiated by addition of the MLL1$^{3762-C'}$ protein at a final concentration of 0.5 μM and allowed to proceed for 30 min before preparing scintillation counting. To count samples, reactions were spotted on separate squares of P81 filter paper (Whatman) and precipitated by submerging in freshly prepared 50 mM sodium bicarbonate buffer with pH=9.0.

Protein Interaction Studies

GST-Pulldown. GST-tagged MLL fragments were combined with WDR5, RbBP5 and Ash2L at 2.5μM in 1x PBS, supplemented with 0.1μg/μl BSA, 0.1% NP40, PMSF and benzamidine, and

incubated with glutathione 4B sepharose (GE Healthcare) for 1 hour at RT. Resin was washed 3x at RT and eluted in equal resin volume 1X SDS loading dye.

FLAG-WDR5. Immunoprecipitation. Stable transfection and nuclear extract preparation of FLAG-WDR5 nuclear extract was performed as described [86]. 0.5ml nuclear extract was combined with inhibitors at the indicated concentrations, incubated with M2 agarose and eluted according to the manufacturers directions.

co-Immunoprecipitation. MLL1$^{3754-C'}$ was cloned into pCDNA3.1Myc (Invitrogen) on BamHI and EcoRI sites. WDR5 was cloned into pIRESNeo, as described previously [86]. Constructs were transfected into 293T with Lipofectamine2000 (Invitrogen) according to the manufacturer's directions and harvested, as described, after 48 hrs. and immunoprecipitated with M2 Agarose [86].

Surface Plasmon Resonance.

Surface Plasmon Resonance binding assays were performed as described [130].

Western Blotting. Westerns were blotted with anti-FLAG monoclonal (SIGMA), anti-MLL-C [54], anti-GST (GE Healthcare), anti-RbBP5 (Cell Signaling), HRP-conjugated anti-His (Qiagen) or anti-Myc.

Cell Culture

MLL1-AF9 Transformed Mouse Leukemia Cells. MLL1-AF9-transformed mouse bone marrow was cultured in IMDM + 15% FBS and supplemented with 0.01ng/ml IL-3 at each passage, every other day. MLL1-AF9 transformed bone marrow was generated as described [121].

Human Leukemia Cell Lines. Human leukemia cell lines MV4:11, K562, MOLM-13, THP-1 and KOPN8 were maintained in RPMI1460 (GIBCO) supplemented with 10% FBS. Cells were passaged to $1\text{-}2\text{x}10^5$/ml every 3-4 days, depending on cell growth. Inhibitors were added such that DMSO was consistent at 0.2% for all treatments.

Cell Viability Assays. Inhibitors were diluted in DMSO and added in at 0.2% DMSO final concentration. For viability assays, cells were cultured at $1\text{x}10^5$/ml and passaged every 2 days. Viability was monitored using the CellTitreGlo® Kit (Promega) according to the manufacturers directions and luminescence was monitored on a Molecular Dynamics plate reader.

RT-PCR. MLL1-AF9 cells were cultured as described for the viability assays for 4 days with **MM-401** or **MM-NC-401** at 40μM with DMSO at 0.2%. At the end of treatment, cells were harvested by centrifugation at 300x*g* and washed with 1xPBS and then resuspended in 1mL Trizol Reagent (Invitrogen) and stored in −80°C. RNA was extracted by a standard Trizol/RNeasy extraction protocol[87] and reverse transcribed using the SuperScript III kit (Invitrogen) according to the manufacturers directions. qPCR was performed as described [87].

Chromatin Immunoprecipitation. Chromatin immunoprecipitation was performed, as described [87]. Anti-H3K4me3 and anti-H3K79me3 were from Abcam.

References

1.   Luger, K., et al., *Crystal structure of the nucleosome core particle at 2.8 A resolution.* Nature, 1997. **389**(6648): p. 251-60.
2.   Kornberg, R.D., *Chromatin structure: a repeating unit of histones and DNA.* Science, 1974. **184**(4139): p. 868-71.
3.   Kornberg, R.D. and J.O. Thomas, *Chromatin structure; oligomers of the histones.* Science, 1974. **184**(4139): p. 865-8.
4.   Kouzarides, T. and S.L. Berger, *Chromatin Modifications and Their Mechanism of Action*, in *Epigenetics*, M.-L. Caparros, Editor 2006, Cold Spring Harbor Laboratory Press: Cold Spring Harbor, NY.
5.   Workman, J.L. and R.G. Roeder, *Binding of transcription factor TFIID to the major late promoter during in vitro nucleosome assembly potentiates subsequent initiation by RNA polymerase II.* Cell, 1987. **51**(4): p. 613-22.
6.   Sims, R.J., 3rd, R. Belotserkovskaya, and D. Reinberg, *Elongation by RNA polymerase II: the short and long of it.* Genes & development, 2004. **18**(20): p. 2437-68.
7.   Allis, C.D., T. Jenuwein, and D. Reinberg, *Overview and Concepts*, in *Epigenetics*, M.-L. Caparros, Editor 2006, Cold Spring Harbor Laboratory Press: Cold Spring Harbor, NY. p. 23-62.
8.   Jaenisch, R. and A. Bird, *Epigenetic regulation of gene expression: how the genome integrates intrinsic and environmental signals.* Nature genetics, 2003. **33 Suppl**: p. 245-54.
9.   Strahl, B.D. and C.D. Allis, *The language of covalent histone modifications.* Nature, 2000. **403**(6765): p. 41-5.
10.   Kouzarides, T., *Chromatin modifications and their function.* Cell, 2007. **128**(4): p. 693-705.
11.   Jenuwein, T. and C.D. Allis, *Translating the histone code.* Science, 2001. **293**(5532): p. 1074-80.
12.   Robzyk, K., J. Recht, and M.A. Osley, *Rad6-dependent ubiquitination of histone H2B in yeast.* Science, 2000. **287**(5452): p. 501-4.
13.   Martin, C. and Y. Zhang, *The diverse functions of histone lysine methylation.* Nature reviews. Molecular cell biology, 2005. **6**(11): p. 838-49.
14.   Rea, S., et al., *Regulation of chromatin structure by site-specific histone H3 methyltransferases.* Nature, 2000. **406**(6796): p. 593-9.
15.   Marmorstein, R., *Structure of SET domain proteins: a new twist on histone methylation.* Trends in biochemical sciences, 2003. **28**(2): p. 59-62.
16.   Couture, J.F., et al., *Structural basis for the methylation site specificity of SET7/9.* Nature structural & molecular biology, 2006. **13**(2): p. 140-6.
17.   Marmorstein, R. and R.C. Trievel, *Histone modifying enzymes: structures, mechanisms, and specificities.* Biochimica et biophysica acta, 2009. **1789**(1): p. 58-68.
18.   Couture, J.F., et al., *Catalytic roles for carbon-oxygen hydrogen bonding in SET domain lysine methyltransferases.* The Journal of biological chemistry, 2006. **281**(28): p. 19280-7.

19.   Sims, R.J., 3rd, et al., *Human but not yeast CHD1 binds directly and selectively to histone H3 methylated at lysine 4 via its tandem chromodomains.* The Journal of biological chemistry, 2005. **280**(51): p. 41789-92.

20.   Li, B., et al., *Combined action of PHD and chromo domains directs the Rpd3S HDAC to transcribed chromatin.* Science, 2007. **316**(5827): p. 1050-4.

21.   Wysocka, J., et al., *A PHD finger of NURF couples histone H3 lysine 4 trimethylation with chromatin remodelling.* Nature, 2006. **442**(7098): p. 86-90.

22.   Shi, X., et al., *ING2 PHD domain links histone H3 lysine 4 methylation to active gene repression.* Nature, 2006. **442**(7098): p. 96-9.

23.   Pena, P.V., et al., *Molecular mechanism of histone H3K4me3 recognition by plant homeodomain of ING2.* Nature, 2006. **442**(7098): p. 100-3.

24.   Gozani, O., et al., *The PHD finger of the chromatin-associated protein ING2 functions as a nuclear phosphoinositide receptor.* Cell, 2003. **114**(1): p. 99-111.

25.   Flanagan, J.F., et al., *Double chromodomains cooperate to recognize the methylated histone H3 tail.* Nature, 2005. **438**(7071): p. 1181-5.

26.   Han, Z., et al., *Structural basis for the specific recognition of methylated histone H3 lysine 4 by the WD-40 protein WDR5.* Molecular cell, 2006. **22**(1): p. 137-44.

27.   Zhang, Y. and D. Reinberg, *Transcription regulation by histone methylation: interplay between different covalent modifications of the core histone tails.* Genes & development, 2001. **15**(18): p. 2343-60.

28.   Ebert, A., et al., *Su(var) genes regulate the balance between euchromatin and heterochromatin in Drosophila.* Genes & development, 2004. **18**(23): p. 2973-83.

29.   Schotta, G., et al., *A silencing pathway to induce H3-K9 and H4-K20 trimethylation at constitutive heterochromatin.* Genes & development, 2004. **18**(11): p. 1251-62.

30.   Tachibana, M., et al., *G9a histone methyltransferase plays a dominant role in euchromatic histone H3 lysine 9 methylation and is essential for early embryogenesis.* Genes & development, 2002. **16**(14): p. 1779-91.

31.   Tachibana, M., et al., *Set domain-containing protein, G9a, is a novel lysine-preferring mammalian histone methyltransferase with hyperactivity and specific selectivity to lysines 9 and 27 of histone H3.* The Journal of biological chemistry, 2001. **276**(27): p. 25309-17.

32.   Tachibana, M., et al., *G9a/GLP complexes independently mediate H3K9 and DNA methylation to silence transcription.* The EMBO journal, 2008. **27**(20): p. 2681-90.

33.   Cao, R. and Y. Zhang, *The functions of E(Z)/EZH2-mediated methylation of lysine 27 in histone H3.* Current opinion in genetics & development, 2004. **14**(2): p. 155-64.

34.   Cao, R., et al., *Role of histone H3 lysine 27 methylation in Polycomb-group silencing.* Science, 2002. **298**(5595): p. 1039-43.

35.   Pasini, D., et al., *Suz12 is essential for mouse development and for EZH2 histone methyltransferase activity.* The EMBO journal, 2004. **23**(20): p. 4061-71.

36.   Karachentsev, D., et al., *PR-Set7-dependent methylation of histone H4 Lys 20 functions in repression of gene expression and is essential for mitosis.* Genes & development, 2005. **19**(4): p. 431-5.

37.   Santos-Rosa, H., et al., *Active genes are tri-methylated at K4 of histone H3.* Nature, 2002. **419**(6905): p. 407-11.

38.   Bannister, A.J., et al., *Spatial distribution of di- and tri-methyl lysine 36 of histone H3 at active genes.* The Journal of biological chemistry, 2005. **280**(18): p. 17732-6.

39.   Bernstein, B.E., et al., *Genomic maps and comparative analysis of histone modifications in human and mouse.* Cell, 2005. **120**(2): p. 169-81.

40.   Barski, A., et al., *High-resolution profiling of histone methylations in the human genome.* Cell, 2007. **129**(4): p. 823-37.

41.   Qiu, J., et al., *The X-linked mental retardation gene PHF8 is a histone demethylase involved in neuronal differentiation.* Cell research, 2010. **20**(8): p. 908-18.

42.   Chang, P.Y., et al., *Binding of the MLL PHD3 finger to histone H3K4me3 is required for MLL-dependent gene transcription.* Journal of molecular biology, 2010. **400**(2): p. 137-44.

43.   Milne, T.A., et al., *Multiple interactions recruit MLL1 and MLL1 fusion proteins to the HOXA9 locus in leukemogenesis.* Molecular cell, 2010. **38**(6): p. 853-63.

44.   Ruthenburg, A.J., et al., *Recognition of a mononucleosomal histone modification pattern by BPTF via multivalent interactions.* Cell, 2011. **145**(5): p. 692-706.

45.   Lan, F., et al., *Recognition of unmethylated histone H3 lysine 4 links BHC80 to LSD1-mediated gene repression.* Nature, 2007. **448**(7154): p. 718-22.

46.   Vermeulen, M., et al., *Selective anchoring of TFIID to nucleosomes by trimethylation of histone H3 lysine 4.* Cell, 2007. **131**(1): p. 58-69.

47.   Fortschegger, K., et al., *PHF8 targets histone methylation and RNA polymerase II to activate transcription.* Molecular and cellular biology, 2010. **30**(13): p. 3286-98.

48.   Gregory, G.D., et al., *Mammalian ASH1L is a histone methyltransferase that occupies the transcribed region of active genes.* Molecular and cellular biology, 2007. **27**(24): p. 8466-79.

49.   Wilson, J.R., et al., *Crystal structure and functional analysis of the histone methyltransferase SET7/9.* Cell, 2002. **111**(1): p. 105-15.

50.   Nakamura, T., et al., *ALL-1 is a histone methyltransferase that assembles a supercomplex of proteins involved in transcriptional regulation.* Molecular cell, 2002. **10**(5): p. 1119-28.

51.   Milne, T.A., et al., *MLL targets SET domain methyltransferase activity to Hox gene promoters.* Molecular cell, 2002. **10**(5): p. 1107-17.

52.   Gu, Y., et al., *The t(4;11) chromosome translocation of human acute leukemias fuses the ALL-1 gene, related to Drosophila trithorax, to the AF-4 gene.* Cell, 1992. **71**(4): p. 701-8.

53.   Steward, M.M., et al., *Molecular regulation of H3K4 trimethylation by ASH2L, a shared subunit of MLL complexes.* Nature structural & molecular biology, 2006. **13**(9): p. 852-4.

54.   Dou, Y., et al., *Regulation of MLL1 H3K4 methyltransferase activity by its core components.* Nature structural & molecular biology, 2006. **13**(8): p. 713-9.

55.   Lee, S., et al., *Coactivator as a target gene specificity determinant for histone H3 lysine 4 methyltransferases.* Proceedings of the National Academy of Sciences of the United States of America, 2006. **103**(42): p. 15392-7.

56.   Lee, J., et al., *Targeted inactivation of MLL3 histone H3-Lys-4 methyltransferase activity in the mouse reveals vital roles for MLL3 in adipogenesis.* Proceedings of the National Academy of Sciences of the United States of America, 2008. **105**(49): p. 19229-34.

57.   Lee, J., et al., *A tumor suppressive coactivator complex of p53 containing ASC-2 and histone H3-lysine-4 methyltransferase MLL3 or its paralogue MLL4.* Proceedings of the National Academy of Sciences of the United States of America, 2009. **106**(21): p. 8513-8.

58.   Lee, S., R.G. Roeder, and J.W. Lee, *Roles of histone H3-lysine 4 methyltransferase complexes in NR-mediated gene transcription.* Progress in molecular biology and translational science, 2009. **87**: p. 343-82.

59.   Mo, R., S.M. Rao, and Y.J. Zhu, *Identification of the MLL2 complex as a coactivator for estrogen receptor alpha.* The Journal of biological chemistry, 2006. **281**(23): p. 15714-20.

60.   Glaser, S., et al., *Multiple epigenetic maintenance factors implicated by the loss of Mll2 in mouse development.* Development, 2006. **133**(8): p. 1423-32.

61.   Hess, J.L., et al., *Defects in yolk sac hematopoiesis in Mll-null embryos.* Blood, 1997. **90**(5): p. 1799-806.

62.   Yu, B.D., et al., *Altered Hox expression and segmental identity in Mll-mutant mice.* Nature, 1995. **378**(6556): p. 505-8.

63.   Schwab, K.R., S.R. Patel, and G.R. Dressler, *Role of PTIP in class switch recombination and long-range chromatin interactions at the immunoglobulin heavy chain locus.* Molecular and cellular biology, 2011. **31**(7): p. 1503-11.

64.   Daniel, J.A., et al., *PTIP promotes chromatin changes critical for immunoglobulin class switch recombination.* Science, 2010. **329**(5994): p. 917-23.

65.   Wu, J., et al., *PTIP regulates 53BP1 and SMC1 at the DNA damage sites.* The Journal of biological chemistry, 2009. **284**(27): p. 18078-84.

66.   Yagi, H., et al., *Growth disturbance in fetal liver hematopoiesis of Mll-mutant mice.* Blood, 1998. **92**(1): p. 108-17.

67.   Ringrose, L. and R. Paro, *Epigenetic regulation of cellular memory by the Polycomb and Trithorax group proteins.* Annual review of genetics, 2004. **38**: p. 413-43.

68.   Argiropoulos, B. and R.K. Humphries, *Hox genes in hematopoiesis and leukemogenesis.* Oncogene, 2007. **26**(47): p. 6766-76.

69.   Hess, J.L., *MLL: a histone methyltransferase disrupted in leukemia.* Trends in molecular medicine, 2004. **10**(10): p. 500-7.

70.   Krivtsov, A.V. and S.A. Armstrong, *MLL translocations, histone modifications and leukaemia stem-cell development.* Nature reviews. Cancer, 2007. **7**(11): p. 823-33.

71.   Sauvageau, G., et al., *Differential expression of homeobox genes in functionally distinct CD34+ subpopulations of human bone marrow cells.* Proceedings of the National Academy of Sciences of the United States of America, 1994. **91**(25): p. 12223-7.

72.   Lawrence, H.J., et al., *Loss of expression of the Hoxa-9 homeobox gene impairs the proliferation and repopulating ability of hematopoietic stem cells.* Blood, 2005. **106**(12): p. 3988-94.

73.   Ernst, P., et al., *Definitive hematopoiesis requires the mixed-lineage leukemia gene.* Developmental cell, 2004. **6**(3): p. 437-43.

74.   Andreeff, M., et al., *HOX expression patterns identify a common signature for favorable AML.* Leukemia : official journal of the Leukemia Society of America, Leukemia Research Fund, U.K, 2008. **22**(11): p. 2041-7.

75.   Southall, S.M., et al., *Structural basis for the requirement of additional factors for MLL1 SET domain activity and recognition of epigenetic marks.* Molecular cell, 2009. **33**(2): p. 181-91.

76.   Patel, A., et al., *On the mechanism of multiple lysine methylation by the human mixed lineage leukemia protein-1 (MLL1) core complex.* The Journal of biological chemistry, 2009. **284**(36): p. 24242-56.

77.   Cosgrove, M.S. and A. Patel, *Mixed lineage leukemia: a structure-function perspective of the MLL1 protein.* The FEBS journal, 2010. **277**(8): p. 1832-42.

78.   Gori, F. and M.B. Demay, *BIG-3, a novel WD-40 repeat protein, is expressed in the developing growth plate and accelerates chondrocyte differentiation in vitro.* Endocrinology, 2004. **145**(3): p. 1050-4.

79.   Gori, F., P. Divieti, and M.B. Demay, *Cloning and characterization of a novel WD-40 repeat protein that dramatically accelerates osteoblastic differentiation.* The Journal of biological chemistry, 2001. **276**(49): p. 46515-22.

80.   Wang, K.C., et al., *A long noncoding RNA maintains active chromatin to coordinate homeotic gene expression.* Nature, 2011. **472**(7341): p. 120-4.

81.   Wu, M.Z., et al., *Interplay between HDAC3 and WDR5 is essential for hypoxia-induced epithelial-mesenchymal transition.* Molecular cell, 2011. **43**(5): p. 811-22.

82.   Li, X., et al., *The Histone Acetyltransferase MOF Is a Key Regulator of the Embryonic Stem Cell Core Transcriptional Network.* Cell stem cell, 2012. **11**(2): p. 163-78.

83.   Diao, Y., et al., *Pax3/7BP Is a Pax7- and Pax3-Binding Protein that Regulates the Proliferation of Muscle Precursor Cells by an Epigenetic Mechanism.* Cell stem cell, 2012. **11**(2): p. 231-41.

84.   Kawabe, Y.I., et al., *Carm1 Regulates Pax7 Transcriptional Activity through MLL1/2 Recruitment during Asymmetric Satellite Stem Cell Divisions.* Cell stem cell, 2012.

85.   Ang, Y.S., et al., *Wdr5 mediates self-renewal and reprogramming via the embryonic stem cell core transcriptional network.* Cell, 2011. **145**(2): p. 183-97.

86.   Dou, Y., et al., *Physical association and coordinate function of the H3 K4 methyltransferase MLL1 and the H4 K16 acetyltransferase MOF.* Cell, 2005. **121**(6): p. 873-85.

87.   Li, X., et al., *Two mammalian MOF complexes regulate transcription activation by distinct mechanisms.* Molecular cell, 2009. **36**(2): p. 290-301.

88.   Odho, Z., S.M. Southall, and J.R. Wilson, *Characterization of a novel WDR5-binding site that recruits RbBP5 through a conserved motif to enhance methylation of histone H3 lysine 4 by mixed lineage leukemia protein-1.* The Journal of biological chemistry, 2010. **285**(43): p. 32967-76.

89.   Patel, A., V. Dharmarajan, and M.S. Cosgrove, *Structure of WDR5 bound to mixed lineage leukemia protein-1 peptide.* The Journal of biological chemistry, 2008. **283**(47): p. 32158-61.

90.   Patel, A., et al., *A conserved arginine-containing motif crucial for the assembly and enzymatic activity of the mixed lineage leukemia protein-1 core complex.* The Journal of biological chemistry, 2008. **283**(47): p. 32162-75.

91.   Boland, M.J., et al., *Adult mice generated from induced pluripotent stem cells.* Nature, 2009. **461**(7260): p. 91-4.

92.   Jiang, H., et al., *Role for Dpy-30 in ES cell-fate specification by regulation of H3K4 methylation within bivalent domains.* Cell, 2011. **144**(4): p. 513-25.

93.   Gori, F., E.D. Zhu, and M.B. Demay, *Perichondrial expression of Wdr5 regulates chondrocyte proliferation and differentiation.* Developmental biology, 2009. **329**(1): p. 36-43.

94.   Wysocka, J., et al., *WDR5 associates with histone H3 methylated at K4 and is essential for H3 K4 methylation and vertebrate development.* Cell, 2005. **121**(6): p. 859-72.

95.   Ruthenburg, A.J., et al., *Histone H3 recognition and presentation by the WDR5 module of the MLL1 complex.* Nature structural & molecular biology, 2006. **13**(8): p. 704-12.

96.   Couture, J.F., E. Collazo, and R.C. Trievel, *Molecular recognition of histone H3 by the WD40 protein WDR5.* Nature structural & molecular biology, 2006. **13**(8): p. 698-703.

97.   Schuetz, A., et al., *Structural basis for molecular recognition and presentation of histone H3 by WDR5.* The EMBO journal, 2006. **25**(18): p. 4245-52.

98.   Song, J.J. and R.E. Kingston, *WDR5 interacts with mixed lineage leukemia (MLL) protein via the histone H3-binding pocket.* The Journal of biological chemistry, 2008. **283**(50): p. 35258-64.

99.   Cao, F., et al., *An Ash2L/RbBP5 heterodimer stimulates the MLL1 methyltransferase activity through coordinated substrate interactions with the MLL1 SET domain.* PloS one, 2010. **5**(11): p. e14102.

100.   Patel, A., et al., *A novel non-SET domain multi-subunit methyltransferase required for sequential nucleosomal histone H3 methylation by the mixed lineage leukemia protein-1 (MLL1) core complex.* The Journal of biological chemistry, 2011. **286**(5): p. 3359-69.

101.   Thiel, A.T., et al., *MLL-AF9-induced leukemogenesis requires coexpression of the wild-type Mll allele.* Cancer cell, 2010. **17**(2): p. 148-59.

102.   Grembecka, J., et al., *Menin-MLL inhibitors reverse oncogenic activity of MLL fusion proteins in leukemia.* Nature chemical biology, 2012. **8**(3): p. 277-84.

103.   Daigle, S.R., et al., *Selective killing of mixed lineage leukemia cells by a potent small-molecule DOT1L inhibitor.* Cancer cell, 2011. **20**(1): p. 53-65.

104.   Hughes, C.M., et al., *Menin associates with a trithorax family histone methyltransferase complex and with the hoxc8 locus.* Molecular cell, 2004. **13**(4): p. 587-97.

105.   Goo, Y.H., et al., *Activating signal cointegrator 2 belongs to a novel steady-state complex that contains a subset of trithorax group proteins.* Molecular and cellular biology, 2003. **23**(1): p. 140-9.

106.   Strahl, B.D., et al., *Methylation of histone H3 at lysine 4 is highly conserved and correlates with transcriptionally active nuclei in Tetrahymena.* Proceedings of the National Academy of Sciences of the United States of America, 1999. **96**(26): p. 14967-72.

107.   Fingerman, I.M., H.C. Li, and S.D. Briggs, *A charge-based interaction between histone H4 and Dot1 is required for H3K79 methylation and telomere silencing: identification of a new trans-histone pathway.* Genes & development, 2007. **21**(16): p. 2018-29.

108.   Dharmarajan, V., et al., *Structural basis for Win (WDR5 interaction) motif recognition in human SET1 family histone methyltransferases.* The Journal of biological chemistry, 2012.

109.   Chin, H.G., et al., *Catalytic properties and kinetic mechanism of human recombinant Lys-9 histone H3 methyltransferase SUV39H1: participation of the chromodomain in enzymatic catalysis.* Biochemistry, 2006. **45**(10): p. 3272-84.

110.   Patnaik, D., et al., *Substrate specificity and kinetic mechanism of mammalian G9a histone H3 methyltransferase.* The Journal of biological chemistry, 2004. **279**(51): p. 53248-58.

111.   Horowitz, S., et al., *Direct evidence for methyl group coordination by carbon-oxygen hydrogen bonds in the lysine methyltransferase SET7/9.* The Journal of biological chemistry, 2011. **286**(21): p. 18658-63.

112. Wang, P., et al., *Global analysis of H3K4 methylation defines MLL family member targets and points to a role for MLL1-mediated H3K4 methylation in the regulation of transcriptional initiation by RNA polymerase II.* Molecular and cellular biology, 2009. **29**(22): p. 6074-85.

113. Hess, J.L., *Mechanisms of transformation by MLL.* Critical reviews in eukaryotic gene expression, 2004. **14**(4): p. 235-54.

114. Patel, S.R., et al., *The BRCT-domain containing protein PTIP links PAX2 to a histone H3, lysine 4 methyltransferase complex.* Developmental cell, 2007. **13**(4): p. 580-92.

115. Chabner, B.A. and T.G. Roberts, Jr., *Timeline: Chemotherapy and the war on cancer.* Nature reviews. Cancer, 2005. **5**(1): p. 65-72.

116. Noor, S.M., R. Bell, and A.C. Ward, *Shooting the messenger: targeting signal transduction pathways in leukemia and related disorders.* Critical reviews in oncology/hematology, 2011. **78**(1): p. 33-44.

117. Kawagoe, H., et al., *Expression of HOX genes, HOX cofactors, and MLL in phenotypically and functionally defined subpopulations of leukemic and normal human hematopoietic cells.* Leukemia : official journal of the Leukemia Society of America, Leukemia Research Fund, U.K, 1999. **13**(5): p. 687-98.

118. DiMartino, J.F., et al., *A carboxy-terminal domain of ELL is required and sufficient for immortalization of myeloid progenitors by MLL-ELL.* Blood, 2000. **96**(12): p. 3887-93.

119. Byun, J.S., et al., *ELL facilitates RNA polymerase II pause site entry and release.* Nature communications, 2012. **3**: p. 633.

120. Mueller, D., et al., *A role for the MLL fusion partner ENL in transcriptional elongation and chromatin modification.* Blood, 2007. **110**(13): p. 4445-54.

121. Tan, J., et al., *CBX8, a polycomb group protein, is essential for MLL-AF9-induced leukemogenesis.* Cancer cell, 2011. **20**(5): p. 563-75.

122. Bernt, K.M., et al., *MLL-rearranged leukemia is dependent on aberrant H3K79 methylation by DOT1L.* Cancer cell, 2011. **20**(1): p. 66-78.

123. Milne, T.A., et al., *Menin and MLL cooperatively regulate expression of cyclin-dependent kinase inhibitors.* Proceedings of the National Academy of Sciences of the United States of America, 2005. **102**(3): p. 749-54.

124. Chen, Y.X., et al., *The tumor suppressor menin regulates hematopoiesis and myeloid transformation by influencing Hox gene expression.* Proceedings of the National Academy of Sciences of the United States of America, 2006. **103**(4): p. 1018-23.

125. Caslini, C., et al., *Interaction of MLL amino terminal sequences with menin is required for transformation.* Cancer research, 2007. **67**(15): p. 7275-83.

126. Gori, F., E. Schipani, and M.B. Demay, *Fibromodulin is expressed by both chondrocytes and osteoblasts during fetal bone development.* Journal of cellular biochemistry, 2001. **82**(1): p. 46-57.

127. Chen, Y., et al., *Crystal structure of the N-terminal region of human Ash2L shows a winged-helix motif involved in DNA binding.* EMBO reports, 2011. **12**(8): p. 797-803.

128. Zhang, G., et al., *Genome sequence of foxtail millet (Setaria italica) provides insights into grass evolution and biofuel potential.* Nature biotechnology, 2012. **30**(6): p. 549-54.

129. Cho, Y.W., et al., *PTIP associates with MLL3- and MLL4-containing histone H3 lysine 4 methyltransferase complex.* The Journal of biological chemistry, 2007. **282**(28): p. 20395-406.

130.   Kawamoto, S.A., et al., *Analysis of the interaction of BCL9 with beta-catenin and development of fluorescence polarization and surface plasmon resonance binding assays for this interaction.* Biochemistry, 2009. **48**(40): p. 9534-41.